

Modelling Dairy Biofilms for Targeted Control of Thermophilic Bacteria

Isabel Huizi Li

A thesis submitted to Auckland University of
Technology in fulfilment of the requirements for the
degree of Doctor of Philosophy (PhD)

2013

School of Applied Sciences

Table of Contents

List of Figures.....	8
List of Tables	10
Attestation of Authorship.....	11
Co-authored Work.....	12
Acknowledgements	13
Intellectual Property Rights.....	15
Ethical Approval	17
Confidential Material	18
Abstract/Executive Summary	19
Glossary	22
1 Introduction	24
1.1. The Biofilm Problem in the Dairy Industry.....	24
1.2. The Significance of this Study	25
1.3. Temperature cycling and Mathematical Modelling Concept	25
1.4. Aims of this Study	26
2 Literature Review	28
2.1 Background of Biofilms	28
2.1.1 Definition of Biofilms	28
2.1.2 History of Biofilms	28
2.1.3 Nature of Biofilms	29
2.1.3.1 Biofilm Formation	29
2.1.3.2 Mechanism of Attachment.....	34
2.1.3.3 Quorum Sensing	34
2.1.3.4 Endospores.....	36
2.1.3.5 Issues and Problems with Biofilms	36
2.1.4 Factors Influencing Biofilm Growth	37
2.1.4.1 pH.....	37
2.1.4.2 Hydrophobicity and Surface Free Energy	37
2.1.4.3 Temperature	39
2.1.4.4 Surface.....	39

2.1.4.5	Flow	40
2.1.4.6	Age of Biofilm	41
2.1.4.7	Oxygen Availability	41
2.1.4.8	Nutrient Availability	41
2.1.4.9	Composition of Processing Fluid	42
2.1.5	Measurement of Biofilm Growth.....	43
2.1.5.1	Traditional Plating Techniques	43
2.1.5.2	Epifluorescence Microscopy and Staining	44
2.1.5.3	Confocal Microscopy.....	45
2.1.5.4	Impedance	45
2.2	Laboratory Systems for Biofilm Study	46
2.2.1	The Robbins Device	46
2.2.2	Continuous Tube Reactor	47
2.2.3	CDC Reactor	47
2.2.4	Plate Reactor	48
2.3	Control of Biofilm.....	49
2.3.1	Cleaning-in-Place	49
2.3.2	Effect of Different Cleaning Regimes.....	50
2.3.2.1	Caustic and Acid	50
2.3.2.2	Sanitizers and Surfactant	50
2.3.2.3	Biological Enzyme-based Cleaners	51
2.3.2.4	Chemical Cleaners.....	51
2.4	Active Surface Technology	52
2.4.1	Implant Surface with Metal Ions.....	53
2.4.2	Implant Surface with Organic Material	53
2.5	Disruption Technology.....	54
2.5.1	pH.....	54
2.5.2	Water Activity	55
2.5.3	Temperature	55
2.6	Introduction to Thermophilic Bacilli in the Dairy Industry	57
2.6.1	Description of <i>Bacillus licheniformis</i>	58
2.6.2	Description of <i>Anoxybacillus</i>	58
2.6.3	Description of <i>Geobacillus</i>	59

2.7	Mathematical Modelling	59
2.7.1	Introduction to Biofilm Modelling	59
2.7.2	Model Selection	60
2.7.3	Different Models.....	61
2.7.3.1	Analytical Models.....	62
2.7.3.2	Pseudo-analytical Models	63
2.7.3.3	Numerical One-dimensional Dynamic Models	63
2.7.3.4	Numerical One-dimensional Steady-state Models	64
2.7.3.5	Multi-dimensional Numerical Models.....	65
2.8.	Direction for the Current Study	66
3	Materials and Methods	68
3.1.	Chemicals	68
3.2.	Media.....	69
3.2.1.	Reconstituted Skim Milk.....	70
3.3.	Microorganisms.....	70
3.3.1.	Culture Management and Maintenance	72
3.3.2.	Gram Staining Procedures.....	72
3.3.3.	Culture Preparation.....	73
3.3.4.	Inoculation of Biofilm Reactor Systems.....	73
3.4.	Coupons.....	73
3.4.1.	Passivation	73
3.4.2.	Cleaning Procedure	74
3.5.	Enumeration of Bacterial Numbers.....	74
3.5.1.	Spiral Plater.....	74
3.5.2.	Impedance Microbiology Tool: BacTrac.....	74
3.5.2.1.	BacTrac Calibration.....	75
3.5.2.2.	Cleaning Procedures for BacTrac Cells	76
3.6.	Attachment and Growth Assays	76
3.6.1.	Microtitre Plate Attachment and Growth Assays.....	76
3.6.1.1.	Attachment Assay	77
3.6.1.2.	Comparison between Attachment in TSB and UHT Milk.....	77
3.6.1.3.	Staining Procedure for Microtitre Plate Assays	78
3.6.2.	Coupon Attachment Assay.....	79

3.7. Polymerase Chain Reaction Assay for Identification of Thermophilic Bacteria	79
3.7.1. Primer Information	79
3.7.2. PCR Mixture	80
3.7.3. PCR Conditions.....	80
3.7.4. PCR Set-up	81
3.8. Planktonic Growth Rate Studies.....	81
4 Characterisations of Thermophilic Bacteria from Milk Powder	83
4.1 Isolation and Identification of Isolate 1 and Isolate 2	84
4.1.1 Isolation and Cell Morphology of Isolate 1 and Isolate 2	84
4.1.2 PCR Identification	87
4.2 Preliminary Studies on Geo1 and Anoxy2	88
4.2.1 Calibration Curves.....	88
4.2.2 30 Min Coupon Attachment Assay.....	88
4.2.3 Planktonic Growth Rate in UHT Milk.....	90
4.3 Summary	92
5 Factorial Experiments Using CDC Reactors	93
5.1 Outline.....	93
5.2 Testing Boundary Conditions for Experiments Using the BacTrac.....	93
5.2.1 Experimental Procedures: Testing Boundary Conditions	94
5.2.2 Results: Testing Boundary Conditions	95
5.3 CDC Reactor Runs.....	96
5.3.1. CDC Reactor Set-up	96
5.3.2. Factorial Design	97
5.3.3. Experimental Procedures: CDC Reactor Runs	98
5.4 Results and Discussion	99
5.4.1 CDC Reactor Runs: Geo1	99
5.4.2 CDC Reactor Runs: Anoxy2.....	105
5.5 Summary	107
6 Temperature-cycling Experiments	109
6.1 Outline.....	109
6.2 Temperature-cycling Experiments	109
6.2.1. Temperature-cycling System	110
6.2.2. Experimental Procedures: Temperature Cycling.....	111

6.2.3.	Hexagonal Reactor Sampling.....	112
6.2.4.	Cleaning Procedure	112
6.3.	Thermocycling (Sine Wave)	113
6.3.1.	Thermocycler Calibration (Sine Wave)	113
6.3.2.	Factorial Design of Thermocycling (Sine Wave) Experiments.....	113
6.3.3	Results and Discussion of Thermocycling (Sine Wave).....	115
6.3.3.1	55–30°C Thermocycling Regime	115
6.3.3.2	55–35°C Thermocycling Regime	116
6.3.3.3	Discussion on Thermocycling (Sine Wave) Regimes.....	117
6.4	Thermospiking (Square Wave)	118
6.4.1.	Factorial Design of Thermospiking (Square Wave) Experiments	118
6.4.2	Results and Discussion of Thermospiking (Square Wave)	119
6.4.2.1	55–30°C Thermospiking Regime.....	119
6.4.2.2	55–35°C Thermospiking Regime.....	121
6.4.2.3	Discussion on Thermospiking (Square Wave) Regimes	122
6.5.	Biofilm Development in Temperature-cycling Experiments.....	124
6.6.	Investigations of the Preheating Pipes.....	126
6.6.1.	Experimental Procedures: Investigations of the Preheating Pipes	126
6.6.2.	Results and Discussion: Investigations of the Preheating Pipes	127
6.7.	Investigations of Effect of Temperature Step Changes on Bacterial Viability of Geo1.....	129
6.7.1.	Experimental Procedures: Investigations of Temperature Step Changes on Bacterial Viability of Geo1.....	129
6.7.2.	Results and Discussion: Investigations of Temperature Step Changes on the Bacterial Viability of Geo1	129
6.8	Impact of Cold Storage on Spores and Bacterial Counts	131
6.8.1.	Experimental Procedures: Impact of Cold Storage.....	131
6.8.2.	Results and Discussion: Impact of Cold Storage	132
6.9	Summary	132
7	Mathematical Modelling of Preheating Section.....	134
7.1	Outline	134
7.2	Logistic Equation	134
7.3	Mathematical Modelling of Bacterial Growth in the Preheating Pipes	136
7.3.1	Mathematical Model Set-up.....	136

7.3.2	Assumptions of the Mathematical Model	137
7.3.3	Mathematical Model Development	140
7.3.4	Mathematical Model Optimization	145
7.3.5	Justification of the Mathematical Model	146
7.4	Summary	148
8	Mathematical Modelling of Temperature Cycling.....	149
8.1	Outline	149
8.2	Mathematical Model Set-up	150
8.3	Biofilm Growth Rate, Temperature and Time Relationship	151
8.4	Assumptions of the Mathematical Model	155
8.5	Mathematical Model Development.....	160
8.6	Justification of the Mathematical Model	164
8.7	Use of the Mathematical Model	173
8.8	Summary	174
9	Final Discussion and Conclusions	175
9.1	Mathematical Model for Prediction of the Growth of Geol	175
9.2	Effectiveness of Temperature Cycling.....	177
9.3	Application of Temperature Cycling in the Dairy Industry	178
9.4	Suggestions for Future Work	185
9.5	Conclusions	190
	References.....	193
	Appendices.....	203

List of Figures

Figure 1: Processes governing biofilm formation (Breyers & Ratner, 2004).....	31
Figure 2: BacTrac calibration curve M for <i>Geobacillus</i> TRGT 9.	75
Figure 3: PCR temperature profile for identification of Isolate 1 and Isolate 2.	80
Figure 4: Biofilm Growth and Attachment microtitre plate assay.....	83
Figure 5: Biofilm Growth and Attachment microtitre plate assay:.....	83
Figure 6: Isolate 1 and Isolate 2 on TSA plates.	85
Figure 7: Gram staining of Isolate 1 under 100x objectives.....	85
Figure 8: Gram staining of Isolate 2 under 100x objectives.....	86
Figure 9: PCR identification results for Isolate 1 and Isolate 2.	87
Figure 10: A 30 min coupon attachment assay for Samples 1–13, Geo1 and Anoxy2.	89
Figure 11: Planktonic growth of Geo1 in UHT milk.....	90
Figure 12: Water activities versus solids in RSM.....	94
Figure 13: Schematic diagram of CDC reactor set-up.....	97
Figure 14: Biofilm growth curves for Geo1 in 10% solids RSM.	100
Figure 15: Biofilm growth curves for Geo1 in 14% solids RSM.	100
Figure 16: Estimated biofilm growth rates versus actual biofilm growth rates of Geo1.	102
Figure 17: Estimated Geo1 biofilm growth rate equations based on actual growth..	104
Figure 18: Biofilm growth curve for Anoxy2 at 50°C in 10% solids RSM.....	105
Figure 19: Biofilm growth curve for Anoxy2 at 60°C in 10% solids RSM.....	106
Figure 20: Estimated Anoxy2 biofilm growth rate equations based on actual growth.	107
Figure 21: Experimental set-up of the thermocycler system.	111
Figure 22: Thermocycling (sine wave) temperature profile.	114
Figure 23: Geo1 thermocycling (sine wave) normalized data (55–30°C).	115
Figure 24: Geo1 thermocycling (sine wave) normalized data (55–35°C).	116
Figure 25: Summary graph of Geo1 thermocycling (sine wave) data.	117
Figure 26: Thermospiking (square wave) temperature profile.	118
Figure 27: Geo1 thermospiking (square wave) normalized data (55–30°C).	119
Figure 28: Geo1 thermospiking (square wave) normalized data (55–35°C).	121

Figure 29: Summary graph of Geo1 thermospiking (square wave) data. 123

Figure 30: Bacterial attachment on the reactor after 24 h using thermocycling (sine wave)..... 124

Figure 31: Bacterial attachment on the reactor after 24 h using thermospiking (square wave)..... 125

Figure 32: Preheating-pipe-only run for Geo1..... 127

Figure 33: Temperature-cycling run for Geo1 with a 55–30–55°C temperature step change. 130

Figure 34: Temperature-cycling run for Geo1 with a 55–35–55°C temperature step change. 130

Figure 35: Schematic diagram of processes in the preheating pipes. 136

Figure 36: Preheating-pipe-only model: estimated versus actual bacterial counts in the bulk milk phase along time scale. 147

Figure 37: Schematic diagram of process in preheating pipe and hexagonal reactor. 150

Figure 38: Geo1 biofilm growth rate versus temperature relationship in 10% RSM.152

Figure 39: Settling of bacteria from the bulk phase on to the biofilm. 156

Figure 40: Estimated versus actual growth (sine wave, 20 min, 55–30°C). 165

Figure 41: Estimated versus actual growth (sine wave, 20 min, 55–35°C). 165

Figure 42: Estimated versus actual growth (square wave, 55–30°C). 166

Figure 43: Estimated versus actual growth (square wave, 55–35°C). 166

Figure 44: Output graph from R: estimated N_{reactor} (sampling interval: 1 min). 168

Figure 45: Output graph from R: estimated N_{reactor} (sampling interval: 2 h). 168

List of Tables

Table 1: Origins of bacterial strains.....	70
Table 2: Strains isolated from skim milk powder.....	71
Table 3: Plate layout for the attachment assay.....	77
Table 4: Plate layout for the comparison study of attachment in TSB and skim milk	78
Table 5: Set-up for the PCR identifications for Isolate 1 and Isolate 2.....	81
Table 6: BacTrac calibration equations developed for Geo1 and Anoxy2.....	88
Table 7: Planktonic growth rates of Geo1 and Anoxy2 in UHT milk.....	91
Table 8: Testing boundary conditions of experiments for factorial design work.....	95
Table 9: Factorial experimental plan for Geo1 and Anoxy2 CDC reactor runs.....	96
Table 10: Factorial design of CDC reactor runs.....	97
Table 11: Factorial CDC reactor run results for Geo1.....	99
Table 12: Estimated biofilm growth rate versus observed biofilm growth rate of Geo1	102
Table 13: Thermocycler calibration to achieve sine wave heating.....	113
Table 14: Factorial design of thermocycling (sine wave) experiments for Geo1.....	114
Table 15: Factorial design of thermospiking (square wave) experiments for Geo1..	119
Table 16: Bacterial and spore counts of Geo1 during 24 h of cold storage.....	132
Table 17: Geo1 maximum specific biofilm growth rate versus temperature relationship in 10% RSM.....	153
Table 18: Options for successful temperature-cycling regimes controlling Geo1	180

Attestation of Authorship

I hereby declare that this submission is my own work and that, to the best of my knowledge and belief, it contains no material previously published or written by another person (except where explicitly defined in the acknowledgements), nor material which to a substantial extent has been submitted for the award of any other degree or diploma of a university or other institution of higher learning.

Candidate Name Printed: _____

Candidate Signature: _____

Date: _____

Co-authored Work

Most of the experimental work in this study was done solely by Isabel Huizi Li in the WN Laboratory at Auckland University of Technology, Wellesley Campus (Auckland, New Zealand) from 2009 to 2013.

PCR work was done under the supervision of Kylie Walker at the Fonterra Research & Development Centre (Palmerston North, New Zealand) in 2010. MALDI–ToF work was done by Jacinda Aplin and Dr Denise Lindsay at the Fonterra Research & Development Centre (Palmerston North, New Zealand) in 2012.

Statistical work was done, with extensive help in constructing models and writing R programs by Dr Robin Hankin at Auckland University of Technology, Wellesley Campus (Auckland, New Zealand), in 2013.

Water activity measurements were done by Ms Sreeni Pathirana at the University of Auckland, City Campus (Auckland, New Zealand) in 2013.

Acknowledgements

I would like to express my deepest appreciation to the following people, who helped me extensively in my past 4 years of research.

This research would neither have come together well nor be completed without my supervisors' kind help, comprehensive knowledge and strong support throughout my hardest 4 years. I would like to pass on my special appreciation to my supervisory team of Professor John Brooks from Auckland University of Technology, Professor Steve Flint from Massey University, Dr Denise Lindsay from Fonterra and Dr Tuan Truong from Fonterra.

Although Dr Robin Hankin from Auckland University was not in my original supervisory team, he offered me massive help in constructing mathematical models and provided me with useful statistical suggestions.

I would also like to thank the Ministry of Science and Innovation and Fonterra as my sponsors. This project could not have gone ahead with their continuous financial and experimental material support.

Furthermore, I would like to thank my partner, parents and friends for giving me endless love and support. Thanks Tony for being with me in the laboratory for so many late nights to guard my safety. Thanks to my parents for financially supporting my fourth year. Thanks to all the technicians, especially Ms Meie Zou, who is more of a friend than my colleague, for providing me with all possible help in times of trouble. I could not have made it through this 4-year journey without all of you being there and supporting me.

Last, but not the least, I would like to thank Auckland University of Technology for providing me with laboratories and instruments, and academic, experimental and administration support throughout my journey.

Intellectual Property Rights

According to my contract with the Ministry of Science and Innovation (formerly a Technology in Industry Fellowship) and Fonterra:

All Intellectual Property will be owned by Fonterra. Notwithstanding the above, the University and the Student will retain the right to:

1. Use any Intellectual Property, except information which is confidential or commercially sensitive to Fonterra, for research and educational purposes;
2. Publish results from the Project, subject to written permission from Fonterra. (Fonterra will grant or withhold permission – and advise The University of its decision – within 20 days of Fonterra's receipt of a request from The University or the Student to publish. Fonterra will only withhold permission on the grounds that the proposed publication: (a) is not of a quality or a standard suitable for submission to and publication by an internationally recognised medical or scientific journal; (b) contains trade secrets belonging to Fonterra; (c) contains trademarks or describes brands belonging to Fonterra which Fonterra does not wish to be included in the publication; (d) is inconsistent with, or not supported by, the conclusions or results from the Project; (e) or presents Fonterra in a manner which Fonterra reasonably considers is likely to be unfair or damaging to the goodwill, reputation, trademarks or brands of Fonterra. Where Fonterra withholds permission, then it will consult with The University to determine whether amendments can be made to the publication so that permission to publish will be granted);
3. Submit the Student's thesis for examination, provided that: (a) the Student must obtain Fonterra's prior written consent to the use of any of Fonterra's Confidential Information or any Intellectual Property in the thesis; (b) Fonterra will grant or withhold consent – and advise The University of its decision – within 20 days of Fonterra's receipt of a request from The University or the Student to publish; (c) Fonterra will only withhold consent on the grounds set out in paragraph 2 above;

(d) where Fonterra withholds consent, then it will consult with The University to determine whether amendments can be made to the thesis so that consent to submit will be granted; (e) where Fonterra grants consent, then it may require as a condition of consent that the examiner(s) enters into a Confidentiality Agreement with Fonterra prior to receipt of the thesis; and (f) Fonterra may require the thesis to be embargoed for a period of up to 2 years from the end of the Project or such longer period as may be reasonably required by Fonterra and approved by The University's Assistant Vice-Chancellor (Research). (Fonterra acknowledges that an embargo will only be extended beyond 2 years in exceptional circumstances).

Ethical Approval

Ethical approval was not required for this project. No experimental testing was done on any form of animal or human. Only microorganisms and milk powder were used in this project. No hazardous material in this project was imported from outside New Zealand. The microorganisms and milk powder used exist locally or were produced in New Zealand.

Confidential Material

According to my contract with the Ministry of Science and Innovation (formerly a Technology in Industry Fellowship) and Fonterra:

“Submit the Student's thesis for examination, provided that: (a) the Student must obtain Fonterra's prior written consent to the use of any of Fonterra's Confidential Information or any Intellectual Property in the thesis; (b) Fonterra will grant or withhold consent – and advise The University of its decision – within 20 days of Fonterra's receipt of a request from The University or the Student to publish; (c) Fonterra will only withhold consent on the grounds set out in paragraph 2 above; (d) where Fonterra withholds consent, then it will consult with The University to determine whether amendments can be made to the thesis so that consent to submit will be granted; (e) where Fonterra grants consent, then it may require as a condition of consent that the examiner(s) enters into a Confidentiality Agreement with Fonterra prior to receipt of the thesis; and (f) Fonterra may require the thesis to be embargoed for a period of up to 2 years from the end of the Project or such longer period as may be reasonably required by Fonterra and approved by The University's Assistant Vice-Chancellor (Research). (Fonterra acknowledges that an embargo will only be extended beyond 2 years in exceptional circumstances).”

The temperature-cycling experiments were the key confidential part of this study. The results from this study are being kept confidential at this stage because they may have business benefits for Fonterra. This project also allows Fonterra to understand biofilm formation and thermophilic bacteria in more detail and depth as factors influencing the growth of thermophilic bacteria were studied.

Abstract/Executive Summary

Biofilms are the main source of bacterial contamination in dairy manufacturing plants. Strategies to mitigate biofilm development in dairy manufacture aim to improve the quality of the products manufactured and to maximize the run length of manufacturing plants. Substantial economic benefits can be made through maximizing the use of manufacturing plants. A simple strategy involves creating an unstable environment for microbial growth by manipulating conditions, such as temperature, on a sufficiently frequent basis to disrupt biofilm growth, and yet maintaining the ability to manufacture dairy products.

Isolates of thermophilic bacilli were provided by Massey University and Fonterra at the beginning of the project. These isolates were screened with different attachment assays, such as 30 min of attachment on to stainless steel coupons in tryptone soy broth and reconstituted skim milk and a microtitre plate assay with Crystal Violet staining.

Two additional thermophilic bacteria were isolated from milk powder and were added into this project. Geo1 was identified as *Geobacillus stearothermophilus* and Anoxy2 was identified as *Anoxybacillus flavithermus*. After preliminary studies, as Geo1 and Anoxy2 were wild strains with fast growth rates, they were preferred for further experiments.

A series of factorial experiments was conducted to investigate the effect of different temperatures and water activities (% solids milk) on the attachment of Geo1 and Anoxy2 to stainless steel coupons in the CDC (Centres for Disease Control and Prevention) reactor. The temperatures tested were 40, 50 and 60°C. The solids contents tested were 10, 14 and 18% for Geo1 and 10, 12 and 14% for Anoxy2. The optimum growth and attachment ranges for Geo1 were found to be between 50 and 60°C with 10–14% solids milk, whereas Anoxy2 grew only at 50 and 60°C with 10% solids milk.

Geo1 was selected for the temperature-cycling experiments because of its wider growth range. Sine wave (thermocycling) and square wave (thermospiking) regimes were

tested in the temperature-cycling experiments. The effect of these two different regimes was trialled using temperature fluctuations of 55–30°C and 55–35°C for different durations or periods. An initial decrease in bacterial counts in the outflowing milk was observed in the 55–35°C experiments. This phenomenon could not be clearly understood and explained at this stage. Some hypotheses were made including the differences in maintenance energy, settling process, sporulation and germination processes between 30°C and 35°C. This could also be explained by the 35°C being in a range where metabolism was continuing perhaps in an unbalanced manner, resulting in more overall damage than cycling to 30°C, where metabolism was more seriously reduced. Thermocycling at 55–35°C for periods of 10 min had the most obvious effect of prolonging the lag phase and giving an initial reduction in bacterial counts in the outflowing milk amongst all the thermocycling runs. This regime would offer the industry a better quality product in the first 12 h of manufacturing runs. Among the other thermocycling regimes, 55–30°C for periods of 50 min seemed to be an alternative option. This regime had a shorter lag phase, but produced a 1 – 1.5 log reduction in the bacterial numbers in the milk after 24 h, which would have the potential of prolonging the total run length of manufacturing runs.

Thermospiking regimes of 55–35°C were shown to prolong the lag phase from 2 to 12 h, whereas thermospiking regimes of 55–30°C prolonged the lag phase to 4 h. The square wave regimes of 55–35°C produced > 2 log reductions in bacterial counts in the prolonged lag phase, which would allow the industry to produce a much better quality product within the first 12 h of manufacture. The square wave regime of 55°C/15 min, 30°C/35 min may have the potential to extend the manufacturing run length because of a < 1.5 log reduction after 12 h and a < 1 log reduction after 24 h.

Preheating pipes submerged in a 55°C water bath for 24 h were required for the temperature-cycling experiments. This may have had an influence on the counts in the outflowing milk, with the results showing thermophilic bacteria in the milk from the preheating system and attached to the preheating pipes. A mathematical model based on logistic growth theory was designed to take account of this effect. The parameters of the preheating-pipe-only model (settling e-folding time of the pipe, growth e-folding time of the pipe, and the carrying capacity of the pipe) were optimized based on the correlation with observed data. The estimated outflow from the preheating-pipe-only

model was calculated using the optimal parameters, and then fed as the inflow condition into the model designed for the whole reactor system. The reactor model allowed us to predict the bacterial concentration of the outflowing milk and the bacterial count of the biofilm on the surfaces of the reactor. The reactor model did not predict well during the initial lag phase, but predicted well during the growth phase and the final stationary phase. The mathematical models designed from this study were unique and robust and represent a new method for analysing and managing growth in a dairy manufacturing plant.

Glossary

Notation	Definition	Unit
$\text{Area}_{\text{pipe}}$	Curved surface area of the whole pipe	cm^2
$\text{Area}_{\text{reactor}}$	Surface area of the hexagonal reactor	cm^2
δx	Distance travelled by the bacteria before attachment	cm
δt	Time taken for the bacteria to travel that distance	s
$\frac{dF}{dt}$	Rate of change of biofilm counts on the preheating pipe	cfu/s
$\frac{dM}{dt}$	Rate of change of bulk milk counts in the preheating pipe	cfu/s
$\frac{dN}{dt}$	Rate of change of bulk milk counts in the hexagonal reactor	cfu/s
$\frac{dR}{dt}$	Rate of change of biofilm counts on the hexagonal reactor	cfu/s
F	Bacterial counts in the biofilm on the preheating pipe	cfu
F_0	Initial counts in the biofilm on the preheating pipe at time 0	cfu
Flowrate	The system flowrate	ml/min
$\text{Growth}_{\text{pipe}}$	Rate of change of biofilm growth in the preheating pipe	cfu/s
$\text{Growth}_{\text{reactor}}$	Rate of change of biofilm growth in the reactor	cfu/s
$\text{Inflow}_{\text{pipe}}$	Rate of change of the inflow of milk from the reservoir	cfu/s
$\text{Inflow}_{\text{reactor}}$	Rate of change of the inflow into the hexagonal reactor, which is the rate of change of the outflow from the preheating pipe	cfu/s
k	Carrying capacity of the system	cfu
k_{pipe}	Carrying capacity of the preheating pipe	cfu
k_{reactor}	Carrying capacity of the hexagonal coupon reactor	cfu
M	Bacterial counts of the bulk milk in the preheating pipe	cfu
M_0	Initial counts of the bulk milk in the preheating pipe at time 0	cfu
$\text{Milk conc}_{\text{income}}$	Concentration of the incoming milk from the reservoir	cfu/ml
N	Bacterial counts of the bulk milk in the hexagonal reactor	cfu
N_0	Bacterials count of the bulk milk in the reactor at time 0	cfu
$\text{Outflow}_{\text{pipe}}$	Rate of change of the outflow of the bulk milk from the preheating pipe into the hexagonal coupon reactor	cfu/s
$\text{Outflow}_{\text{reactor}}$	Rate of change of the outflow of the bulk milk from the hexagonal coupon reactor to waste	cfu/s

P	Population of the system in the logistic equation. In this study, it means the bacterial population	cfu
Period	The period of the sine wave	min
R	Bacterial counts of the biofilm on the reactor surface	cfu
r	Growth rate of the population in the logistic equation	/h
Settling_{pipe}	Rate of change of the bacteria settling process from the bulk milk on to the biofilm in the preheating pipe	cfu/s
Settling_{reactor}	Rate of change of the bacteria settling process from the bulk milk on to the biofilm in the hexagonal coupon reactor	cfu/s
Sloughing_{pipe}	Rate of change of the bacteria sloughing-off from the biofilm into the bulk milk in the preheating pipe	cfu/s
Sloughing_{reactor}	Rate of change of the bacteria sloughing-off from the biofilm into the bulk milk in the hexagonal coupon reactor	cfu/s
t_{0,pipe}	Settling e-folding time of the preheating pipe	s
t_{0,reactor}	Settling e-folding time of the hexagonal coupon reactor	s
t_{G,pipe}	Growth e-folding time of the preheating pipe	s
t_{G,reactor}	Growth e-folding time of the hexagonal coupon reactor	s
t_D	Doubling time of the microorganism	min
t_{high}	Time spent at high temperature (55°C) in the thermospiking experiments	min
t_{low}	Time spent at low temperature (30 or 35°C) in the thermospiking experiments	min
T_{min}	Minimum temperature in the thermospiking experiments (30 or 35°C)	°C
T_{max}	Maximum temperature in the thermospiking experiments (55°C)	°C
Velocity	Specific settling velocity	cm/s
Volume_{pipe}	Volume of the preheating pipe	cm ³
Volume_{reactor}	Volume of the hexagonal coupon reactor	cm ³

1 Introduction

1.1. The Biofilm Problem in the Dairy Industry

Biofilms are defined as the bacteria living preferentially in matrix communities growing on surfaces and are often associated with a polysaccharide material known as a glycocalyx (Costerton & Wilson, 2004) (Parkar, Flint, & Brooks, 2004) (Sutherland, 2001).

Biofilms are the main contamination source in the dairy industry. The bacteria that produce biofilms and can colonize the whole plant (Brooks & Flint, 2008a). Biofilms can be found in many places and cause many problems in a dairy plant. In daily dairy processing, plants have to be shut down periodically for cleaning to remove foulant in heat exchangers, or because end products are contaminated (Bremer, Fillery, & McQuillan, 2006) (Hinton, Trinh, Brooks, & Manderson, 2002). (Parkar, Flint, & Brooks, 2004) (Tamime, 2008).

Thermophilic bacilli, *Geobacillus stearothermophilus* (10.8%) and *Anoxybacillus flavithermus* (43.4%), are the main contaminants responsible for economic loss in milk powder production all over the world (Rueckert, Ronimus, & Morgan, 2004). They usually come into the plant, mainly in their vegetative form, in a low count (10-30 cfu/ml with <10 cfu/ml spores detected) from the raw milk. During powder production, they grow and form spores in evaporation passes (thermophile count $>10^5$ cfu/ml, spore count $> 10^3$ cfu/ml) and heat exchangers (thermophile count $>10^4$ cfu/ml, spore count $> 10^2$ cfu/ml) within the 18 h production time, where temperature is in their wide growth range (Scott, Brooks, Rakonjac, Walker, & Flint, 2007). They are the crucial cause of shortening of the run length of daily manufacturing runs and downgrading or spoilage of the quality of products, because they can act as a reservoir of contamination, persisting thorough cleaning (Brooks & Flint, 2008a) (Rueckert, Ronimus, & Morgan, 2004) (Sharma & Anand, 2002). According to a Fonterra December 2006 assessment, if the run length of all Fonterra milk powder manufacturing plants can be increased by

1 h, a potential total financial benefit of \$36 million/year can be attained (Brooks & Flint, 2008b).

1.2. The Significance of this Study

Because of the significant economic loss caused by thermophilic biofilms, there is an urgent need to study these thermophilic bacteria, their growth, and biofilm behaviour in more detail. Reducing or delaying this contamination will enable an improvement in product quality and an extension of the run length for milk powder manufacturing plants.

1.3. Temperature cycling and Mathematical Modelling Concept

The literature cites many strategies for control of biofilms, have been implemented in the dairy industry, such as conventional cleaning and sanitizing regimes with caustic and acid solutions, and cleaning regimes using biological based solutions, such as enzymes and phages (Bremer, Fillery, & McQuillan, 2006) (Parkar, Flint, & Brooks, 2004).

Other than different cleaning regimes, there is a novel technology, called temperature cycling. Bacterial count in the milk product stream is proven to be proportional to the size of the surface area in contact with milk as well as the time of milk spent in the growth region of the target species (Hinton, Trinh, Brooks, & Manderson, 2002). The temperature cycling approach is designed based on this concept, involving creating an unstable environment for microbial growth by manipulating conditions, such as temperature, on a sufficiently frequent basis to disrupt biofilm growth, and yet limiting the amount of dangerous chemicals and maintaining the ability to manufacture dairy products hygienically (Brooks & Flint, 2008b) (Knight, Nicol, & McMeekin, 2004). This approach has been shown to be effective in controlling one group of bacteria, the

thermophilic streptococci (Knight, Nicol, & McMeekin, 2004). Attempts to control other groups, in particular the thermophilic bacilli, have not been successful (Aplin & Flint, 2007).

Success involves understanding the parameters for biofilm growth of the particular group of bacteria of concern, *Geobacillus stearothermophilus* and *Anoxybacillus flavithermus*. The most effective way to achieve this is through creating and using a comprehensive mathematical model that incorporates all the parameters required for growth of the group of thermophilic bacilli in dairy system. The model would then be used to generate conditions that are unsuitable for bacterial growth (Knight, Nicol, & McMeekin, 2004). Thus, the dairy industry could use this model as a decision making-aid and management tool, which can provide an instantaneous prediction of thermophile level in the product for a known level of incoming thermophilic bacteria, using microbiology techniques with short detection time, such as flow cytometry.

1.4. Aims of this Study

My research question is whether a mathematical model can represent the biofilm behaviour of targeted thermophilic bacilli in the dairy industry and whether this model can be used to optimize methods to control these bacteria and thus minimize thermophile counts in the final products. The following were the aims of this project:

- To study the planktonic and biofilm growth behaviour of the thermophilic bacilli, *Geobacillus* and *Anoxybacillus*.
- To study the effect of various factors, such as pH, temperature and water activity, on the growth of biofilms of thermophilic bacilli.
- To develop a successful control strategy based on different temperature-cycling regimes under different conditions.

- To design a comprehensive model incorporating various processes of the formation of biofilms, such as settling and sloughing, to predict the behaviour of bacteria under temperature-cycling conditions.
- To make suggestions and recommendations to the dairy industry on the control of biofilms, based on the outcome of the model.
- To suggest possible alterations to processing conditions or physical plants to extend the manufacturing run time of milk powder based on the temperature-cycling results.

2 Literature Review

2.1 Background of Biofilms

2.1.1 Definition of Biofilms

Biofilms may be defined as bacteria living preferentially in matrix communities growing on surfaces and are often associated with a polymeric material known as a glycocalyx (Costerton & Wilson, 2004) (Parkar, Flint, & Brooks, 2004) (Sutherland, 2001).

2.1.2 History of Biofilms

Biofilms became recognized in the 1980s. Biofilms first came to scientists' attention was because the concept of planktonic cells could not explain some problems and abnormalities in their experiments. (Costerton & Wilson, 2004). Microbial ecologists and engineers have started to apply biofilm concepts to resolve anomalies as well as problems in natural and industrial systems. Microbiologists and medical practitioners started to apply this new concept in medical areas such as diagnosis in chronic infections (Costerton & Wilson, 2004). Biofilms were believed to play a very important role, being the root cause of all infections associated with medical devices, and most other chronic bacterial infections (Costerton & Wilson, 2004). In the mid-1980s, these medical biofilms were found to be resistant to antibiotics, whereas environmental biofilms were found to be more resistant to biocides than the planktonic bacteria (Costerton & Wilson, 2004).

By the mid-1990s, biofilms were studied in more depth. By this time, biofilms were found to be associated with many chronic infections, such as chronic rhinosinusitis. The course and the duration of the chronic infection could be predicted and treated by appropriate therapies (Costerton & Wilson, 2004). By the end of the decade, biofilms

were found in any natural or industrial process wherever fouling or material degradation occurred. (Costerton & Wilson, 2004).

2.1.3 Nature of Biofilms

The thickness of biofilms varies from a few microns to several millimetres. Biofilms contain 90–97% water (Sutherland, 2001) (Kokare, Chakraborty, Khopade, & Mahadik, 2009). They are most commonly formed by mixed species of bacteria but, under some circumstances, such as in food manufacturing plants, they may consist of mono species of bacteria in certain parts of the process because of the selective pressures in that environment (Scott, Brooks, Rakonjac, Walker, & Flint, 2007). In mixed-species films, many other molecules accompany the bacterial cells, including a variety of extracellular polysaccharides, enzymes and other proteins, bacteriocins and low mass solutes, and also nucleic acids (Sutherland, 2001).

Mixed-species biofilms have been found to be more stable than mono-species biofilms. Biofilm formation may be enhanced by the existence of other microorganisms (Mosteller & Bishop, 1993). For example, *Campylobacter jejuni* does not grow and form a single-species biofilm readily at around 30 °C; however, it can form a mixed biofilm with enterococci at this temperature (Trachoo & Brooks, 2005). The attachment of *C. jejuni* to stainless steel increases by 1–2 log cfu/cm² because of the presence of *Enterococcus* species (Trachoo & Brooks, 2005). Another example is that the attachment and survival of *Listeria* can be enhanced by the presence of *Pseudomonas fragi* (Sasahara & Zottola, 1993).

2.1.3.1 Biofilm Formation

A biofilm is formed from planktonic bacteria in the bulk aqueous phase. Bacteria are attracted onto to the product contact surface as the bulk stream passes through the plant

(Costerton & Wilson, 2004). Attraction of bacteria is initiated by electrostatic and van der Waals' forces and may involve a pre-conditioning film (Breyers & Ratner, 2004). Some researchers have used the DLVO (Derjaguin, Landau, Verwey and Overbeek) theory to explain the driving force of this initial attachment before the secretion of Extracellular Polymeric Substances (EPS) (Hermansson, 1999) (Rijnaarts, Norde, Bouwer, Lyklema, & Zehnder, 1995). The DLVO theory explains the interaction between a charged surface and the bulk aqueous phase; it also quantitatively describes that the driving force of particles on to the surface as the combined effect of van der Waals' attraction and electrostatic force repulsion (Palmer, Flint, & Brooks, 2007).

The DLVO theory explains that the attraction or repulsion between the substratum and the bacteria is the net result of van der Waals attraction and the repulsive interaction between them (Hermansson, 1999). Both the substratum and bacteria are normally negatively charged in nature ecosystems (Hermansson, 1999) (Tang, Flint, Brooks, & Bennett, 2008). In the liquid, there is a very thin layer between the substratum and the bulk liquid, ions in which have more thermal motion, and is referred to as the diffuse electric double layer (Hermansson, 1999). The electric double layer interaction is caused by the osmotic pressure between the ions touching each other in the electric double layer, which can be approximated as the repulsive interaction in the DLVO theory. The electric double layer interaction is closely related to the surface zeta potential and the measure of the thickness of the electric double layer "the inverse of Debye length" (Hermansson, 1999). The thickness of the electric double layer then is inversely related to the ionic strength (I). So when the I value is high, the thickness of the electric double layer is thin, and there is attraction between substratum and bacteria due to the van der Waals attraction. When the I value is low, the substratum and bacteria repel each other, whereas the bacteria appear to be "reversibly attached" to the substratum when I is at medium values (Hermansson, 1999). Previous experiments also showed that decrease in the zeta potential increased bacterial attachment, since the repulsion interaction decreased and overcame by the van der Waals attraction (Tang, Flint, Brooks, & Bennett, 2008). The DLVO theory offers us some basic mechanisms of how bacteria are attracted to substratum, but there are some limitations on using the DLVO theory, such as the surface roughness (Hermansson, 1999).

After the initial attachment, attachment of bacteria to the surface becomes irreversible with the secretion of the glycocalyx (Costerton & Wilson, 2004) (Donlan & Costerton, 2002). The biofilm gradually becomes thicker and thicker in some environments and forms a mushroom-like structure (Cunningham, Lennox, & Ross, 2011). Then part of the biofilm structure is sloughed back into the bulk stream and can seed and contaminate the downstream process (Breyers & Ratner, 2004).

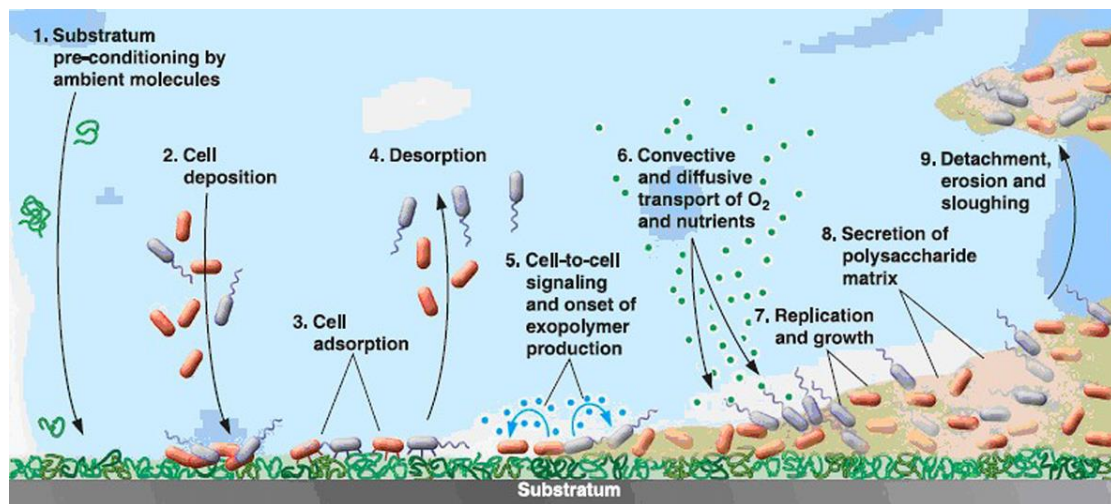


Figure 1: Processes governing biofilm formation (Breyers & Ratner, 2004).

Courtesy of the American Society for Microbiology.

2.1.3.1.1 Attachment

After the planktonic cells attach on to the product contact surface, the first stage of biofilm formation process is attachment. The attachment process can be divided into three different stages, based on their occurrence over time.

A conditioning film on the surface, formed by macromolecules from the bulk phase (such as nutrients), is often required before microbial adhesion can occur (Breyers & Ratner, 2004) (Donlan & Costerton, 2002) (Palmer, Flint, & Brooks, 2007). Adsorption events may also be dependent on the structural characteristics of the conditioning film (Kirtley & McGuire, 1989). Biofilm formation can also occur without a conditioning

film. Neither streptococci nor *Bacillus* species require a conditioning film for biofilm formation (Flint & Brooks, 2001). For some species, the emission of a large quantity of sensing molecules is crucial during the initial stage of biofilm formation (Donlan & Costerton, 2002). In contrast, it has been found that the initial bacterial attachment may be inhibited or influenced by the presence of some macromolecules. The initial attachment of biofilms of thermophilic bacilli is negatively influenced by the presence of skim milk on the stainless steel surface (Parkar, Flint, & Brooks, 2003).

After attraction, reversible attachment of the bacteria to the surface occurs by a two-step process, comprising the adhesion of cells on to the solid surface and cell-cell adhesion (Breyers & Ratner, 2004) (Jenkinson & Lappin-Scott, 2001). The reversible binding is facilitated initially by weak electrostatic and van der Waals' forces, which hold the bacterium close to the surface, according to the DLVO theory (Donlan & Costerton, 2002) (Palmer, Flint, & Brooks, 2007) (Zottola, 1994). Then stronger attachment can occur rapidly through a combination of both physical and chemical forces (Jenkinson & Lappin-Scott, 2001).

Soon after attachment to the surface, adhesion-specific genes are upregulated by the cells and ready to produce enzymes for the production of exopolysaccharide (Costerton & Wilson, 2004) (Donlan & Costerton, 2002). The new EPS material must be produced by the attached bacterial cells to secure the bacterial adhesion onto the surface as well as to neighbouring cells in the developing biofilm. (Donlan & Costerton, 2002). This process can occur very rapidly; in some species, such as thermophilic streptococci and *B. cereus*, it can be shorter than 60 s (Flint, Brooks, Bremer, Walker, & Hausman, 2002).

2.1.3.1.2 Growth of Biofilm

The microcolony is the basic structural unit of the biofilm (Costerton & Wilson, 2004). After structural analysis of a number of mono-specie *in vitro* biofilms and multi-species biofilms from nature, Breyers and Ratner's group has discovered the fact that

microcolonies are ‘communities’ of mono-specie or multi-species bacterial cells that are discretely grouped/packed by a matrix of EPS material. (Breyers & Ratner, 2004) (Costerton & Wilson, 2004). The composition of microcolony varies from 10–25% cells and 75–90% EPS matrix, owing to species variation. The EPS materials may often be found to be thicker, denser and more congregated in the area that is closer to the core of the microcolony (Breyers & Ratner, 2004). Structural analysis of microcolonies showed that bacterial cells tended to form a ‘mushroom-like’ shape within the matrix owing to the lack of Brownian motion. (Cunningham, Lennox, & Ross, 2011). There were more bacterial cells found in the ‘crown’ of the mushroom and far fewer found in the ‘stalk’. In very thick sessile communities, the geometry of the microcolonies was sometimes described as forming vertical arrays (Costerton & Wilson, 2004) (Cunningham, Lennox, & Ross, 2011). However, this mushroom-like structure is not usually seen in dairy biofilms because of the high shear, e.g. *Geobacillus* and *Anoxybacillus* biofilms are often found as even thin layers of a few cells thick (Brooks & Flint, 2008a) (Scott, Brooks, Rakonjac, Walker, & Flint, 2007).

2.1.3.1.3 Release of Bacteria from Biofilms (Biomass Transfer)

The detachment of cells from biofilm colony, either as a single cell or a group of cells, (known as sloughing-off) is a very important process of the biofilm lifecycle. The sloughed off cells may spread and form new biofilms that colonize new surfaces (Breyers & Ratner, 2004) (Costerton & Wilson, 2004) (Donlan & Costerton, 2002). Enzymes, such as dispersin B and deoxyribonuclease, have the ability to break down EPS materials in the matrix, hence may influence the detachment process. These enzymes could be utilized to enhance the detachment process, owing to their ability to break down the EPS materials. (Davies & Geesey, 1995) (Davies et al., 1998). Some researchers have found that a fatty acid messenger, cis-2-decenoic acid, could be used as an ‘anti-biofilm’ agent, since it can enhance the detachment process and inhibit microcolony formation. (Davies & Geesey, 1995).

The sloughed-off pieces of biomass from the biofilm can contaminate product downstream in a flowing system (Brooks & Flint, 2008a) (Flint & Brooks, 2001). The vegetative cells and spores from the biomass can also attach to a surface and start another cycle of biofilm formation (Hinton, Trinh, Brooks, & Manderson, 2002) (Scott, Brooks, Rakonjac, Walker, & Flint, 2007). The biomass from the dispersion also has a 'biofilm-like' behaviour because it does not have a lag phase when it reattaches on to a new surface and it grows more rapidly (Rice, Hamilton, & Camper, 2000).

2.1.3.2 Mechanism of Attachment

Long fimbriae sticking out of the cell surface and a thick EPS material coat around the cells are often associated with wild strain bacteria. (Costerton & Wilson, 2004). Those long fimbriae facilitate the specific adhesion to specific binding sites on tissue surfaces, while the EPS enables non-specific adhesion to inert surfaces (Costerton & Wilson, 2004). Researchers also found that adhesion based on interactions of proteins was not as strong as specific adhesions aided by fimbriae. (Costerton & Wilson, 2004). In order to test the functionality of those fimbriae, sonication was used to remove fimbriae from cell surfaces. Experimental results showed that the functionality of the fimbriae was to line up the bacterial cells onto the corresponding tissue-specific receptors. (Costerton & Wilson, 2004). The sites of fimbriae and specific receptor associated adhesion serve as a site for the later irreversible adhesion formed by layers of EPS. In aquatic ecosystems, the distance between EPS polymers and the surface is very small. The EPS polymers may serve as non-specific ligands for adhesion. (Costerton & Wilson, 2004).

2.1.3.3 Quorum Sensing

The discovery of communication between bacteria changed our human's perception of these microorganisms. It became clear that bacteria are not simply independently living single cells; they release signalling molecules into the environment and communicate with neighbouring cells. (Davies et al., 1998). Besides the ability to release the

signalling molecules into the neighbourhood, bacteria are also capable of quantifying the concentration of these molecules within a matrix of surrounding populations. The term 'quorum sensing' describes the aforementioned ways of bacterial communication – detecting concentration of molecules accumulated and releasing the cell's own signalling molecules into the environment. (Davies et al., 1998).

Bacterial behaviour, such as biofilm formation, is often regulated and associated with quorum sensing. Bacteria need to respond and adapt quickly to environmental changes. Adaptations may be in response to the available level of nutrients, defence against other competitors for same nutrients, and to avoid harmful substances. (Davies et al., 1998). In order to invade the host successfully, the pathogenic bacteria need to 'co-ordinate' its virulence so they can seep through the immune response during infection of a host (Cunningham, Lennox, & Ross, 2011).

Signalling molecules may not be seen during the attachment process, but are often associated with the development process during the biofilm formation. Extracellular chemicals, such as amino acids and butyrolactone/butanolide metabolites, are often utilized by Gram-positive bacteria (Kleerebezem, Quadri, Kuipers, & de Vos, 1997), whereas N-acetyl-homoserine lactones are the signalling molecules for Gram-negative bacteria (Kaiser, 1996). Signalling genes may have influence over the thickness of the film formed (Davies et al., 1998). However, the mechanism and the role of signalling molecules in the biofilm formation remain unclear. The debate over this topic has continued for years. Some researchers believe that there is no correlation between signalling molecules and biofilm production (Van Houdt, Aertsen, Jansen, Quintana, & Michiels, 2004). Others have shown that there are some cyclic growth patterns for some films. They hypothesize that quorum sensing and signalling may be involved in biofilms (Parkar, Flint, & Brooks, 2003).

2.1.3.4 Endospores

Thermophilic bacilli form endospores (Bergey's Manual Trust, 2009) (Scott, Brooks, Rakonjac, Walker, & Flint, 2007). An endospore is a dormant, tough, non-reproductive structure that is resistant to many chemical and physical conditions. Its primary function is to ensure bacterium can survive under periods of environmental stress (Flint, Palmer, Bloemen, Brooks, & Crawford, 2001). Endospores are often found to be resistant to many treatments or stress conditions, including physical treatments such as ultraviolet light, gamma radiation, desiccation, temperature, starvation and chemical and biological treatments, such as chemical disinfectants and lysozyme (Scott, Brooks, Rakonjac, Walker, & Flint, 2007). Most commonly used technologies in the dairy industry are targeted towards the inactivation of vegetative cells, but not the killing of endospores (Bremer, Fillery, & McQuillan, 2006). This is a problem for dairy manufacturing plants, because these spores can germinate and contaminate the plant after their survival through processing. These spores can be released into product, where they can germinate and cause spoilage, shortening the shelf life, reducing product quality and causing spoilage in the final product manufactured with ingredients containing spores (Brooks & Flint, 2008a) (Scott, Brooks, Rakonjac, Walker, & Flint, 2007).

2.1.3.5 Issues and Problems with Biofilms

Biofilms are a persistent problem for the dairy industry. Bacteria that produce biofilms can accumulate on food surfaces, colonize milk storage tanks, cause fouling of heat exchangers and spores may adhere to the pipe walls of manufacturing plant (Hinton, Trinh, Brooks, & Manderson, 2002). Some heat-resistant spores can survive through the pasteurization and evaporation, and can pass through to the final product. They can germinate and contaminate the product (Brooks & Flint, 2008a) (Scott, Brooks, Rakonjac, Walker, & Flint, 2007). These hazards threaten the quality of the product and sometimes the health of customers. The formation of biofilms can also cause energy loss, through reduced heat transfer, and blockages, resulting in reduced flow in

equipment (Hinton, Trinh, Brooks, & Manderson, 2002). Biofilms increase the fouling of the pipes and accelerate corrosion and material deterioration. They also cause increased resistance to cleaning procedures. As a manufacturing plant has to be shut down periodically for cleaning, the manufacturing run time is shortened. The costs of shortened run times and poor quality products are enormous, as much as NZ\$36 million/year (Brooks & Flint, 2008b).

2.1.4 Factors Influencing Biofilm Growth

2.1.4.1 pH

In South African dairy factories, researchers isolated *Bacillus* species from the alkaline wash solutions used for cleaning in place (Lindsay, Br özel, & von Holy, 2005). It was suggested that the microbial residue from washes can make contact with surfaces and act as a contamination source for the next run (Bremer, Fillery, & McQuillan, 2006) (Lindsay, Br özel, & von Holy, 2005). It was found that all isolated *Bacillus* strains grow in a pH range between 4.5 and 9.5 in buffered standard nutrient broth, and from pH 4 to pH 10 in 1% milk medium. It was found that all isolates examined attach to stainless steel at pH 4, 7 and 10 in 1% milk medium. Generally, most isolates attach better at pH 4 and 10 than at pH 7. The results also shown that all isolates exhibit low hydrophobicity at all pH values, even though attachment to stainless steel occurs at the same pH values (Lindsay, Br özel, & von Holy, 2005).

2.1.4.2 Hydrophobicity and Surface Free Energy

The attachment is influenced by the level of hydrophobicity of the surface, surface free energy as well as microbial cell hydrophobicity.

Polytetrafluoroethylene (PTFE) is highly hydrophobic and can be utilized as a ‘non-stick’ coating for food contact surfaces and is also used in some valve seats. However, there is marked attachment of *Salmonella* and *Listeria* on PTFE (Sinde & Carballo, 2000) (Teixeira, Lopes, Azeredo, Oliveira, & Vieira, 2005). After a thermodynamic analysis, Duncan-Hewitt (1990) described the hydrophobic effect as “*spontaneous, highly temperature dependent and thermodynamically favourable*”, however, the true nature of the hydrophobicity effect has proven to be debatable. Later on, Parkar, Flint, & Brooks (2003) found that there was no relationship or consistent trend between the level of bacterial attachment and surface hydrophobicity or surface zeta potentials.

Previous study also showed that attachment was favourable towards increase in hydrophobicity of the isolate in whey permeate, but the correlation between hydrophobicity of the isolate and attachment was not clear in whey or phosphate buffer solutions (Tang, Flint, Brooks, & Bennett, 2004).

The bacterial attachment onto a substratum is thermodynamically favourable if the total surface free energy of adhesion is negative (Teixeira, Lopes, Azeredo, Oliveira, & Vieira, 2005). The correlation between the surface free energy and the level of bacterial attachment is known as the “Baier’s Curve” (Baier, 1980). It shows that as the bacterial attachment is minimized when surface energy is around 25mM/m (Baier, 1980). At any other surface energy level beyond or below this level there will be an increase in bacterial attachment. In the other studies, this relationship was proven to exist using *Pseudomonas aeruginosa* strain AK1 strain in the range of 20 – 27 mM/m (Pereni, Zhao, Liu, & Abel, 2006). Later on, it was also found that minimal adhesion occurs when the van der Waals’ polar component of the surface free energy is about 25.3 mM/m (Zhao & Liu, 2006).

2.1.4.3 Temperature

Holding bacteria on a large surface area at the optimum temperature will encourage the growth of biofilms. There is minimal growth at the low and high ends of the growth temperature range. Applying temperature spikes and heat waves periodically may influence the growth by shifting the target bacteria out of the suitable growth temperature range. Knight, Nicol, & McMeekin (2004) developed a method using temperature step changes to disrupt thermophilic streptococci, whereas Fonterra developed a heat wave method for thermophilic bacilli (Aplin & Flint, 2007). Knight, Nicol, & McMeekin (2004) applied temperature step changes periodically to the heating section of the heat exchanger to control the formation of biofilms of *Streptococcus thermophilus*. Temperature changes are likely to influence biofilm development via the disruption of the logarithmic growth phase of the microorganisms or via triggering sporulation by exposing the target microorganisms under unfavourable conditions (Aplin & Flint, 2007). In addition, fouling was significantly reduced in the temperature wave trial (Aplin & Flint, 2007). A temperature wave around the optimum growth temperature has little effect on biofilm growth, although it has an effect on the sporulation of thermophilic bacilli (Aplin & Flint, 2007).

2.1.4.4 Surface

Flint (1998) described the relationship between the topography of the surface and the attachment of bacteria. Surface roughness describes and quantifies the vertical derivation of the roughness of the surface from the mean line. The most commonly used roughness amplitude parameter is the R_a , which is the arithmetic mean roughness of the absolute values (Misumi, 1994). Some studies show a strong relationship between surface roughness and adhesion (Coquet et al., 2002). However, Flint, Brooks, & Bremer (2000) showed little correlation of surface roughness with the attachment of thermo-resistant streptococci. Some studies found that bacteria prefer to adhere to stainless steel and zinc rather than to other metals or glass. More bacteria prefer to

attach to stainless steel of grade 316L than to that of grade 304L, because of its slightly greater hydrophobicity (Flint, Brooks, & Bremer, 2000).

Fouling may be a factor that influences biofilm formation. Analysis of the thermophile concentrations in bulk milk samples from a tube heat exchanger failed to differentiate between the numbers of thermophiles on the pre-fouled tubes and the numbers on the initially clean tubes (Hinton, Trinh, Brooks, & Manderson, 2002). More bacteria were found on the pre-fouled side than on the initially clean side. They also found that the rate of increase in colonies on both sides was similar, but that colonization took place 8 h later on the initially clean tubes compared with the pre-fouled tubes (Hinton, Trinh, Brooks, & Manderson, 2002). Fouling may enhance the attachment of thermophiles. Foulant protects bacteria from heating and has a higher affinity for bacterial attachment (Hinton, Trinh, Brooks, & Manderson, 2002). Foulant provides a rough surface and thus provides a larger surface area for attachment than clean stainless steel (Hinton, Trinh, Brooks, & Manderson, 2002).

2.1.4.5 Flow

Biofilms form differently under different flow conditions, such as laminar flow and turbulent flow (Stoodley, Dodds, Boyle, & Lappin-Scott, 1999). Biofilms growing in turbulent flow can be complex in structure. Structures such as cell clusters and ripples can travel along solid surfaces into downstream process. The viscoelasticity of the biofilm allows it to deform structurally when exposed to different shear stresses (Stoodley, Dodds, Boyle, & Lappin-Scott, 1999). Thick biofilms grown under laminar flow are irregular in shape and consist of clusters of cells cell separated by interstitial voids, whereas biofilms grown under turbulent flow are structurally different, being thinner and filamentous. The filaments have a complex cohesive structure, known as the “biofilm streamers”, and are formed by microcolonies of non-filamentous bacteria enclosed or tangled in filamentous sheathed bacteria (Stoodley, Dodds, Boyle, & Lappin-Scott, 1999) (Stoodley, Sauer, Davies, & Costerton, 2002). This type of

structure is unlikely to be seen in milk evaporators, in which the biofilms are normally monocultures and thin (Scott, Brooks, Rakonjac, Walker, & Flint, 2007).

2.1.4.6 Age of Biofilm

The age of the biofilm can greatly influence the success of the cleaning of the surfaces. When the film is older, it is harder to clean off the surface because more EPS is produced as well as spores are more likely to be present (Kokare, Chakraborty, Khopade, & Mahadik, 2009) (Brooks & Flint, 2008a). Older biofilms may be in the maturation and dispersion phase. Cells may be dispersed from the biofilms and may seed somewhere downstream in the process (Brooks & Flint, 2008a) (Costerton & Wilson, 2004) (Cunningham, Lennox, & Ross, 2011).

2.1.4.7 Oxygen Availability

Oxygen availability may be quite important in the growth of biofilms. Currently, there is little information in this area. During processing, milk is put through a deaeration process (Alfa Laval/Tetra Pak, 1995). The total volume of air in milk in the udder can be 4.5–6%, of which oxygen constitutes about 0.1%, nitrogen constitutes about 1% and carbon dioxide constitutes 3.5–4.9% (Alfa Laval/Tetra Pak, 1995). During handling, the air content of milk can increase to 10%. Dispersed air in the milk can cause inaccurate measurements and reduce the stability of ingredients or products (Alfa Laval/Tetra Pak, 1995).

2.1.4.8 Nutrient Availability

It is found that biofilms will grow on surfaces in very dilute nutrient solutions, which do not favour growth of planktonic cells (Stoodley, Dodds, Boyle, & Lappin-Scott,

1999). This observation supports the argument that a biofilm may serve as an adsorbent layer for the subsequent planktonic growth, gathering organic materials and nutrients from the bulk aqueous phase. Biofilms grown under high nutrient concentrations are thicker, more mushroom-like and denser than biofilms grown under low nutrient concentrations (Stoodley, Dodds, Boyle, & Lappin-Scott, 1999).

Stoodley, Dodds, Boyle, & Lappin-Scott (1999) also showed that a mature mixed-species biofilm can morphologically transform from the loose ‘ripples and streamers’ to densely packed ‘mound-like structures’ when the nutrients increase by 10-fold. These more densely packed biofilms are more sensitive to shear and can be torn off from the surface more readily and easily than the ripples and streamers formed at lower concentration (Stoodley, Dodds, Boyle, & Lappin-Scott, 1999). In contrast, Stoodley, Dodds, Boyle, & Lappin-Scott (1999) also showed that the detachment rate of an *Aeromonas hydrophila* biofilm is higher when the nutrients are limited.

2.1.4.9 Composition of Processing Fluid

Flint & Hartley (1996) found that stainless steel surface coated with skim milk proteins decreases the biofilm attachment of vegetative cells as well as spores. Milk of different composition results in different fouling of the surface; for example, aggregated proteins can cause more fouling (Toyoda, Schreier, & Fryer, 1994). Jeurnink & de Kruif (1995) found that varying the calcium content of milk compared with normal milk results in a decrease in heat stability of the milk and induces more fouling. The fat present in the milk did not affect the level of fouling (Foster, Britten, & Green, 1989) (Visser & Jeurnink, 1997). However, it is found that reducing pH can result an increase of fat content in the deposits (Lewis & Heppell, 2000).

Klausen et al. (2003) showed that different carbon sources from nutrients can affect the structure of *Pseudomonas aeruginosa* PAO1 biofilms. Biofilms grown under glucose

conditions show the typical “mushroom-like” structure separated by water channels, whereas biofilms grown under citrate conditions are flat, are homogeneous and lack evidence of water channels (Klausen et al., 2003).

2.1.5 Measurement of Biofilm Growth

2.1.5.1 Traditional Plating Techniques

Before the invention of modern microscopy and impedance methods, plating methods were always used to enumerate bacteria. There are two common methods: the spread plate method and the drop plate method (Miles–Misra method) (Herigstad, Hamilton, & Heersink, 2001).

In the traditional spread plate method, 0.1 ml of an aqueous sample is inoculated onto an agar plate. The liquid sample is then spread evenly onto the agar with a flame-sterilized glass rod, fixing the cells on the surface of the agar (Herigstad, Hamilton, & Heersink, 2001). The colony-forming units (cfus) are counted after an appropriate incubation period, the duration and temperature varies for different bacteria. For the drop plate method, the sample volume is dispensed on the different sectors of the agar plate as a fixed number of small individual drops (Herigstad, Hamilton, & Heersink, 2001). After incubation of the plates, the colonies within the drops (with the highest number of full-sized discrete colonies – usually sectors containing 2–20 colonies – are counted) are counted using either the naked eye or a plate reader and the counts are scaled up using the following equation to calculate the total number of cfus in the initial volume.

$$CFU/ml = \text{Average number of colonies for a dilution} \times 50 \\ \times \text{dilution factor}$$

Because each drop is counted separately, the drop plate method is not recommended for organisms that are highly motile (Herigstad, Hamilton, & Heersink, 2001). Some researchers have developed a method to standardize the drop method, which has a better design than random plating (Herigstad, Hamilton, & Heersink, 2001). The drop plate method shows many positive characteristics, such as the plating and counting procedures are less labour intensive and less time consuming compared with the traditional plate method. The plating and counting steps are convenient in routine work and require less materials to gain the same information (Herigstad, Hamilton, & Heersink, 2001). The drops take less time to absorb and dry fully compared with a whole spread plate.

2.1.5.2 Epifluorescence Microscopy and Staining

Epifluorescence microscopy is a standard method for observing biofilms on solid surfaces (Lichtman & Conchello, 2005). Normal transmission microscopy is unsuitable when a solid surface is being examined. Specific stains can be used to highlight cell viability, or to identify different cell types in the biofilm. Acridine orange and DAPI (4,6-diamidino-2-phenylindole) are commonly used for biofilm work to stain the DNA (Schaule, Griebel, & Flemming, 2000). Acridine orange targets genetic material in the microorganisms and can discriminate between deoxyribonucleic acid (DNA) and ribonucleic acid (RNA) (The Gale Group Inc., 2003).

Both living and dead bacteria and other microorganisms contain nucleic acid to which Acridine orange can bind. Therefore, the dye is not able to tell the difference between living microbes from dead microbes, although a green fluorescing cell has little RNA and is therefore not actively metabolizing (John Brooks, personal communication, 2009). However, Acridine orange has proven to be a useful tool for counting the total number of microbes in a sample, such as in a biofilm (The Gale Group Inc., 2003).

2.1.5.3 Confocal Microscopy

Confocal scanning laser microscopy (CSLM) has been used for biofilm studies in recent years. This has overcome difficulties in obtaining clear photomicrographs of aggregated bacteria clusters under hydrated conditions (Silyn-Roberts & Lewis, 1997). CSLM allows visualization and documentation of the cell morphology and physiology in three dimensions *in situ* (Silyn-Roberts & Lewis, 1997).

The confocal laser microscope has several advantages. It has much higher resolution than epifluorescence microscopes. It gives a real time *in situ* picture of the situation, rather than an *in vitro* picture. It also provides a detailed three-dimensional reconstruction of the cells rather than the original two-dimensional image from an ordinary microscope (Silyn-Roberts & Lewis, 1997). Unfortunately, it is not widely used in many laboratories because of its high costs – a research-grade cryostat (\$20,000) and a high quality epifluorescence microscope (\$25,000) cost far less than a confocal microscope (up to \$700,000) (Silyn-Roberts & Lewis, 1997).

2.1.5.4 Impedance

Impedance is a very fast microbiological tool used to enumerate bacteria in a suspension, as well as detecting biofilm (Flint & Brooks, 2001) (Silley & Forsythe, 1996). Impedance is defined as resistance to alternating current flow (Silley & Forsythe, 1996). An appropriate medium must be selected for the detection of different species of microorganisms. Then the impedance method can be developed and used for biofilm related experiments, such as evaluating different disinfectants for control of biofilms (Mosteller & Bishop, 1993). Impedance can be used to enumerate *Geobacillus stearothermophilus* bacteria in a very short detection period (< 8 h for estimates of 100 vegetative cells or more) and gives reproducible estimates (Flint & Brooks, 2001). The impedance method can also be developed to estimate levels of thermophilic bacilli in

foods, such as milk, and to enumerate growth on stainless steel coupons, and has enabled further studies on attachment and development (Flint & Brooks, 2001).

One device that is used in impedance microbiology is the BacTrac (BacTrac 4300, Sy-Lab, Neupurkersdorf, Vienna, Austria) (Sy-Lab, 2009). Two impedance measurements (known as detection times) are taken at each sampling interval per sample, the M-value (media) and the E-value (electrode). These series of detection times can be used individually or in combination to calculate the growth of the bacteria in the sample (Centers for Disease Control and Prevention, 2009). The measurement principle is to monitor the change in impedance related to bacterial growth in the medium over time and to determine the 'impedance detection time', which is related to the initial concentration of bacteria in the measurement cell.

2.2 Laboratory Systems for Biofilm Study

2.2.1 The Robbins Device

Many systems have been developed to study the growth of biofilms of microorganisms. The Robbins device is the most widely used and well-known system. It was first developed and later modified by McCoy, Bryers, Robbins, & Costerton (1981) in 1981 and is called the modified Robbins device (Kharazmi, Giwercman, & Højby, 1999). It is essentially a length of pipe that can be fitted into a process pipeline and provides a means of sampling the wall of the pipe for biofilm growth.

There are many types of modified Robbins device for different applications, such as different flow or pressure conditions. One commercially available unit consists of number of ports (12 or 25) arranged along a rectangular cross-sectioned pipe. It can be made from stainless steel or polymer (vinyl chloride) (PVC). Each port is made up of a press-fit plug and a sample coupon (surface area of 50 mm²) (Tyler Research, 2009).

Coupons can be made of different materials, such as stainless steel and polycarbonates. When the plug is pressed in, the surface of the coupon becomes part of the channel wall. The bacteria enter the system via the flow stream and form biofilm on the channel wall and the coupons. Then the coupons can be removed and analysed individually at any time with minimal disruption to the experiment (Tyler Research, 2009). It was also used to monitor an industrial heat exchanger in a previous study (Scott, Brooks, Rakonjac, Walker, & Flint, 2007).

2.2.2 Continuous Tube Reactor

A continuous tube reactor is described by Flint, Palmer, Bloemen, Brooks, & Crawford (2001). A series of inoculated stainless steel coupons is inserted into silicone tubing of 9 mm diameter. Fresh milk is added to and removed from the reactor at a rate determined by the doubling time of the bacteria. The dilution rate should be greater than the bacterial growth rate to avoid planktonic growth of bacteria in the milk. Samples can be taken by excising a piece of silicone tubing containing the coupon, which is then removed from the tube aseptically (Flint, Palmer, Bloemen, Brooks, & Crawford, 2001).

The concept can be adapted by connecting a few reactors in series, using rubber tubing. This whole chain of reactors is placed in a water bath set at the desired temperature. A reactor can be disconnected for sampling without contaminating others by simply aseptically disconnecting one part of the rubber tubing. The disadvantage of this method is that growth is tested at one temperature only, rather than by exposure to temperature waves or spikes (Flint, Palmer, Bloemen, Brooks, & Crawford, 2001).

2.2.3 CDC Reactor

The CDC reactor is designed for growing laboratory biofilms under high shear conditions. It is suitable for modelling many different environments (Centers for

Disease Control and Prevention, 2009). It has a 1 L vessel with an effluent spout at approximately 400 ml, an impeller for continuous mixing and eight independent rods, each of which holds three removable coupons for growing biofilms. The removable rods allow for intermittent removal to monitor the development of biofilms over time (Centers for Disease Control and Prevention, 2009).

For establishing biofilms on the coupons, the dilution rate is set higher than the planktonic growth rate of the bacteria. Samples from set intervals can be taken out by removing coupons aseptically. The continuous flow and agitation simulate conditions in a manufacturing plant.

2.2.4 Plate Reactor

An hexagonal plate reactor (picture in Appendix 1) was developed at Fonterra for temperature-spiking experiments (Aplin & Flint, 2007). The hexagonal stainless steel chamber has two stainless steel tubes on either side, allowing milk to be fed into and out of the reactor. Silicone tubing connected to the stainless steel tubes allows the reactor to be connected to a continuous flow of medium (Aplin & Flint, 2007). Milk is pumped through the silicone tubing into a stainless steel preheating tube in a water bath. From there, the liquid passes through the reactor before discharging to waste. The reactor is placed on the heating block of a modified PCR (polymerase chain reaction) thermal cycler to generate temperature spikes for experiments. Temperature spiking can be achieved by programming the thermal cycler and running it in continuous mode (Aplin & Flint, 2007). Thermocouples are inserted into inlets and outlets of the reactor and cycler to monitor the temperature profile. At the end of the experiment, the top plate of the reactor can be opened and the inner surfaces of the reactor are sampled or stained to visualize the biofilms on the stainless steel (Aplin & Flint, 2007).

This reactor was designed to simulate the stainless steel surfaces of a plate heat exchanger that could be exposed to different temperatures, as described by Knight, Nicol, & McMeekin (2004).

2.3 Control of Biofilm

Traditionally and most of the time, in manufacturing plants, biofilms on surfaces are removed and controlled by cleaning and sanitizing using different agents (Bremer, Fillery, & McQuillan, 2006) (Parkar, Flint, & Brooks, 2004). Spores and single cells may still remain on the rough areas of the surface after the cleaning-in-place process and act as seed recontaminating the plant post cleaning (Bremer, Fillery, & McQuillan, 2006) (Flint, 1998).

Modern engineering technologies offer an alternative for controlling biofilms, called surface treatment. Surface treatment of the contact surfaces provides the possibility to prevent and hence control the bacterial attachment in the first place (Brooks & Flint, 2008a).

2.3.1 Cleaning-in-Place

Cleaning of processing or manufacturing equipment in various industries can be completed without the need of dismantling. This concept is known as Cleaning-in-place (CIP) (Tamime, 2008). Until the 1950s, closed manufacturing systems were disassembled with manual cleaning (Tamime, 2008). The establishment of CIP provides possibilities for industries to clean their manufacturing systems frequently with minimum disruption to production. Industries such as dairy, beverage, brewing, processed foods, pharmaceutical and cosmetics industries, benefit from CIP most (Tamime, 2008). The CIP has a lot of advantages compared with traditional manual cleaning methods, including less time consuming, less labour intensive and can be done

more frequently, less chemical exposure risk to people and less disruption to production (Tamime, 2008).

2.3.2 Effect of Different Cleaning Regimes

2.3.2.1 Caustic and Acid

Standard caustic (2%, 75 °C, 30 min) and nitric acid (1.8%, 75 °C, 30 min) treatment at Reynolds numbers greater than 2000 is currently used in dairy plants. It dissolves cells and milk residues and removes calcium deposits (Parker, Flint, & Brooks, 2004). Under ideal conditions, this method is the most effective of all the caustic and acid treatments that are used to treat biofilms. The removal of cells and the polysaccharide matrix from the stainless steel surface by this method is radical (Parker, Flint, & Brooks, 2004). Full strength caustic (2% NaOH) at both 50 and 60 °C and half strength caustic (1% NaOH) at 60 °C can produce a 6–7 log₁₀ cells/cm² reduction in viability but only a 2 log₁₀ cells/cm² reduction in total cells of the thermophilic bacilli detected by epifluorescence microscopy (Parker, Flint, & Brooks, 2004). Alternative caustic chemicals are no better than the standard sodium hydroxide (Bremer, Fillery, & McQuillan, 2006). Lower concentrations of sodium hydroxide can cause a large variation in the effectiveness of the cleaning of dairy biofilms (Bremer, Fillery, & McQuillan, 2006). Lower temperatures can also leave residues of bacterial cells on the surface, which provide a base for further biofilm development (Marshall, 1994) (Parker, Flint, & Brooks, 2004).

2.3.2.2 Sanitizers and Surfactant

Cleaning and sanitation are traditionally regarded as being separate and distinct steps in a good cleaning programme. The incorporation of a sanitizing step, designed to kill any cells remaining after cleaning, does not always show any further reduction in viable

cells following the current standard caustic and acid cleaning (Bremer, Fillery, & McQuillan, 2006).

Eliminator (Orica Chemnet, New Zealand), a caustic additive that contains chelating and sequestering agents and surface-active wetting agents, reduces the number of cells remaining on stainless steel compared with the standard method (Bremer, Fillery, & McQuillan, 2006). Eliminator acts as a surfactant and sequestering agent, which helps to remove fat and protein as well as to minimize the effects of hard water (Bremer, Fillery, & McQuillan, 2006) (Parkar, Flint, & Brooks, 2004).

2.3.2.3 Biological Enzyme-based Cleaners

Enzyme cleaners are an alternative, environmentally friendly group of cleaning agents. Basically, two types of product are available: protease cleaners, attacking protein and polysaccharidase-based cleaners, consisting of a combination of enzymes such as amylase and cell wall peptidoglycan hydrolase, targeting the polysaccharide matrix (Parkar, Flint, & Brooks, 2004).

Enzymes do not achieve 100% killing of the biofilm and leave visible residual polysaccharide when used to treat biofilms of thermophilic bacilli. However, the viability and the total counts decrease by $3.6\text{--}6.6 \log_{10} \text{ cells/cm}^2$ and $4\text{--}5 \log_{10} \text{ cells/cm}^2$ respectively (Bremer, Fillery, & McQuillan, 2006) (Parkar, Flint, & Brooks, 2004).

2.3.2.4 Chemical Cleaners

Oxidizing chemicals are general pro-oxidants, which can generate reactive oxygen and/or chlorine. The main mechanism of activity is the initiation of oxidative attack on the bacterial -SH group-containing components, such as enzymes, together with peroxidative attack targeting unsaturated fatty acids in the cell membrane (Bremer,

Fillery, & McQuillan, 2006) (Parkar, Flint, & Brooks, 2004). Quaternary ammonium compounds have three actions: the breaking down of cell membranes, intracellular potassium efflux and followed with cellular protein/nucleic acid damage (Bremer, Fillery, & McQuillan, 2006).

Most oxidizing chemicals, when tested using the recommended strength at ambient temperature for 5 min, are very effective against biofilms with a loss of viability and removal ranging from 5.5 to 7.0 \log_{10} cells/cm² and from 1 to 2 \log_{10} cells/cm² respectively. Quaternary ammonium, using the recommended strength at ambient temperature for 30 min, has been shown to produce a reduction in viability and total cells of 7 \log_{10} cells/cm² and 2 \log_{10} cells/cm² respectively (Bremer, Fillery, & McQuillan, 2006) (Brooks & Flint, 2008a) (Parkar, Flint, & Brooks, 2004).

2.4 Active Surface Technology

Stainless steel is extensively used in food processing industries owing to its ideal heat transfer efficiency, cleanability, strength and corrosion resistance (Brooks & Flint, 2008a). Active surface technology was developed to inhibit or decrease bacterial attachment and biofilm formation. The following possible strategies are available for surface modifications (Muller-Steinhagen & Zhao, 1997) (Zhao, 2004) (Zhao & Liu, 2006) (Zhao, Liu, & Wang, 2005) (Zhao, Liu, Wang, Wang, & Muller-Steinhagen, 2005).

- Implantation of ions to lower the surface energy.
- Generation of diamond-like carbon surfaces.
- Formation of silica surfaces to produce either a hard glass-like surface or a hydrophilic anionic surface.
- Incorporation of PTFE into the surface.
- Coating with a molecular brush.
- Generation of bioactive surfaces.
- Coating with antimicrobial chemicals.

2.4.1 Implant Surface with Metal Ions

SiF_3^+ ions can be used in surface implantation to reduce the surface free energy of stainless steel, thereby reducing attachment (Muller-Steinhagen & Zhao, 1997). Antimicrobial coatings of electroless Ni–P–PTFE on stainless steel can reduce bacterial attachment by 82–97% (Zhao & Liu, 2006). Electroless Ag–PTFE has a similar antimicrobial effect (Zhao, 2004). Zhao, Liu, & Wang (2005) have demonstrated that an Ag–PTFE ion coating is able to reduce the attachment of *Escherichia coli* by 94–98% compared with other surfaces such as silver-coated stainless steel and titanium surfaces. They have also shown that the Ag–PTFE coating can be applied to environments containing salt.

2.4.2 Implant Surface with Organic Material

Passive coating of surfaces with organic polymers containing microbial inhibitors is a novel approach to controlling biofilms, but may not be acceptable for the food industry (Brooks & Flint, 2008a). An example of this type of control is the development of an ethylene vinyl acetate polymer together with a low solubility commercial quaternary amine complex, which reduces the viability and adherence of some microbes more than surfaces coated with a control polymer without the quaternary amine complex (Price, Sawant, & Ahearn, 1991). It slows the bacterial growth and preserves the plastic materials from microorganisms that metabolize and attack plastics.

Coating surfaces to control biofilms has been used in a wide range of areas, including the shipping and oil industries, but has only recently been tested in the food manufacturing industry. Health concerns with many of these coatings have been raised, with leaching into food, microbial degradation and heat/cool breakdown of the compounds being unacceptable in food applications. There are also concerns with coating breakdowns in other industries, such as coatings on shipping hulls made from

toxic materials, which can cause serious environmental problems. If scientists could overcome these problems, this approach would be beneficial for the future control of biofilms (Brooks & Flint, 2008a).

2.5 Disruption Technology

The concept of disruption technology is to minimize the area of the surface that is held at the optimum biofilm growth conditions as well as to ensure the transit of product fluid through the growth temperature bands as quickly as possible (Brooks & Flint, 2008a). This is a very cutting-edge approach to biofilm control and disruption that relies on changing environmental parameters such as pH, temperature and water activity while maintaining the product quality and lowering chemical use (Brooks & Flint, 2008b) (Knight, Nicol, & McMeekin, 2004). Creating unstable or unfavourable conditions periodically during the exponential growth phase of the targeted control bacteria can reduce bacterial growth dramatically (Brooks & Meers, 1973) (Knight, Nicol, & McMeekin, 2004).

2.5.1 pH

pH is crucial for microbial growth and in dairy processing (Alfa Laval/Tetra Pak, 1995). Most bacteria have an optimal pH for growth of around 7.0. Cow's milk has a pH around 6.5–6.7. The isoelectric point of casein, which is the main protein of milk, is around 4.6. Thus, milk sours and curdles when the pH falls below 4.6 (Alfa Laval/Tetra Pak, 1995). The pH in dairy manufacture cannot be altered for many processes, except for the manufacture of acid casein and cheese or other fermented dairy products. Altering the pH will change the appearance, functional properties and taste of milk (Alfa Laval/Tetra Pak, 1995)

2.5.2 Water Activity

Bacteria are generally unable to grow when the water activity drops below 0.9. Milk has a moisture content of 87% prior to processing (Alfa Laval/Tetra Pak, 1995). Milk products for making milk powder are usually concentrated from an initial solids content of 9–13% to a final concentration of 40–50% total solids during evaporation process before being pumped to the drier (Alfa Laval/Tetra Pak, 1995). The products to be evaporated, such as milk, are usually heat sensitive and can be significantly damaged / destroyed by overheating. To reduce this heat impact, the evaporation process is normally conducted under partial vacuum, allowing temperatures to be reduced down to 40 °C at some points (Scott, Brooks, Rakonjac, Walker, & Flint, 2007). In addition, the evaporator is designed to have as short a residence time as possible. There are opportunities for bacterial colonization and germination in the stainless steel tubes of the evaporator effects and on distribution plates and other zones of the evaporator at which the water activity and the temperature are within the growth range for bacteria (Scott, Brooks, Rakonjac, Walker, & Flint, 2007). The water activity does change during evaporation, so that microbial growth is unlikely to occur in the later stages (Scott, Brooks, Rakonjac, Walker, & Flint, 2007). Using variations in water activity as a disruptive technology would be difficult to manipulate but some advantage of the natural change in water activity during evaporation may be used to control growth. For example, using temperatures outside the growth range for most bacteria in the early stages of evaporation could control bacteria at this stage, with lower temperatures being used in the later stages of evaporation. This is generally what is done in a falling film evaporator anyway, except that the temperatures in the early stages of evaporation are generally within the growth range that is suitable for thermophilic-spore-forming bacilli (Scott, Brooks, Rakonjac, Walker, & Flint, 2007).

2.5.3 Temperature

Heat treatment, such as pasteurization, is an important part of dairy manufacture to ensure the microbiological safety of dairy products. Severe heat treatments, such as

UHT treatment, have adverse effects on the appearance, taste and nutritional properties of milk. Intense heating will create a cooked and then burnt flavour in the end product and will accelerate the denaturation of the milk proteins, causing fouling on surfaces and impairing cheesemaking (Alfa Laval/Tetra Pak, 1995). The choice of the time/temperature combinations for heat treatment is therefore important to minimize damage and yet to ensure safety.

Altering the temperature in specific zones of a manufacturing plant (e.g. plate heat exchangers) within defined limits at frequent time periods will ensure the safe treatment of milk, prevent damage to the milk and potentially control biofilm growth. This concept was first developed by Knight, Nicol, & McMeekin (2004) using temperature spikes to control the growth of *Streptococcus thermophilus*. This enabled disruption of the growth of the biofilm, which enabled longer pasteurizer runs in the cheesemaking industry. The spike consisted of a temperature step change programme introduced to the regeneration section of a plate heat exchanger, involving an increase in temperature at the inlet of the cold end of the regeneration section (outlet from the first heating section) from its normal operating temperature to 55 °C for 10 min with an interval of 1 h between spikes. This programme extended the production cycle to 16 h, an extension of 6 h (Knight, Nicol, & McMeekin, 2004). However, the economic balance between the cost of plant modification and increased energy consumption needs to be justified and balanced with the economic benefits gained from the extended run time and less cleaning/shut-down time. If a manufacturing plant has excess capacity in the availability of plate heat exchangers, calculations show that the advantages of extending run times do not balance with the increased costs involved with adapting to temperature cycling regimes (Brooks & Flint, 2008a).

Aplin & Flint (2007) investigated the use of a temperature wave programme consisting of sine wave temperature cycling in laboratory-scale reactors for the control of the thermophilic bacilli in plate heat exchangers. A heat wave of 30–50 °C over a 20 min cycle is effective in controlling the growth of thermophilic bacteria in a laboratory system for up to 14 h. A heat wave of 45–58 °C over a 20 min cycle does not produce the same effect, showing the importance of setting the correct parameters (Aplin & Flint,

2007). However, this work demonstrated the potential of disruptive technology in the form of a cyclical heat wave to control the growth of biofilms of thermophilic bacilli.

2.6 Introduction to Thermophilic Bacilli in the Dairy Industry

Thermophilic bacilli are commonly found in the milk powder manufacturing process, with high numbers of *Geobacillus* spp. and *Anoxybacillus* spp. spores often being found in the end products (Scott, Brooks, Rakonjac, Walker, & Flint, 2007) (Seale, Flint, McQuillan, & Bremer, 2008). Studies showed that several strains of *Geobacillus stearothermophilus*, *Anoxybacillus flavithermus* and *Bacillus licheniformis* are the dominating contaminants (91.9% amongst all screened samples) contaminants found in milk powder samples all over the world (Rueckert, Ronimus, & Morgan, 2004) as well as in the New Zealand dairy manufacturing plants (Ronimus et al. 2003).

These spores usually exist in low numbers in the ingredient raw milk. The source of these spores in product may be silage on the farm or thermophilic bacteria growing on the surfaces of the heat exchangers and evaporators (Seale, Flint, McQuillan, & Bremer, 2008). Heat-resistant spores can survive through pasteurization and germinate when the growth conditions permit (Scott, Brooks, Rakonjac, Walker, & Flint, 2007) (Seale, Flint, McQuillan, & Bremer, 2008). These bacteria form biofilms on the stainless steel surfaces of pipes and equipment or seal materials. They may slough off and contaminate the bulk flow. Spores can be found at levels as high as 10^5 /g of milk powder. This results in a reduction in the value of the product in the market (Seale, Flint, McQuillan, & Bremer, 2008). These spores not only cause direct economic loss to the manufacturer but also cause indirect economic loss because of the frequent cleaning required (Brooks & Flint, 2008a) (Scott, Brooks, Rakonjac, Walker, & Flint, 2007).

2.6.1 Description of *Bacillus licheniformis*

This group of bacteria was first reported as ‘feather-degrading bacteria’ (Williams, Richter, Mackenzie, & Shih, 1990). *B. licheniformis* is described as a Gram-positive, motile, spore-forming, facultatively anaerobic rod. The optimal growth temperature for *B. licheniformis* is 50 °C, but its vegetative cells have the ability to tolerate much higher temperatures (Bergey's Manual Trust, 2009). Dairy products tend to have a higher chance of being contaminated with toxin-producing isolates of *B. licheniformis* (Williams, Richter, Mackenzie, & Shih, 1990). *B. licheniformis* strain F does not show a regional pattern, suggesting that it originates from soil, having been commonly found in milk powder samples (37.7% of 742 isolates) all over the world (Rueckert, Ronimus, & Morgan, 2004).

2.6.2 Description of *Anoxybacillus*

Anoxybacillus are aerobic, facultatively aerobic or facultatively anaerobic, alkaliphilic, moderately thermophilic, straight or slightly curved short rods (Bergey's Manual Trust, 2009). The cells are Gram-positive, motile or non-motile, and catalase variable. They are spore formers with no more than one various shaped terminal endospore. The growth temperature of different species varies between 30 and 70 °C, with the optimum temperature around 50 to 62 °C. The pH range for growth is between 4.5 and 11, with the optimum around 6.0 to 8.5 (Bergey's Manual Trust, 2009). This group of bacteria may utilize fermentation pathways when they cannot utilize oxygen and nitrate as electron acceptors (Bergey's Manual Trust, 2009). *Anoxybacillus flavithermus* strain C has been identified as the most common contaminant (43.2% of all contaminants) in the milk powder around world, especially as the dominant strain when the total thermophile count of the milk powder exceeds 500 cfu/g (Rueckert, Ronimus, & Morgan, 2004).

The targeted species for the dairy industry is *Anoxybacillus flavithermus*. The cells are Gram-positive, straight, motile rods with a terminal endospore. Colonies are round, smooth and yellow pigmented. The bacterium is facultatively anaerobic, catalase positive and oxidase positive (Bergey's Manual Trust, 2009). It does not hydrolyse starch but does hydrolyse gelatine. It grows in 2.5% NaCl broth, but not in 3% NaCl. The pH range for growth is around 6–9. The growth temperature is between 30 and 72 °C, with optimum temperatures at 60 °C (aerobic) and 65 °C (anaerobic) (Bergey's Manual Trust, 2009) (Pikuta et al., 2000).

2.6.3 Description of *Geobacillus*

This group of bacteria are rod-shaped motile cells either singly or in short chains. The bacteria are mainly Gram-positive with possibility of varied Gram reaction (Bergey's Manual Trust, 2009). They are aerobic or facultatively anaerobic spore formers, producing one ellipsoidal or cylindrical endospore per cell terminally or sub-terminally. *Geobacillus* can grow at any temperature between 37 and 75 °C, with the optimum temperature between 55 and 65 °C. *Geobacillus* can survive when the pH is around 6–8.5, with an optimum at pH 6.2–7.5. Most species within this genus are catalase-positive and do not produce acid from lactose (Nazina et al., 2001).

The main targeted species for the dairy industry is *Geobacillus stearothermophilus* (Scott, Brooks, Rakonjac, Walker, & Flint, 2007). Previous study showed that *Geobacillus stearothermophilus* strain A is the third commonly found contaminant (10.8% amongst all the isolates), responsible contamination of nearly 50% of the milk power samples from all over the world (Rueckert, Ronimus, & Morgan, 2004).

2.7 Mathematical Modelling

2.7.1 Introduction to Biofilm Modelling

A biofilm is a system consisting of four compartments: a bulk liquid, the boundary layer of the liquid on the contact surface, the biofilm itself and the substratum (Wanner et al., 2006). A mathematical model is defined as a systematic and logical way to simulate or translate a real-world system into mathematical terms. The aim of modelling biofilms is to gain some understanding of biofilm behaviour, to enhance the growth of ‘good’ biofilms and to eliminate ‘bad’ biofilms in various industries (Wanner et al., 2006). Another objective is to provide industry with a tool to predict the development of biofilms in real time during a production run.

2.7.2 Model Selection

Except where specifically indicated, the material in this section is extracted, summarised and reproduced from (Wanner et al., 2006).

According to the International Water Association (IWA) task group, there are six steps in designing and using a mathematical model for biofilms.

- Identify important processes and variables existing in the system.
- Express these identified processes in mathematical terms.
- Implement Mass, energy or momentum balances to combine the mathematical expressions together.
- Assign appropriate values (such as values according to literature or experiments) to the mathematical terms in the modelled equations.
- Solve the mathematical equations by suitable techniques (this may require only normal analytical techniques, or may involve numerical solutions techniques for more complicated equations).
- The output of the model solution can be represented by the model variables. For example, the model may describe the growth rate of the bacteria at different depths in the biofilm over time.

The first step in the selection of the model is to identify important processes and variables existing in the system being modelled.

Different sections of the biofilm system are defined as ‘compartments’. There are four compartments in a typical biofilm system: the bulk liquid flowing past the biofilm, boundary liquid layer formed between bulk and biofilm (a very thin liquid layer – particles within have less momentum due to the reduced flow), the biofilm itself and the substratum underneath the biofilm. There are several components within each compartment, such as biomass, substrates, products and any other material that is important to the model. The components undergo transformation, transport and transfer processes. The components and processes are linked with mathematical equations.

After identifying variables and processes, the appropriate mass balance needs to be determined, together with expressions for each variable within. There are two types of parameter: system specific and universal. System-specific parameters are dependent on the targeted biofilm system and may vary when the system varies, such as biofilm thickness and density. Universal parameters are obtained from the literature or from other experiments that are independently conducted on the biofilm being modelled. Universal parameters, such as kinetic parameters for microbial reactions, do not change with the system.

2.7.3 Different Models

The conservation of mass is one of the most important principles of any quantitative systems. The mass balance can be expressed as (reproduced from Wanner et al., 2006):

$$\begin{aligned}
 & \textit{Net rate of Accumulation of mass of component in the system} \\
 & = \textit{Net rate of mass influx of component transported into the system} \\
 & + \textit{Net rate of generation of the component in the system}
 \end{aligned}$$

Most of the following models are derived from the principal mass balance. The differences between these models are more or less assumptions, computations and flexibility.

2.7.3.1 Analytical Models

Analytical models are widely used for modelling of general biofilm systems, since it does not require high level of mathematics knowledge and can be solved using mathematical derivation, omitting the need of numerical techniques. The advantage of the analytical model is that it is in a less complex mathematical format. Also, each of the terms and their effects can be analysed directly and separately. The disadvantage is that systems having multiple components and complex geometry cannot be studied using this model. The analytical model can be used for a simple biofilm system with simple conditions, for example a biofilm that is homogeneous and having only one rate-limiting substrate.

The analytical model is often applied to biofilm systems having one dominant process, such as nitrification. However, it can also be applied to multi-species and multi-substrate systems when sufficient information on biofilm composition is known. The most important obstacle of the analytical model is the Monod relationship, which is defining in which rate substrates utilized or synthesized. The problem is simplified by making assumptions using the half-saturation concentration of the limiting substrate as the cut-off point. An assumption of zero-order kinetics is used where the concentration of the bulk is higher than half saturation, whereas first-order kinetics are used for lower than the half-saturation concentration.

2.7.3.2 Pseudo-analytical Models

A pseudo-analytical model is a simplified alternative to an analytical model. Assumptions need to be made to simplify the conditions to maintain robustness and predictive power of the model. A simplified form of pseudo-analytical model can be designed only for a highly specific system with a lot of known parameters, such as known biofilm thickness, whether the system is single-substrate limited or known kinetics, and whether it is under first-order or zero-order. This model is simpler than an analytical model, so the algebraic equations within it are solvable by hand or using simple computer-aid skills such as spreadsheets. An example for a pseudo-analytical model is a model of mass balance designed for a reactor system using the concentration of the bulk as input and concentration in the outflow as output variable based on the conservation of mass principle (Rittmann & S  ez, 2004).

The basic pseudo-analytical model applies only to a highly specific system such as a steady-state biofilm with one microbial species and one rate-limiting substrate (Rittmann, Pettis, Reeves, & Stahl, 1999). However, it can be adapted to fit a multi-species environment, which makes the multi-species system model more accessible to non-specialist modellers. It illustrates the important interactions between different materials or biomasses in a multi-species biofilm system, such as the *Geobacillus/Anoxybacillus* biofilms in the dairy industry.

2.7.3.3 Numerical One-dimensional Dynamic Models

A dynamic model is often used if the prediction is about how a biofilm forms and develops within the system along time in one dimension. This model is normally applied to more complex systems, such as a multi-species biofilm in a multi-substrate environment. It is more complex than the basic and pseudo-analytical models, but is less complicated than multi-dimensional models. This model is often used to study the biofilm formation process with time, microbial composition of the system and the

impact of the detachment process on biofilm. A computerized simulation, AQUASIM, has been developed. This program can achieve fast calculation on the simulation using one-dimensional dynamic models while allowing some flexibility to the model in various aspects (Reichert & Wanner, 1997), such as whether there are some dissolved or particulate components in the system, and the order of kinetics.

One of the advantages of the one-dimensional dynamic model is that it allows modellers to calculate the values of different types of particulate variables (i.e. dissolved or attached) differently using various methods. Another advantage of the model is that the outputs of the model can be a wide range of estimations of different particulate components, including spatial information on different particulate components within the system. There are many steady-state processes that can be considered using this model, including transformation processes (i.e. in biochemical reactions, one substance may be consumed then transformed into another), and attachment and detachment of cells to estimate biofilm thickness (Picioreanu, Van Loosdrecht, & Heijnen, 2000a).

Wanner et al., (2006, page 92), it is stated that *“The limitations of this model are that all gradients of variables and parameters in the biofilm are expressed only in the direction perpendicular to the substratum and that all quantities represent averages over planes parallel to the substratum.”* Therefore the dimension properties of the substratum in relation to the dimension properties of the biofilm must be considered, and whether local prediction still holds true when applied to the whole dimension. Another limitation is that this model considers the bulk liquid as a fully mixed homogenous environment without any clusters of microbes, sediments, lumps, or aggregation of other particulate (such as protein) in the system.

2.7.3.4 Numerical One-dimensional Steady-state Models

Analytical and pseudo-analytical models involve describing key processes and variables using linear algebraic expressions. They are simplified linear versions of the

numerical one-dimensional steady-state model, made by approximation using linear assumptions. Compared with a one-dimensional dynamic model, this model excludes consideration of the dynamic development of the biofilm with time. Due to this nature, the assumptions of this model need to be carefully planned and laid out. It requires the modeller to have good knowledge of the system being modelled to apply this model and to simplify the situation by setting up appropriate assumptions. However, this model may still involve differential equations to solve in some cases, since it has dimension parameters and non-linearity.

2.7.3.5 Multi-dimensional Numerical Models

This type of model can simulate the heterogeneity of complex biofilm systems. Whether biofilm structure is heterogeneous or homogenous depends on how the biofilm forms and the environment biofilm within (Picioreanu & Van Loosdrecht, 1998). This type of model can model the heterogeneity of the environment of the system, hence can provide modeller some insight into the details such as how bacteria interact with each other, how bacteria interact with substratum, and how they form different biofilms (Picioreanu & Van Loosdrecht, 2002).

Some assumptions of the less complicated analytical models and the one-dimensional models no longer hold true and cannot be applied in multi-dimensional models. Some assumptions are no longer simplified and being modelled in the multi-dimensional models instead, such as, in many cases, biofilm is assumed as a uniform structure with cells evenly distributed in the microcolony (Picioreanu, Van Loosdrecht, & Heijnen, 2000c). This model is much more complicated and realistic than any of the aforementioned models, with far fewer idealised and simplified assumptions. A biofilm is a three dimensional structure in the real world. The multi-dimensional model allows us to simulate more realistic situations, such as flows into and out of the biofilm (Picioreanu, Van Loosdrecht, & Heijnen, 2000b).

The crucial limitation on application of this type of model to use in the industries is the complexity of the mathematical equations. These models are not straightforward and understandable by untrained people. Such models do have much more freedom, but they are no longer solvable by hand or with simple computer skills. Solving multi-dimensional models requires super computer power and the useful information gained from these models may still be limited. Thus there is no guarantee of more predictive power, and there may be loss of the robustness in the model.

2.7.4 Models Used in the Current Study

From the summary provided above, a model that would include the majority of the processes (such as settling, growth and sloughing) and assumptions should be used. The ideal model should include the mass balance equations for all major processes occurring with all components in every compartments (such as bulk liquid phase and biofilm phase) under defined conditions within the growth boundary.

In the current study, the major variables were the temperature, water activity and flow of the bulk fluids and the composition of the bulk fluid. A model between an analytical model and a one-dimensional dynamic model was considered. In this way, some assumptions could be made to simplify the system, but could also allow us to capture most of the effects of the components and conditions.

2.8. Direction for the Current Study

The attachment of biofilms has been studied extensively. Some modelling research has been conducted by the Picioreanu group (Picioreanu, Van Loosdrecht, & Heijnen, 2000c) (Ratkowsky, Lowry, McMeekin, Stokes, & Chandler, 1983). The aim of this project was to generate a predictive model of biofilm activity – attachment, development and inhibition. Few modelling studies have been done on the two targeted bacteria, *Geobacillus* species and *Anoxybacillus flavithermus* (Xavier, Picioreanu, &

Van Loosdrecht, 2005). These bacteria have emerged recently and have drawn major attention from the dairy industry. This study attempted to provide the dairy industry with a tool to predict the behaviour of biofilms in the milk evaporation process and thus to enable the plant to be run in a manner that minimizes biofilm growth.

3 Materials and Methods

This chapter has described the methods used in the preliminary studies for this project. The preliminary studies included microbial attachment to coupons, microtitre plate assays and growth rate studies. These experiments allowed us to determine the attachment and growth behaviours of these thermophilic bacilli under planktonic and biofilm conditions.

3.1. Chemicals

Crystal violet, safranin, glacial acetic acid and methanol were used in the microtitre plate assay staining process. **Crystal violet** (0.5%) was made according to the instructions on the package by diluting the appropriate amount of Crystal Violet powder (Biolab, Mulgrave, VIC, Australia) in deionized water with adequate stirring. **Safranin** (0.5%) was made using the same procedure as for Crystal Violet but with safranin powder (Sigma–Aldrich, St. Louis, MO, USA). **33% (v/v) glacial acetic acid** was made by reconstituting 99.7% glacial acetic acid (Ajax Finechem, Seven Hills, NSW, Australia) in the appropriate amount of deionized water. **99.5% methanol** (Fisher Scientific, Leicester, England) was used in the microtitre plate assay.

75% ethanol was made up by diluting 99.5% ethanol (Thermo Fisher Scientific, Scoresby, VIC, Australia) in deionized water for sanitizing and cleaning of BacTrac cells.

Glycerol was added to bacterial cultures before freezing to reduce ice crystal formation and damage to bacterial cells on defrosting. **Glycerol** (BDH Laboratory Supplies, Poole, England) was added to the bacterial culture to achieve a final concentration of 15%.

Standard alkali and acid washes were made up according to the washes used in CIP in the dairy manufacturing plants to clean and passivate stainless steel coupons and reactors. **Alkali wash** (2% NaOH) was made from NaOH pellets (Thermo Fisher Scientific, Scoresby, VIC, Australia) dissolved in deionized water. **Acid wash** (1.8% HNO₃) was made by diluting 70% HNO₃ (ACI Labscan, Bangkok, Thailand) in deionized water.

The **Gram's Iodine** solution used for gram staining was made up by diluting 500 ml of the stock solution in 1500 ml distilled water before use. The stock solution was made up by 10 g of Potassium Iodide (KI) (Scientific Supplies, Auckland, New Zealand) dissolving in 500 ml of distilled water followed by dissolving 20 g of Iodine crystals (Scientific Supplies, Auckland, New Zealand) and appropriate amount of distilled water to make up to 1 L with vigorous mixing.

3.2. Media

Tryptone soy broth (TSB) (Becton Dickinson Labware, Franklin Lakes, NJ, USA) and **tryptone soy agar plates** (TSA plates) (Becton Dickinson Labware, Franklin Lakes, NJ, USA) were made up according to the instructions on the package and were autoclaved at 121°C for 15 min before use for growth of *Geobacillus* and *Anoxybacillus*.

Skim milk medium: 10% (w/v) skim milk was made by mixing skim milk powder (bought from a local supermarket) and the appropriate amount of deionized water. The skim milk was autoclaved at 121°C for 15 min before use. Skim milk medium with 15% glycerol (final concentration, v/v) was used for long term storage of bacterial cultures in the -80°C freezers.

UHT skim milk: Supermarket shelf-bought UHT milk was used in part of this project (Fonterra, New Zealand).

3.2.1. Reconstituted Skim Milk

The skim milk used in the experiments was made with gamma-sterilized skim milk powder and sterile deionized water. The skim milk powder was provided by Fonterra and was gamma irradiated by Schering–Plough, Wellington, New Zealand.

Sterile milk powder (100 g) was reconstituted with 910 ml of sterile deionized water to make up 1 L of reconstituted skim milk (RSM) with 10% (w/v) solids. RSMs of different solids percentages were made by weighing the appropriate amount of sterile milk powder and making up to 1 or 4 L with stirring followed by vigorous shaking in the reservoir. Then the RSM was stored in a cold room overnight and shaken well before use.

The water activities of the RSMs with different solids percentages were tested using a dew point water activity meter (AquaLab 4TE, AquaLab, Pullman, WA, USA) at below 25°C.

3.3. Microorganisms

Thirteen isolates were provided by Professor Steve Flint at the beginning of the study. Five were reference cultures and the others were isolated from dairy manufacturing plants. These cultures were provided on frozen media containing glycerol.

Table 1: Origins of bacterial strains

Laboratory Identification Number	Fonterra Identification Number	Description
Sample 1	DSM 2641	Reference strain: <i>A. flavithermus</i>
Sample 2	DSM 14791	Reference strain: <i>G. thermoleovorans</i>
Sample 3	DSM 11667	Reference strain: <i>G. thermoleovorans</i>
Sample 4	DSM 5934	Reference strain: <i>G. stearothermophilus</i>
Sample 5	DSM 1550	Reference strain: <i>G. stearothermophilus</i>
Sample 6	CBF 4	Wild strain: <i>A. flavithermus</i> (Clandeboye, 2003)

Sample 7	CBF 5	Wild strain: <i>A. flavithermus</i> (Clandeboye, 2003)
Sample 8	TT 1	Wild strain: <i>Geobacillus</i> sp. (Clandeboye, 2003)
Sample 9	TRGT 6	Wild strain: <i>Geobacillus</i> sp. (Te Rapa, powder, August 2008)
Sample 10	TRGT 7	Wild strain: <i>Geobacillus</i> sp. (Te Rapa, powder, August 2008)
Sample 11	TRGT 8	Wild strain: <i>Geobacillus</i> sp. (Te Rapa, powder, August 2008)
Sample 12	TRGT 9	Wild strain: <i>Geobacillus</i> sp. (Te Rapa, powder, August 2008)
Sample 13	CGT 1	Wild strain: <i>Geobacillus</i> sp. (Complaint from Taiwan)

Samples 1–13 were provided by Fonterra and Massey University at the beginning of the study in 2009.

A. flavithermus = *Anoxybacillus flavithermus*
G. thermoleovorans = *Geobacillus thermoleovorans*
G. stearothermophilus = *Geobacillus stearothermophilus*
 Clandeboye = near Christchurch, South Island of New Zealand
 Te Rapa = near Hamilton, North Island of New Zealand

Later in the study, two new strains were isolated from the skim milk powder provided by Fonterra using TSB and TSA plates. These two strains were identified using molecular biological methods including polymerase chain reaction (PCR) and mass spectrometry (matrix-assisted laser desorption/ionization time of flight (MALDI–ToF)).

Table 2: Strains isolated from skim milk powder

Laboratory Identification Number	Origin	Identification
Geo1	Skim milk powder (2010)	<i>G. stearothermophilus</i>
Anoxy2	Skim milk powder (2010)	<i>A. flavithermus</i>

Geo1 and Anoxy2 were isolated from skim milk powder in 2010.

A. flavithermus = *Anoxybacillus flavithermus*
G. stearothermophilus = *Geobacillus stearothermophilus*

3.3.1. Culture Management and Maintenance

All stock cultures were kept in a -80°C freezer in the autoclaved skim milk medium at all times. These cultures were rarely used to prevent contamination and therefore maintained purity. The viability and the purity of these cultures were checked every 6 months.

A batch of working culture vials was made from the stock cultures. A loopful of stock culture was inoculated on to a TSA plate and grown aerobically at 55°C for 24 h. Cells from that TSA plate were inoculated into 100 ml of TSB and grown aerobically in a 55°C water bath for 4–8 h until really cloudy. Sterile glycerol (15% v/v final concentration) was added into the TSB broth and mixed well. An aliquot (1 ml) of the culture mix was added to an Eppendorf tube. All vials were frozen in the -80°C freezer. The working culture tube was completely defrosted and shaken well before use. The culture management system flow chart is shown in Appendix 2.

3.3.2. Gram Staining Procedures

A well isolated colony from an overnight culture was picked off and suspended in a drop of saline on a glass slide. The smear was completely air-dried and then the slide was passed through the flame 5 times to heat fix the smear. The heat fixed smear was exposed to 0.5% Crystal Violet for 1 min. After the Crystal Violet was poured off, the slide was gently rinsed with deionised water for 10 s. The smear was then covered with Gram's Iodine for 1 min. After the iodine was poured off, the slide was gently rinsed with deionised water for 10 s followed by a gentle wash of 95% ethanol for 30 s to decolorize. Then the smear was covered with 0.5% Safranin for 1 min. The slide was rinsed gently with deionized water and blot dried using tissue. The smear was observed using 100 times objective with oil immersion.

3.3.3. Culture Preparation

The defrosted 1 ml working culture was poured and spread evenly on to a TSA plate to grow into a lawn culture. The plate was incubated aerobically at 55°C for 24 h. An area of 1 cm² (1 cm x 1 cm) of culture on the agar plate was swabbed and used to inoculate 100 ml of TSB medium, which was incubated in the 55°C water bath for 4–8 h to reach 10⁷ cfu/ml.

3.3.4. Inoculation of Biofilm Reactor Systems

For **the inoculation of the milk supply**, cultures were prepared as described previously (Section 3.3.3) and were diluted to an approximate concentration of 10⁵ cfu/ml. An aliquot of 40 ml of the culture was inoculated into 4 L of prepared sterile skim milk at the start of the reactor run. The milk container was kept cold in an ice-filled bucket during the experiment.

For **the inoculation of the hexagonal reactor**, cultures were prepared as described previously (Section 3.3.3). Two additional sections of autoclaved silicone tubing (about 5 cm long) were fitted on to the inlet and outlet of each of the two metal reactors aseptically. Cultures were injected into the reactors fully using a sterile syringe and needle with very slow injection to ensure a full coverage of culture in the reactor. Then each of the silicone tubes was clamped. The reactor was left on the bench to incubate for 1 h prior to the temperature-cycling experiment.

3.4. Coupons

3.4.1. Passivation

Square stainless steel (316L with 2B finish) coupons (1 cm² (1 cm x 1 cm)) were used in coupon attachment experiments. Round stainless steel (0.5 cm thickness, 316L with 2B finish) coupons (1 cm diameter) were used later in the CDC reactor experiments.

These coupons were treated with 50% HNO₃ at 75°C for 30 min and were autoclaved at 121°C for 15 min initially before use. This treatment was needed only before the first experiment after the coupons had been sourced from the manufacturer.

3.4.2. Cleaning Procedure

The coupons were rinsed in deionized water and then soaked in a 75°C alkali wash (2% NaOH) for 30 min followed by a 75°C acid wash (1.8% HNO₃) for 30 min with five deionized water rinses in between. The coupons were then dried using paper towels and sterilized by autoclaving in 121°C for 15 min.

3.5. Enumeration of Bacterial Numbers

3.5.1. Spiral Plater

An automatic spiral plater system (Whitley automated spiral plater, Don Whitley Scientific, Shipley, England) was used to enumerate the bacterial cells on the coupons. The plater was set up to plate triplicate TSA plates logarithmically with 100 µl of sample on each plate using the valve injection mode.

3.5.2. Impedance Microbiology Tool: BacTrac

The impedance microbiology tool BacTrac (BacTrac 4300, Sy-Lab, Vienna, Austria) was used in this study to enumerate bacteria. Impedance microbiology first came to attention in the late 1990s and was later used widely in testing various aspects in the food industry (Silleby & Forsythe, 1996).

The BacTrac measures the time taken for the impedance change, caused by bacterial growth, by certain levels, in the medium (M) or at the electrodes (E). The threshold used in this project was 3% and the medium used was TSB. Therefore, the detection time M and E values used in this project refer to ‘the time taken for the impedance caused by a certain strain to change by 3% in the TSB or at the electrodes’.

3.5.2.1. BacTrac Calibration

At the beginning of the study using the BacTrac system, the BacTrac needed to be calibrated for each strain of bacteria. The calibration process allowed us to establish the relationship between known bacterial counts and detection time measurements. Therefore, later in the experiment, this relationship could be used to determine unknown bacterial concentrations from measured detection times. The relationship between the detection times M or E values and bacterial counts (log count converted) had to be established for each strain.

The bacterial culture was grown up according to Section 3.3.3. It was serially diluted to 10^{-8} . Samples (1 ml) of each dilution were pipetted into BacTrac cells containing 9 ml of TSB, placed into the BacTrac at 55°C and monitored for 24 h. At the same time, the culture was counted on TSA plates. The \log_{10} count of each dilution was plotted against the detection time M and E values to obtain a calibration curve that could be used to determine equivalent counts of samples drawn from experimental reactors.

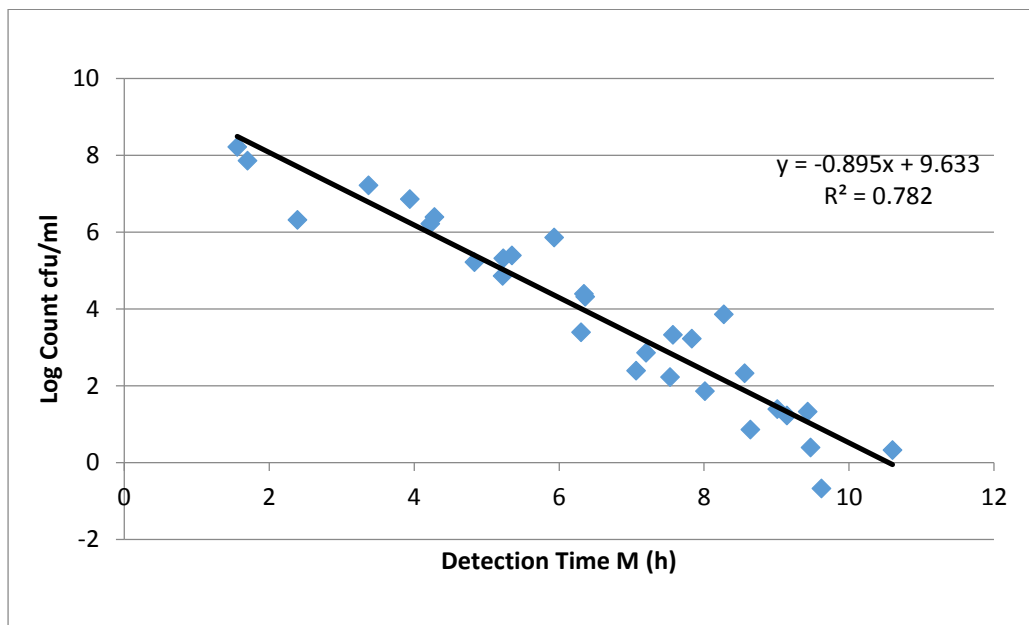


Figure 2: BacTrac calibration curve M for *Geobacillus* TRGT 9.

Geobacillus TRGT 9 calibration curve. The BacTrac calibration was done using standard strength TSB and growth at 55°C. Calibration curves and data for all 13 Massey isolates are shown in Appendix 2 in the data CD. The detection limit of BacTrac for liquid sample is 1 /ml and 10/g for solid samples.

A trend line was drawn for each graph and the equations for the trend lines were examined. The relationship between the log count converted bacterial count and the detection time should be linear. Some bacteria may have better readings in M, whereas some may have better readings in E. The trend with the highest R^2 value (the trend had better fit with the data in either M or E) was chosen as the calibration curve. The equation was in the format

$$\log_{10}(\text{bacteria counts}) = \pm \text{constant} \times \text{Detection time M/E value} \pm \text{constant}$$

In the example in Figure 2, the equation obtained from the calibration curve of *Geobacillus* TRGT 9 was:

$$\log_{10}(\text{unknown conc of TRGT9}) = -0.895 \times \text{Detection time M} + 9.633$$

Later, the unknown bacterial concentration (abbreviation conc) could be calculated using the calibration curve and the known measured detection time M or E value.

3.5.2.2. Cleaning Procedures for BacTrac Cells

The BacTrac cells were autoclaved after the run. Each individual cell was brushed gently with hot tap water and detergent (Pyroneg, Thermo Fisher Scientific, Scoresby, VIC, Australia). After rinsing with deionized water, each cell was filled and soaked overnight with 5 ml of 75% ethanol to clean the electrodes thoroughly. Each cell was rinsed with deionized water and autoclaved before use.

3.6. Attachment and Growth Assays

3.6.1. Microtitre Plate Attachment and Growth Assays

Sterile hydrophobic polystyrene plates (96 wells) (Becton Dickinson Labware, Franklin Lakes, NJ, USA) were used in this set of experiments. Cultures were grown

and prepared as described previously in Section 3.3.3 to a final concentration of 10^7 cfu/ml. All 13 isolates from Massey were tested in this part of experiments.

3.6.1.1.Attachment Assay

Prepared cultures were diluted to approximately 10^5 cfu/ml in TSB. Then the diluted culture was diluted 1:1 in UHT milk. Standard strength TSB and UHT milk were used in this experiment.

The wells of a microtitre plate were inoculated with 200 μ l of diluted culture with 12 replicates being prepared for each isolate (Table 3). Then, the plate was incubated at 55°C for 30 min before staining (Section 3.6.1.1). Sterile TSB or sterile UHT milk was used as a blank. Readings were taken using the microplate reader at wavelength of 550 nm.

Table 3: Plate layout for the attachment assay

		10^5 cfu/ml (12 replicates)
Sample 1	ROW A	Column 1 → Column 12
↓	↓	
Sample 7	ROW G	
Blank	ROW H	Blank

Attachment assay for Samples 1–13 in standard TSB medium. The absorbance readings were taken at wavelength of 550 nm.

3.6.1.2.Comparison between Attachment in TSB and UHT Milk

Serial 10-fold dilutions in standard TSB brought the final concentration of the prepared culture to 10^5 cfu/ml. Standard strength TSB and UHT skim milk were used in this experiment.

Dilutions of 1:1 and 1:10 (culture: TSB or culture: skim milk) were made in test tubes. Six replicates of 200 μ l of each isolate at each concentration were aliquoted into the

wells according to Table 4. Then, the plate was incubated at 55°C for 30 min before staining (Section 3.6.1.1). Sterile TSB or adjusted UHT skim milk (1:1 or 1:10 TSB: UHT milk) was used as a blank. The readings were taken in the microplate reader at wavelength of 550 nm.

Table 4: Plate layout for the comparison study of attachment in TSB and skim milk

		10⁵ cfu/ml (6 replicates) 1:1 (Culture: TSB/milk)	10⁵ cfu/ml (6 replicates) 1:10 (Culture: TSB/milk)
Sample 1	ROW A	Column 1 → Column 6	Column 7 → Column 12
↓	↓		
Sample 7	ROW G		
Blank	ROW H	For milk 1:1 (TSB: milk) For TSB: 200 µl of TSB	For milk 1:10 (TSB: milk) For TSB: 200 µl of TSB

Comparison study of attachment of Samples 1–13 on to microtitre plates in standard TSB medium and UHT skim milk. The absorbance readings were taken at wavelength of 550 nm.

3.6.1.3. Staining Procedure for Microtitre Plate Assays

After incubation, the optical density of the isolates were measured in the plate after staining. The contents of the microtitre plate were poured out and discarded. The plate was then washed three times with 200 µl of deionized water and blot-dried on tissue paper. Methanol (200 µl) was distributed into each well and held for 15 min to fix the cells. The methanol was poured out and the plate was dried in the incubator. Crystal violet (200 µl) was distributed into each well and held for 5 min to stain the biofilm. Then the Crystal Violet was poured out and the plate was washed five times with 200 µl of deionized water to remove excess stain. The plate was dried in the 55°C incubator for 1 h. Then 200 µl of 33% v/v glacial acetic acid was distributed into each well to release the Crystal Violet stain from the cells. Final endpoint readings were taken. The optical density of the wells was read at wavelength of 550 nm using a microplate reader (FLUOstar Omega, BMG LABTECH, Offenburg, Germany).

3.6.2. Coupon Attachment Assay

Each culture was grown to approximately 10^7 cfu/ml according to the conditions in Section 3.3.3. The culture was then diluted 1:10 in sterile TSB or UHT skim milk. Six previously treated (Section 3.4.1) coupons were submerged into each of the diluted cultures for 30 min. Then, each coupon was washed separately five times in sterile deionized water by gentle rotation. After washing, each coupon was inserted into one sterile BacTrac cell containing 10 ml of sterile TSB medium. The BacTrac was run overnight before data collection.

3.7. Polymerase Chain Reaction Assay for Identification of Thermophilic Bacteria

The PCR identification procedure was performed in the Fonterra Research & Development Centre laboratories in Palmerston North according to the procedure developed by Flint, Ward and Walker (2001). The experiments used to identify the two new isolates from this study were done using the following procedure.

3.7.1. Primer Information

A specific primer designed for either *Anoxybacillus flavithermus* (Flavo) (5'-TAACGCCAGTTACTACGCTACTTG-3') or *Geobacillus thermoleovorans* (Levo) (5'-CGCCGCCCTCTTCGAACGGCGCTCC-3') was used in combination with the universal primer Y1 (5'-TGGCTCAGAACGAACGCTGGCCCG-3') (Flint, Ward, & Walker, 2001). *Geobacillus stearothermophilus* shows 99% similarity in 16S rRNA sequence with *Geobacillus thermoleovorans*. Primers designed using sequence of *Geobacillus thermoleovorans* 16S rRNA enables identification of any closely related *Geobacillus* species (Flint, Ward, & Walker, 2001).

3.7.2. PCR Mixture

The master mix for the PCR was made from 460 μl of H_2O , 40 μl of 20x buffer (Tfl), 80 μl of 25 mM MgCl_2 , 160 μl of dNTP mix (Promega), 1 μl of each primer (Flavo + Y1 or Levo + Y1) and 10 μl of Tfl polymerase (MasterAmp Tfl DNA polymerase, Epicentre Technologies, Madison, WI, USA). A 50 μl aliquot of this mix was dispensed into each tube. Then, 5 μl of template (fresh overnight culture) was added to the appropriate tube. A negative control tube was set up; it contained 50 μl of PCR mix and 5 μl of sterile H_2O . Two positive control tubes for the *Geobacillus* samples were set up; one tube contained 50 μl of PCR mix and 5 μl of *Geobacillus* sp. (AM) and the other tube contained 50 μl of PCR mix and 5 μl of *Geobacillus thermoleovorans* (DSM 5366). A positive control tube for the *Anoxybacillus* samples was also set up; it contained 50 μl of PCR mix and 5 μl of *Anoxybacillus flavithermus* (DSM 2641).

3.7.3. PCR Conditions

The tubes were placed in the PCR machine and run with the following temperature profile (Figure 3). A 1 kb DNA ladder (Invitrogen, Life Technologies, Auckland, New Zealand) was used. The PCR products around 500 bp were visualized by electrophoresing on a 2% agarose gel at 80 V (10 μl of sample per well, 1 μl for the ladder), staining with GelStar (Lonza, Basel, Switzerland) for 20–30 min (diluted to 1x strength, 5 μl /50 ml of TE buffer) and observing the band under UV light.

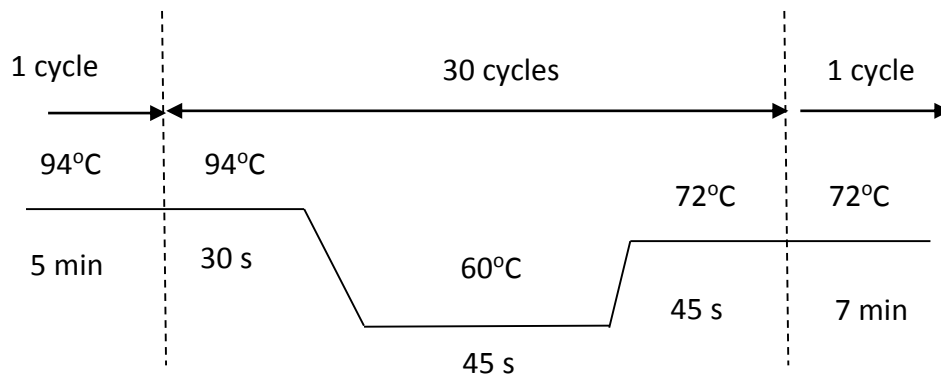


Figure 3: PCR temperature profile for identification of Isolate 1 and Isolate 2.

The PCR method was developed for the identification of thermophilic bacilli using procedures in (Flint, Ward, & Walker, 2001).

3.7.4. PCR Set-up

The PCR assay was set up as shown in Table 6. The reaction was separated into two sets: the Flavo set for the detection of *Anoxybacillus flavithermus* and the Geo/Levo set for the detection of *Geobacillus* species. The positive control used for the Flavo set was the reference strain *Anoxybacillus flavithermus* (DSM 2641). The positive controls used for the Geo/Levo set were the reference strain *Geobacillus* sp. (AM) and *Geobacillus thermoleovorans* (DM 5366). The negative control used for both sets was autoclaved deionized H₂O.

Table 5: Set-up for the PCR identifications for Isolate 1 and Isolate 2

Lane	Description of the Lane	Note
1	Ladder (1 kb, Invitrogen)	
2	Negative Control: H ₂ O	Flavo set for the detection of <i>Anoxybacillus flavithermus</i>
3	<i>Anoxybacillus</i> DSM 2641	
4	Geo sp. (AM)	
5	Geo thermo DSM 5366	Positive control in this set was the reference strain <i>Anoxy</i> DSM 2641
6	Isolate 1	
7	Isolate 2	Negative control was H ₂ O
8	Ladder (1 kb, Invitrogen)	
9	Negative Control: H ₂ O	Geo/Levo set for the detection of <i>Geobacillus</i> sp.
10	<i>Anoxybacillus</i> DSM 2641	
11	Geo sp. (AM)	
12	Geo thermo DSM 5366	Positive controls in this set were the reference strains <i>Geobacillus</i> sp. (AM) and Geo thermo DSM 5366
13	Isolate 1	
14	Isolate 2	Negative control was H ₂ O
15	Ladder (1 kb, Invitrogen)	

PCR identification of Isolate 1 and Isolate 2 using known *Geobacillus* species and *Anoxybacillus flavithermus* as positive controls. *Anoxy* = *Anoxybacillus flavithermus*; Geo thermo = *Geobacillus thermoleovorans*; Geo sp. = *Geobacillus* species.

3.8. Planktonic Growth Rate Studies

The planktonic growth rates of Sample 7 (*A. flavithermus*, CBF 5) and Sample 12 (*Geo* sp., TRGT 9) with two replicates were tested under TSB and skim milk conditions. This experiment procedures were also performed using Geo1 and Anoxy2.

The culture was grown as described previously (Section 3.3.3) to a concentration of approximately 10^7 cfu/ml. Serial 10-fold dilutions of the culture in TSB brought the cell concentrations to approximately 10^6 and 10^5 cfu/ml. For both these concentrations, 1 ml was diluted in 99 ml of sterile TSB or sterile UHT skim milk and was maintained at 55°C in a shaking water bath for 6–8 h.

For TSB experiments: A 200 µl sample was withdrawn into a microtitre plate for reading every 30 min. The plate was scanned at 550 nm.

For UHT milk experiments: A 1 ml sample was withdrawn into a BacTrac cell containing 9 ml of sterile TSB medium. The BacTrac was run for 24 h before data collection.

4 Characterisations of Thermophilic Bacteria from Milk Powder

Preliminary studies were done on the *Geobacillus* and *Anoxybacillus* isolates from Massey University to screen isolates for further studies, based on their biofilm attachment and growth in TSB and milk.

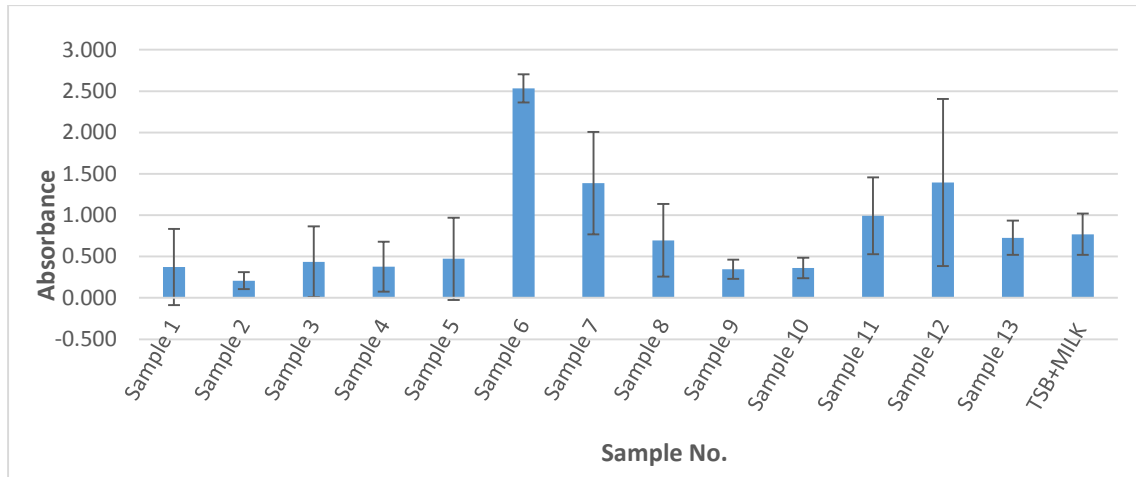


Figure 4: Biofilm Growth and Attachment microtitre plate assay

The absorbance readings of growth and attachment for all 13 samples in UHT milk as medium, stained after incubating in 55°C incubator for 8 h (Sample 1-13, 550nm, crystal violet stained, water as blank, error bars are representing + / - one standard deviation ;);

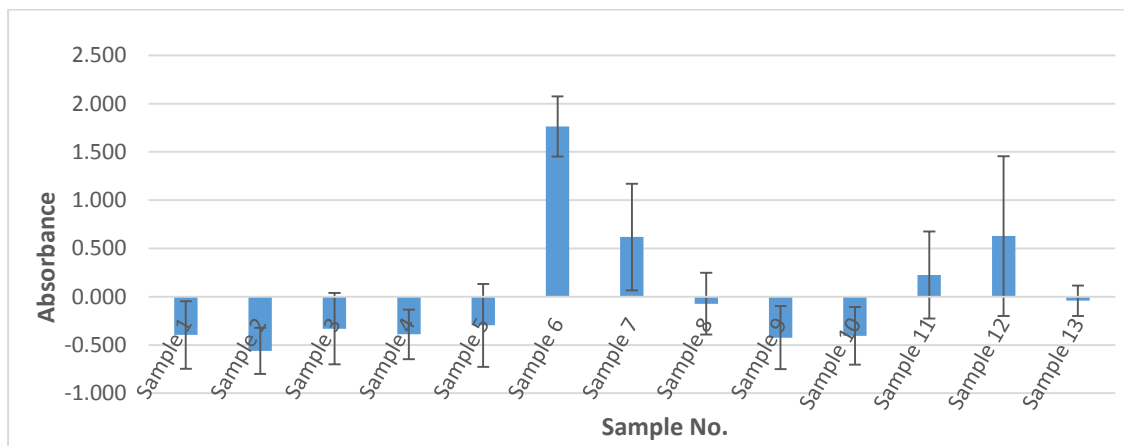


Figure 5: Biofilm Growth and Attachment microtitre plate assay:

The absorbance readings of growth and attachment for all 13 samples in UHT milk as medium, stained after incubating in 55°C incubator for 8 h (Absorbance, Sample 1-13, 550nm, crystal violet stained, TSB + milk + water as blank, error bars are representing + / - one standard deviation ;);

From comparison between Figure 4 and Figure 5, milk proved not to be suitable for use in the microtitre plate assay to screen biofilm attachment because of the over-

shadowing effect from the attachment of milk protein on to the plate (detailed data shown in Appendix 7-9 in the data CD).

When biofilm attachment in milk was screened using the BacTrac, thermophilic bacteria in the milk powder affected the growth of the target microorganism. Two strains of thermophilic bacteria were isolated from skim milk powder. They were distinguished on the basis of colony morphology.

4.1 Isolation and Identification of Isolate 1 and Isolate 2

4.1.1 Isolation and Cell Morphology of Isolate 1 and Isolate 2

Thermophilic bacteria were found in the non-gamma-irradiated milk powder. They could grow rapidly and could compete with the target thermophilic bacteria in the experiment. The non-irradiated milk powder was diluted with sterile water, spiral plated on to TSA plates and incubated at 55°C for 24 h. Two types of colonies with different morphologies were found. Each type of colony was isolated on to another TSA plate.

On TSA plates (Figure 6), Isolate 1 colonies were small, flat, round and white in colour. Isolate 2 colonies appeared to be medium, smooth, shiny, round and cream in colour. Both Isolate 1 and Isolate 2 appeared to be long Gram-positive rods (Gram staining procedures in Section 3.3.2) with terminal endospores (Figures 7 and 8).

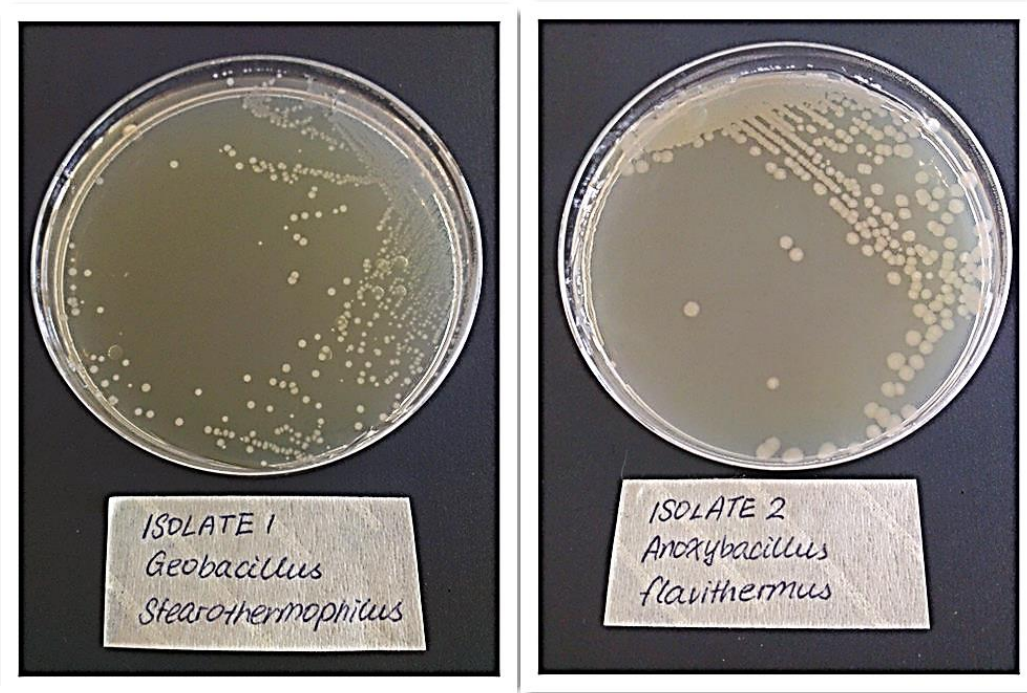


Figure 6: Isolate 1 and Isolate 2 on TSA plates.

After 24 h of aerobic growth in the 55°C incubator on TSA plates.



Figure 7: Gram staining of Isolate 1 under 100x objectives.

Gram stained (Section 3.3.2), 100x objective (Olympus PLN100x on Olympus BX41), oil immersion. (Picture was taken using Leica camera system fitting over the eyepiece of the microscope)

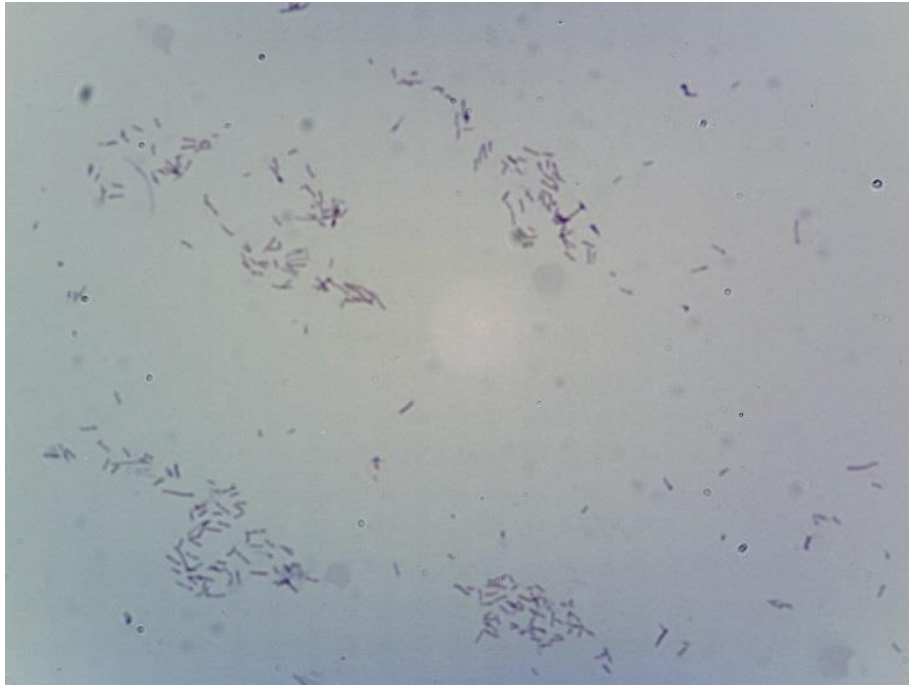


Figure 8: Gram staining of Isolate 2 under 100x objectives.

Gram stained (Section 3.3.2), 100x objective (Olympus PLN100x on Olympus BX41), oil immersion. (Picture was taken using Leica camera system fitting over the eyepiece of the microscope)

Bergey's Manual Trust (2009) states that reference strains of *Anoxybacillus* have a wider growth range than *Geobacillus* with respect to both temperature and pH.

The reference *Anoxybacillus* strain DSM 2641 has a strong, yellow pigment. It grew (within 4 h) and then died very rapidly (within 6 h) in TSB in the 55°C water bath. In contrast, Isolate 2 had only minor yellow pigmentation, compared with DSM 2641, and survived in TSB in the 55°C water bath for longer than 8 h. Isolate 1 was able to grow from 35 to 70°C on TSA plates both aerobically and anaerobically.

It seemed that these two wild strains from milk powder had quite different behaviour from the reference strains (Burgess, Brooks, Rakonjac, Walker, & Flint, 2009) (Flint, Palmer, Bloemen, Brooks, & Crawford, 2001).

4.1.2 PCR Identification

PCR identification (Section 3.7) results for Isolate 1 and Isolate 2 are shown below in Figure 9. The set on the left hand side of Figure 9, Lane 2 – Lane 7 is the PCR set for testing *Anoxybacillus flavithermus*, using *Anoxybacillus flavithermus* as the positive control. The set on the right hand side of Figure 9, Lane 9 – Lane 14 is the PCR set for testing presence of *Geobacillus species*, using *Geobacillus species* and *Geobacillus thermoleovorans* as positive controls.



Figure 9: PCR identification results for Isolate 1 and Isolate 2.

Using the method and layout described in Section 3.7; Lanes 1, 8 and 15 = 1 kb ladder; Lanes 2 and 9 = negative control H₂O; Lanes 3 and 10 = positive control *Anoxybacillus flavithermus*; Lanes 4 and 11 = positive control *Geobacillus* sp.; Lanes 5 and 12 = positive control *Geobacillus thermoleovorans*; Lanes 6 and 13 = Isolate 1; Lanes 7 and 14 = Isolate 2.

From the PCR gel (Figure 9), Isolate 2 (lane 7) corresponded to the reference positive control *Anoxybacillus flavithermus* in lane 3. Isolate 1 in lane 13 produced a band corresponding to the positive control of *Geobacillus* species in lane 11. This identification showed that Isolate 1 was a *Geobacillus* species and that Isolate 2 was *Anoxybacillus flavithermus*.

This identification was confirmed using mass spectrometry (MALDI–ToF) identification (Denise Lindsay, Fonterra, 2012, personal communication): Isolate 1 was confirmed as *Geobacillus stearothermophilus* and Isolate 2 was confirmed as *Anoxybacillus flavithermus*.

4.2 Preliminary Studies on Geo1 and Anoxy2

4.2.1 Calibration Curves

Using the standard calibration method in Section 3.5.2.1, BacTrac calibration equations for Geo1 and Anoxy2 were produced and were used later to determine the bacterial counts in unknown concentrations of Geo1 and Anoxy2.

Table 6: BacTrac calibration equations developed for Geo1 and Anoxy2

Lab ID	M/E Value Used	Calibration Equation
Geo1	M	$\text{Log}_{10}(\text{Unknown}) = -0.9162 \times M + 11.253$
Anoxy2	M	$\text{Log}_{10}(\text{Unknown}) = -0.7117 \times M + 10.382$

Detailed calibration curves are included in Appendix 3 in the data CD;

4.2.2 30 Min Coupon Attachment Assay

Figure 10 below shows the bacterial attachment of all 13 Massey isolates and two new milk isolates onto 1 cm² stainless steel coupons after incubation in TSB or RSM for 30 min (Section 3.6.2).

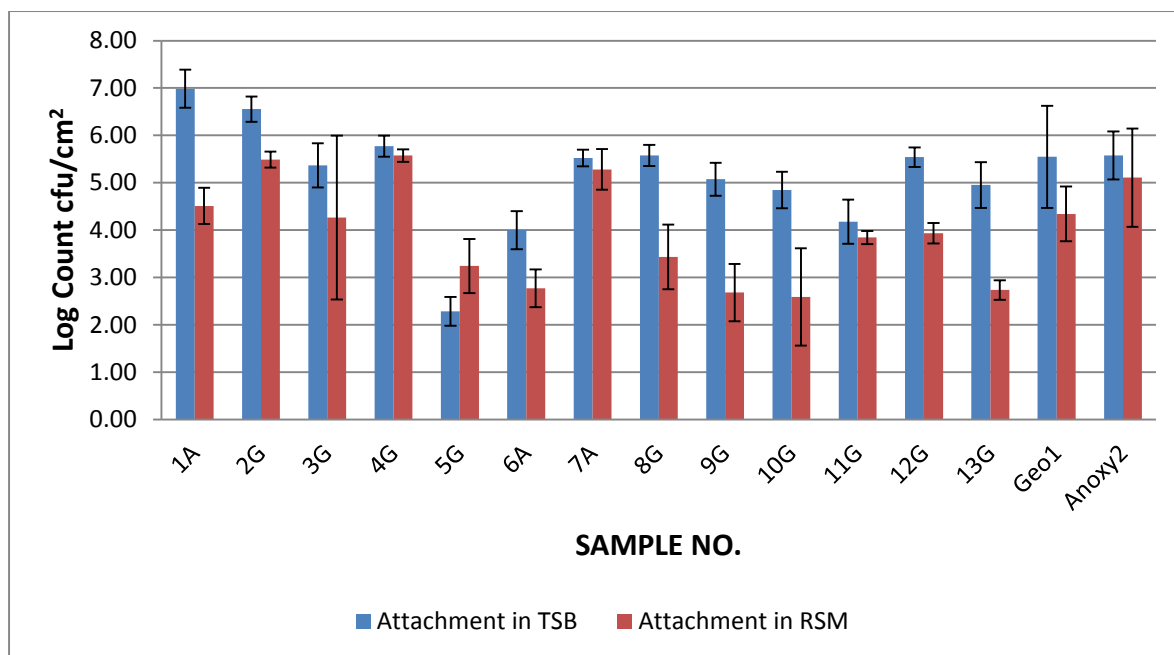


Figure 10: A 30 min coupon attachment assay for Samples 1–13, Geo1 and Anoxy2.

A 30 min coupon attachment assay at 55°C for all 13 Massey isolates and the two new milk isolates in TSB and in RSM. Y-axis = log count converted of bacteria attachment to 1 cm² stainless steel coupons in 30 min (mean and S.D. plotted); A = *Anoxybacillus flavithermus*; G = *Geobacillus* species; blue = attachment in TSB; red = attachment in RSM; 1–5 = reference strains; 6–13, Geo1 and Anoxy2 = wild strains. The attachment data was converted from the bacterial concentration of the TSB based on detection time M/E values from the BacTrac. The bacterial concentration (cfu/ml) x the TSB volume / the coupon area = the bacterial concentration x 10ml / (2 sides x 1cm²); Detailed data is included in Appendix 4-6 in the data CD.

Figure 10 shows that Geo1 and Anoxy2 had more bacterial attachment in 30 min in RSM than other samples except strain 2, 4 and 7. Geo1 had less attachment than the reference *Geobacillus* strains 2 (DSM 14791), 3 (DSM 11667) and 4 (DSM 5934) and more attachment than reference *Geobacillus* strain 5 (DSM 1550). Anoxy2 had similar attachment with *Anoxybacillus* strain 7 (CBF 5), but less attachment than the reference *Anoxybacillus* strain 1 (DSM 2641) in TSB but more attachment in RSM.

There were no consistent trends in biofilm attachment between *Geobacillus* species and *Anoxybacillus flavithermus*. There was also no consistent trends in biofilm attachment between wild strains and reference strains.

4.2.3 Planktonic Growth Rate in UHT Milk

The growth rates of Geo1 and Anoxy2 as planktonic cells were determined in UHT milk at 55°C for 8 h using a shaking water bath and the BacTrac. These growth rate data were used to determine the flowrate for experiments in the CDC reactor. The gradient of log phase of the growth curve is taken for calculating the maximum specific growth rate of the bacteria. The lag phase ends when the bacteria adapt to the environment and start to grow and enter log phase. The log phase starts when we can detect an increase in cell concentration in the suspension or on the coupon surface.

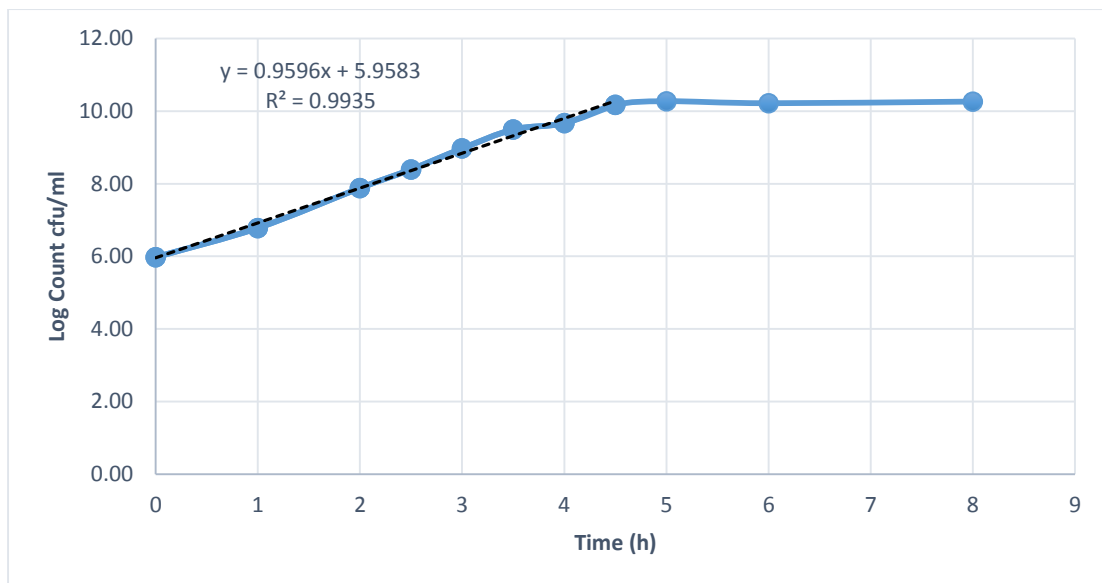


Figure 11: Planktonic growth of Geo1 in UHT milk.

Y-axis = log count converted using BacTrac calibration curve and measured detection time; X-axis = incubation time in the water bath. Equation displayed is used for calculation of the planktonic growth rate. Planktonic growth rate data and calculation for Sample 7 and 12 in TSB is shown in Appendix 10, in UHT milk in Appendix 11, and Geo1/Anoxy 2 growth in UHT milk in Appendix 12.

The BacTrac detection time readings were converted into log counts (cfu/ml) using the BacTrac calibration equations in Table 6. The gradient of the linear portion of the log phase was calculated on the graph (Figure 11).

The maximum specific growth rate was calculated from the ln curve rather than the log curve using the method outlined by Pirt (1975). The conversion between log and ln is:

$$\mu_{max} = \log gradient \times \frac{\ln 2}{\log 2}$$

$$\mu_{max,Geo1} = 0.9596 \times 2.303 = 2.210/hour$$

After calculating the maximum specific growth rate for each isolate, the doubling time (t_D) of each isolate was calculated and is given in Table 7.

$$t_D = \frac{\ln 2}{\mu} = \frac{0.693}{2.210} = 0.314/hour = 18.81 \text{ minutes}$$

Table 7: Planktonic growth rates of Geo1 and Anoxy2 in UHT milk

Lab ID/Species	Growth Rate (/h)	Doubling Time (t_D) (h)	Doubling Time (t_D) (min)
Geo1	2.210	0.314	18.81
Geo1D	2.188	0.317	19.00
Anoxy2	1.749	0.396	23.78
Anoxy2D	1.830	0.379	22.72

Planktonic growth rates of Geo1 and Anoxy2 and duplicates Geo1D and Anoxy2D in 10% solids standard UHT milk at 55°C for 8 h. The calculations were done based on the growth curves in the Appendix 12 in the data CD.

According to Table 7, Geo1 grew faster than Anoxy2. The doubling times of these two microorganisms were around 19 and 24 min respectively, similar to values in the literature (Flint, Palmer, Bloemen, Brooks, & Crawford, 2001) (Parker, Flint, & Brooks, 2003). The volume of the CDC reactor is 300ml. The flowrate for the CDC reactor experiments was set to be 5 ml/min to reduce planktonic growth in the reactor.

$$\mu_{max,Geo1} = 2.20/h \text{ and } \mu_{max,Anoxy2} = 1.79/h$$

$$\begin{aligned} \text{Dilution rate} &= \frac{\text{Flow rate of the System (ml/min)}}{\text{Volume of the System (ml)}} = \frac{5\text{ml/min}}{300\text{ml}} \\ &= 0.017/\text{min} = 1.02/h \end{aligned}$$

If the dilution rate is larger than the maximum specific growth rate, the culture will wash out if not reinoculated.

The planktonic growth in the bulk milk was reduced in the CDC reactor without culture being washing out. The CDC reactor is a stirred reactor, the kinetics show that two pot volumes must flow through the reactor to replace 95% of the medium. It is impossible to prevent planktonic growth since some cells can remain in the liquid phase for very long periods.

4.3 Summary

Geo1 and Anoxy2 showed similar amounts of attachment and similar growth rates. Bacterial attachment within 30 min was 5 log cfu/cm² in TSB and 3–4 log cfu/cm² in RSM. The doubling times of these bacteria were around 19–24 min.

For further studies, wild strains are more preferred than reference strains due to their biofilm behaviours may have adapted to the dairy manufacturing environment. Thus, from the preliminary studies, Geo1 and Anoxy2 were fast growers and attachers compared with the other wild strains (Appendices 6). They were chosen for biofilm studies using the CDC reactor and for thermocycling work.

5 Factorial Experiments Using CDC Reactors

5.1 Outline

The aim of the CDC reactor run experiments was to understand and construct growth response surfaces of the chosen isolates under different combinations of water activity and temperature. The preliminary study tested the boundary conditions for the CDC reactor experiments.

5.2 Testing Boundary Conditions for Experiments Using the BacTrac

To investigate the factors influencing the growth of biofilms of these thermophilic bacteria, preliminary tests examined the growth at various temperatures and water activities using the BacTrac analyser. Geo1 and Anoxy2 were tested.

Bacterial growth depends on temperature, pH and water activity. However, in the dairy industry, the pH cannot be varied easily because the milk proteins will be denatured at their isoelectric point and will adversely alter the properties of the final product. Therefore, the focus of these experiments was on temperature and water activity.

The water activity of milk decreases along with the boiling temperature as milk is concentrated during evaporation. Therefore, the growth of thermophilic bacteria is favoured during early stages of evaporation and is inhibited during the later stages of evaporation.

In evaporation, different water activities were represented by different solids percentages. Higher solids level in the RSM means lower water activity for microbial growth (Figure 12).

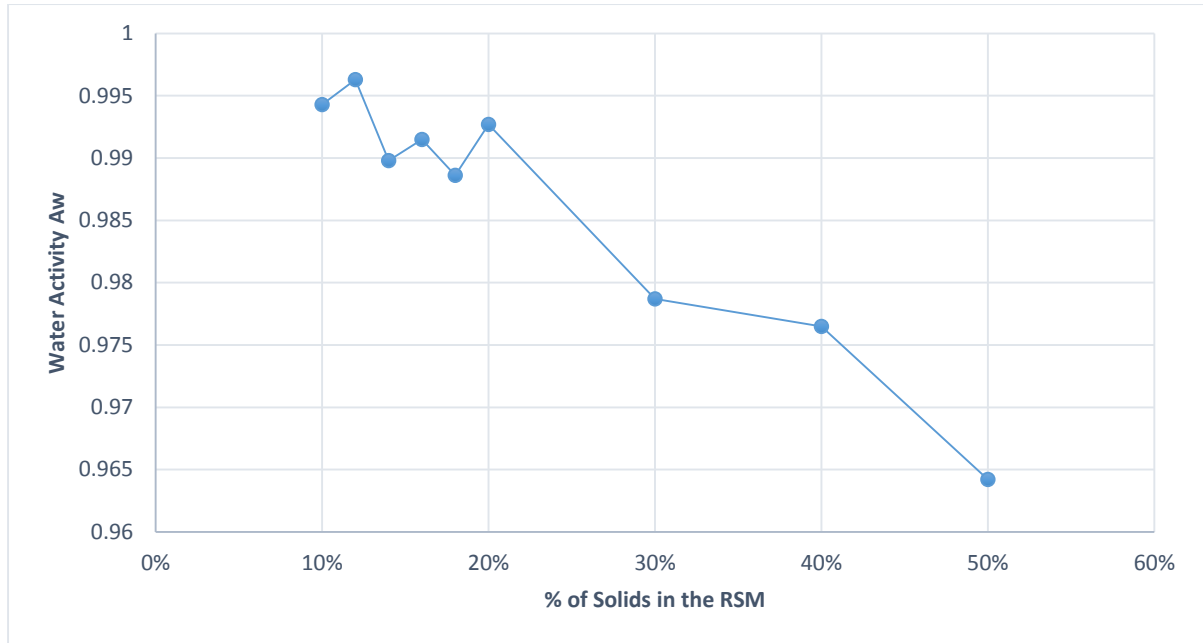


Figure 12: Water activities versus solids in RSM.

Water activities for RSM of different solids – 10, 12, 14, 16, 18, 20, 30, 40 and 50% solids. Graph was reproduced from one-off water activity measurements done by Ms Sreeni Pathirana at the University of Auckland, Auckland, New Zealand, in 2013 using an AquaLab 4TE dew point water activity meter (AquaLab, Pullman, WA, USA).

5.2.1 Experimental Procedures: Testing Boundary Conditions

Cultures were prepared as described in Section 3.3.3. Sterile skim milks with different solids percentages were made according to the milk preparation procedure in Section 3.2.1.

The bacterial culture (1 ml) was diluted in 99 ml of sterile RSM of the appropriate solids and was incubated in the shaking water bath set at the appropriate temperature for 8 h (Table 8). Samples (1 ml) were taken at inoculation (T_0) and after 8 h of incubation (T_8). Triplicate samples were taken for each point and were transferred into separate BacTrac cells containing 9 ml of sterile TSB medium. Then the BacTrac was run and monitored at 55°C for 24 h before readings were taken. Each combination of isolate, temperature and solids was done in triplicate to ensure accuracy.

Table 8: Testing boundary conditions of experiments for factorial design work

No.	Isolate Used	Temperature (°C)	Solids (%)
1	Geo1 and Anoxy2	40, 70	10, 40
2	Geo1 and Anoxy2	40, 65	10, 35
3	Geo1 and Anoxy2	40, 60	10, 30
4	Geo1 and Anoxy2	40, 60	10, 30
5	Geo1 and Anoxy2	40, 60	10, 20, 30
6	Geo1 and Anoxy2	40, 60	15
	CBF 5 and TRGT 9	40, 60	15, 30
7	Geo1 and Anoxy2	40, 60	18
	Anoxy2	70	18
	CBF 5 and TRGT 9	40, 60	25
8	Geo1 and Anoxy2	70	10
	CBF 5 and TRGT 9	40, 60	20
	TRGT 9	70	20

Geo1, Anoxy2, CBF 5 and TRGT 9 were tested under different combinations of temperature and levels of solids in the milk using the BacTrac. Each sample/isolate was tested at all different combinations of temperature and solids listed for each run. Detailed data for each run can be found in the Appendix 13 in the data CD.

5.2.2 Results: Testing Boundary Conditions

The log counts from T_0 and T_8 were compared to determine whether or not there was planktonic growth. These results indicated the realistic boundary limits of the growth range of various strains, such as the highest/lowest temperature and the highest/lowest solids.

For Geo1, the growth temperature range for planktonic growth is 40 – 65°C. The growth rate for Geo1 decreases from 60°C to 65°C. The planktonic growth range of percentage of solids is between 10 – 18%, with no growth at 20%. For Anoxy2, the growth temperature range for planktonic growth is 40 – 70°C. The growth rate for Anoxy2 decreases from 65°C to 70°C. The planktonic growth range of percentage of solids is between 10 – 14%, with no growth at 16% or 18% (tested with CDC reactor run, detailed results not shown).

Table 9: Factorial experimental plan for Geo1 and Anoxy2 CDC reactor runs

Lab ID/Species	Temperature Range (°C)	Solids Range (%)
Geo1	40, 50, 60	10, 14, 18
Anoxy2	40, 50, 60	10, 12, 14

The conditions in this table were summarized and chosen from the testing of the boundary conditions experimental results listed in Appendix 13 in the data CD. The factors for the factorial experiments were temperature and solids, each at three levels.

After refining the results, to study the effect of different temperatures and solids and their interactions, the CDC reactor experiments were designed factorially based on Table 9.

5.3 CDC Reactor Runs

CDC reactors were used to study the factors influencing the growth of biofilms of Geo1 and Anoxy2. The factorial experiments were set up according to the boundary conditions determined by the previous experiments (Section 5.2). The factors studied were solids and temperature. The factorial experiments were of balanced design with two factors and three levels of each factor.

5.3.1. CDC Reactor Set-up

The CDC biofilm reactor was set up as shown in Figure 11. Coupons, as described in Section 3.4.1, were inserted into the eight coupon holders of the reactor. The inoculated RSM was delivered at a flowrate of 5 ml/min throughout the run. The heating temperatures and milk concentrations varied according to the factorial design.

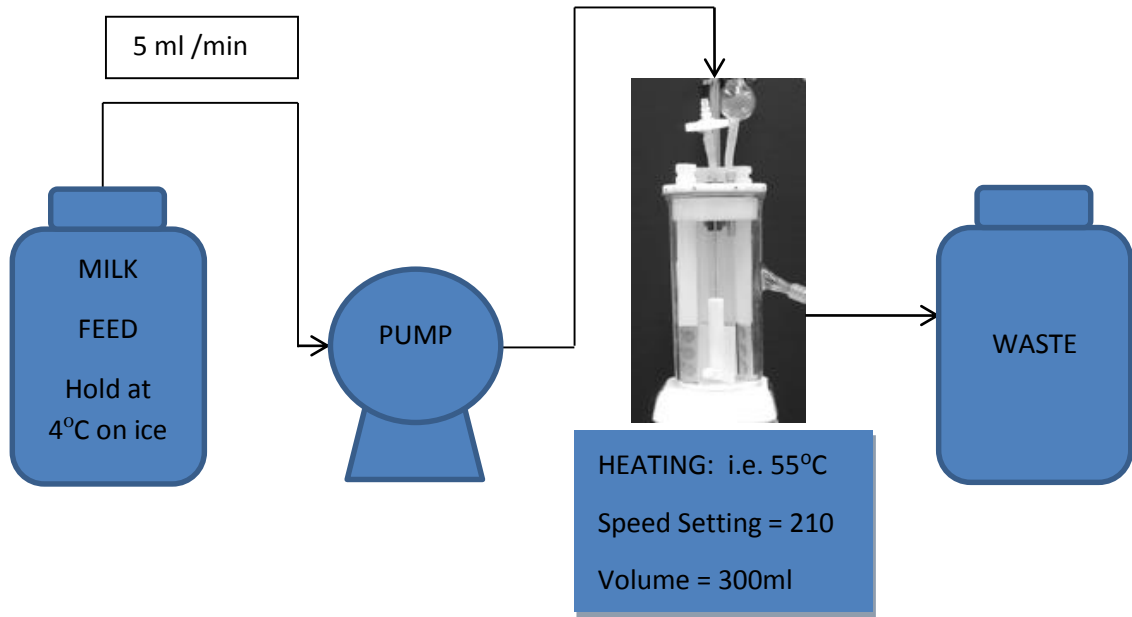


Figure 13: Schematic diagram of CDC reactor set-up.

5.3.2. Factorial Design

The reactor runs were designed factorially and were completed in a randomized order, following the temperature and RSM combinations listed in Table 10.

Table 10: Factorial design of CDC reactor runs

Run No.	Geo1		Anoxy2	
	Temperature (°C)	Solids (%)	Temperature (°C)	Solids (%)
1	40	10	40	10
2	50	10	50	10
3	60	10	60	10
4	40	14	40	12
5	50	14	50	12
6	60	14	60	12
7	40	18	40	14
8	50	18	50	14
9	60	18	60	14

Factorial design of CDC reactor runs for Geo1 and Anoxy2 to test the biofilm growth rate of each microorganism at different temperatures and different levels of solids in the RSM. Detailed data from these experiments can be found in Appendix 14(Geo1) and 17(Anoxy2) in the data CD

5.3.3. Experimental Procedures: CDC Reactor Runs

Cultures were prepared as described previously (Section 3.3.3). RSMs with different solids percentages were prepared as described in Section 3.2.1. The culture was inoculated aseptically into the RSM, using the procedures described in Section 3.3.4, at the start of the reactor run. The milk container was kept cold at 4°C in an ice-filled bucket during the experiment. The system was assembled as shown in Figure 13.

Two coupons were removed from the coupon holders in the CDC reactor at each sampling interval during the 12 h experiment. Coupons were sampled at 1.5 and 3 h and then every hour up to 12 h. Each coupon was inserted into one sterile 15 ml plastic bottle containing 10 ml of sterile TSB. Each coupon was rinsed in the bottle by gentle rotation. Then, the TSB was poured out and each coupon was removed into a separate sterile plastic bottle containing 10 ml of TSB and 5 g of sterile glass beads. The contents of the bottle were vortex mixed thoroughly at maximum speed for 2 min. A 100 µl sample of this TSB was plated on to TSA plates using a spiral plater (Section 3.5.1). Triplicate plates were plated for each coupon using one or two readable dilutions.

Immediately after each run, the reactor was thoroughly rinsed with water to remove any milk residues after the reactor contents had been emptied into a waste reservoir. The reactor was disassembled and soaked in Trigene (Medichem, Barcelona, Spain) overnight to disinfect it. It was then soaked and brushed with detergent (Pyroneg, Thermo Fisher Scientific, Scoresby, VIC, Australia).

The coupons were cleaned according to the cleaning method outlined in Section 3.4.2. The coupons were inserted back into the holders. After rinsing thoroughly in deionized water, the reactor was dried using paper towels and assembled. After covering the ends of all tubing with tin foil, the reactor was autoclaved before the next run.

5.4 Results and Discussion

5.4.1 CDC Reactor Runs: Geo1

The biofilm growth rate and the doubling time of Geo1 at different combinations of temperatures and solids were calculated and are given in Table 11.

Table 11: Factorial CDC reactor run results for Geo1

Run No.	Temperature (°C)	Solids (%)	Lag Phase Length (h)	Growth Rate (/h)	Doubling Time (min)
1	40	10	3	0.847	49.13
2	50	10	1	1.466	28.37
3	60	10	1	1.198	34.72
4	40	14		0	
5	50	14	4	1.238	33.59
6	60	14	1	1.100	37.82
7	40	18		0	
8	50	18		0	
9	60	18		0	

The biofilm growth rate and the doubling time of Geo1 calculated for each different combination of temperature and solids percentage of RSM. Additional temperatures (35°C and 70°C) were checked later in Chapter 8 for establishment of the temperature and growth relationship.

Table 11 shows that the growth rate of Geo1 increased when the temperature was increased from 40 to 50°C and decreased when the temperature was increased from 50 to 60°C.

The growth rate of Geo1 decreased when the solids was increased (solids increases = water activity decreases). There was no growth beyond 18% milk solids. Water activity is a very important factor that influences the growth of Geo1 (Scott, Brooks, Rakonjac, Walker, & Flint, 2007). The growth of Geo1 started to tail off from 14% solids. A concentration of 18% solids inhibited the growth of Geo1. The growth was slowed when the temperature was above 60°C or below 40°C, or the water activity was low (i.e. the solids were above 14%).

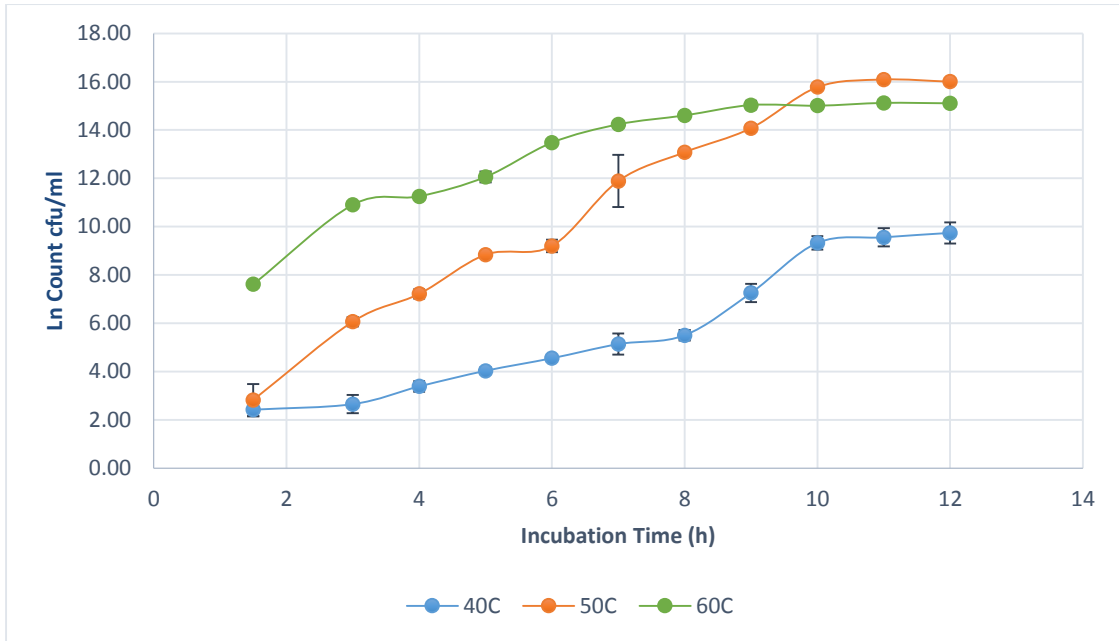


Figure 14: Biofilm growth curves for Geo1 in 10% solids RSM.

The biofilm growth rates of Geo1 at temperatures of 40, 50 and 60°C in 10% solids RSM in the CDC reactor after 12 h. The lag phase ends when the bacteria adapt to the environment and start to grow and enter log phase. The log phase starts when we can detect an increase in cell concentration in the suspension or on the coupon surface. Lag phase for 40°C = 3 h; Lag phase for 50°C = 1 h; Lag phase for 60°C = 1 h;

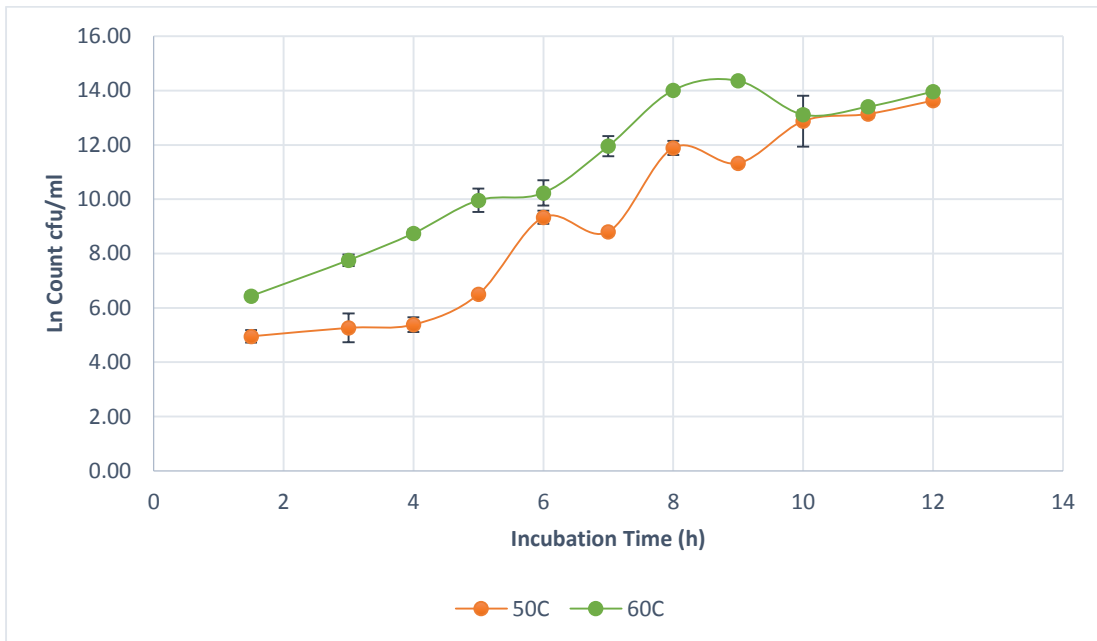


Figure 15: Biofilm growth curves for Geo1 in 14% solids RSM.

The biofilm growth rates of Geo1 at temperatures of 50 and 60°C in 14% solids RSM in the CDC reactor after 12h. There was no growth at 40°C. The lag phase ends when the bacteria adapt to the environment and start to grow and enter log phase. The log phase starts when we can detect an increase in cell concentration in the suspension or on the coupon surface. Lag phase for 50°C = 4 h; Lag phase for 60°C = 1 h;

The lag phase ends when bacteria adapt to the environment and start to grow and enter log phase. The log phase starts when an increase in cell concentration in the suspension or on the coupon surface can be detected. From Figure 14 and Figure 15, the lag phase for the growth of Geo 1 decreased from 3 h to 1 h and 4 h to 1 h, when the temperature was increased from 40 to 60°C, at 10% and 14% solids respectively. According to the growth rate estimation study in the literature (Ratkowsky, Lowry, McMeekin, Stokes, & Chandler, 1983), it was thought that the optimum growth temperature for Geo1 would be between 50 and 60°C at 10% solids.

The factorial experiments were analysed using the statistical software package Minitab. The data were analysed using factorial regression and response surface regression. The results are included in Appendices 3 and 4 (same as Appendix 15 and 16 in the data CD).

The factorial regression allowed us to examine the effects of the main factors and the effects from interactions. The estimated function for the biofilm growth rate using factorial regression is:

Biofilm Growth Rate

$$= -0.048 + 0.055 \times \text{Temperature} - 0.037 \times \% \text{Solids} - 0.002 \\ \times \text{Temperature} \times \% \text{Solids}$$

The response surface regression allowed us to examine not only the effect of the linear terms but also the effects from the two-way interactions and the square terms. The estimated function for the biofilm growth rate using response surface regression is:

Biofilm Growth Rate

$$= -11.482 + 0.432 \times \text{Temperature} + 0.303 \times \% \text{Solids} - 0.004 \\ \times \text{Temperature}^2 - 0.012 \times \% \text{Solids}^2 - 0.002 \times \text{Temperature} \\ \times \% \text{Solids}$$

These regressions were compared with the actual observed growth rates of Geo1 under different conditions (Table 12). Also, additional CDC reactor runs at 35 and 70°C in 10% solids RSM were done to test out the two extreme temperatures of the response surface with 10% solids.

Table 12: Estimated biofilm growth rate versus observed biofilm growth rate of Geo1

Temperature	% of Solids	Actual Growth Rates	Estimated Growth Rates using Response Surface Regression	Estimated Growth Rates using Factorial Regression
oC	%	/h	/h	/h
35	10	0	0.05	0.74
40	10	0.85	0.68	0.90
50	10	1.47	1.36	1.23
60	10	1.20	1.29	1.56
70	10	1.05	0.45	1.89

Estimated biofilm growth rates using response surface regression and factorial regression compared with observed biofilm growth rates of Geo1 at different temperatures in 10% solids RSM. The 40°C, 50°C and 60°C data were extracted from the Table 11. Some additional CDC reactor runs at 35 and 70°C in 10% solids RSM were done to test out the two extreme temperatures of the response surface with 10% solids.

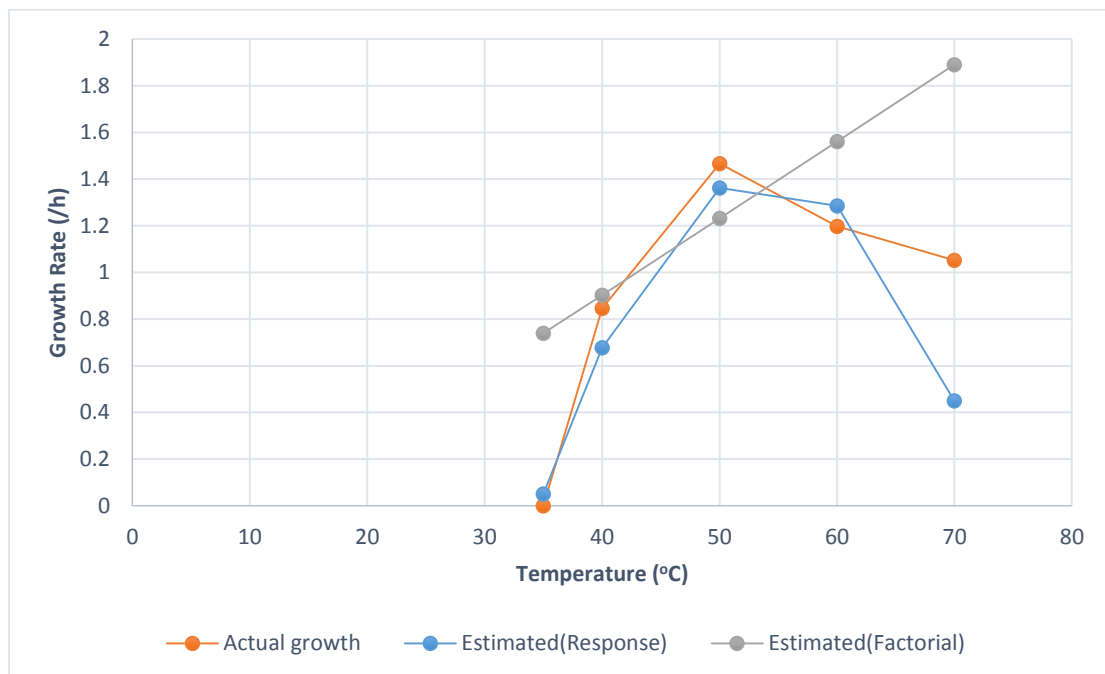


Figure 16: Estimated biofilm growth rates versus actual biofilm growth rates of Geo1.

Estimated biofilm growth rates of Geo1 using factorial and response surface regressions (Minitab) compared with the actual biofilm growth rates in 10% solids RSM at different temperatures.

Figure 16 shows that the response surface regression did take account of the non-linearity, but the discontinuity of the data was not included (i.e. the growth rates were zero at temperatures lower than 35°C). Because of the nature of microbial growth and the activity of key enzymes, microorganisms do not grow above or below certain temperatures and water activities (Ratkowsky, Lowry, McMeekin, Stokes, & Chandler, 1983). As there are always constraints on microbial growth, the growth rates under different conditions will always be discontinuous (i.e. there is no growth above or below certain temperatures).

The constraints for Geo1 were:

$$\text{Growth rate} = 0, \text{ when Temperature} > 80^{\circ}\text{C}$$

$$\text{Growth rate} = 0, \text{ when Temperature} < 35^{\circ}\text{C}$$

$$\text{Growth rate} = 0, \text{ when \% Solids} > 18\%$$

The above models did not include the constraints listed and the discontinuity of the data (i.e. no growth beyond constraint conditions). After consulting with statistician Dr Robin Hankin (2013, personal communication), it was suggested that there was no readymade regression that would fit the data and would consider the discontinuity of the data. The model would give invalid output (negative growth rates) if the discontinuity of the data were not considered.

However, it was also suggested that estimation could be achieved by joining two adjacent data points and using the straight line to estimate the growth rate within that range (Figure 17).

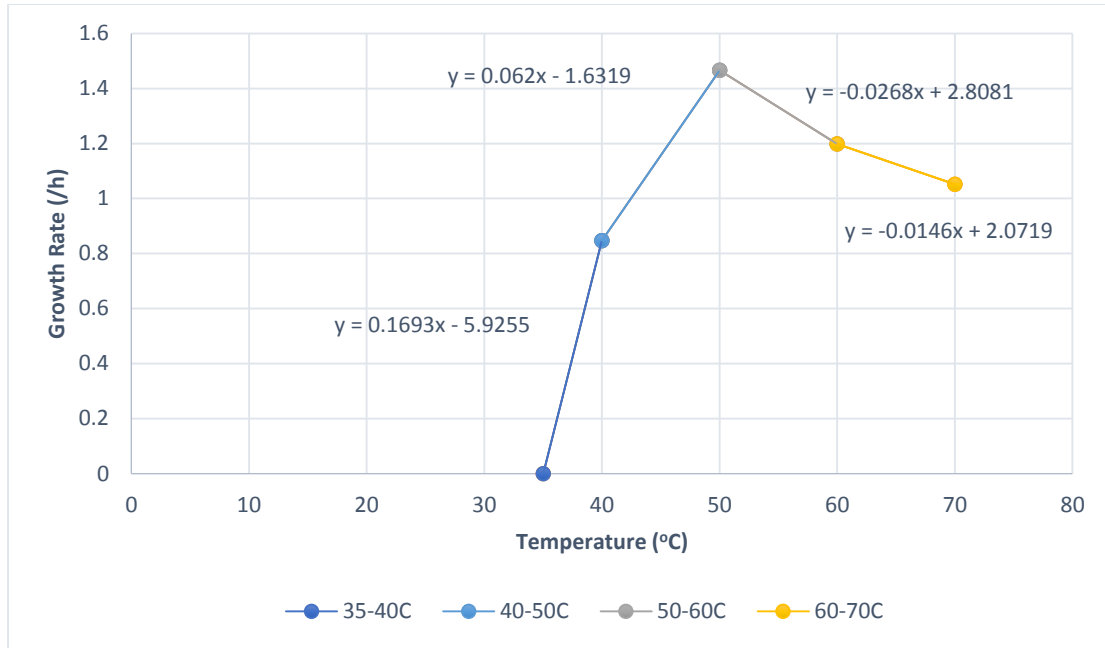


Figure 17: Estimated Geo1 biofilm growth rate equations based on actual growth.

Estimated biofilm growth rate equations for the different temperature ranges based on the actual biofilm growth rates of Geo1 in 10% solids RSM. Equations were developed by joining two adjacent data together by a straight line.

The equations for calculating biofilm growth rate of Geo1 under 10% RSM from Figure 17 based on different temperatures are:

$$\text{Biofilm Growth Rate}_{35-40^{\circ}\text{C}} = 0.169 \times \text{Temperature} - 5.926$$

$$\text{Biofilm Growth Rate}_{40-50^{\circ}\text{C}} = 0.062 \times \text{Temperature} - 1.632$$

$$\text{Biofilm Growth Rate}_{50-60^{\circ}\text{C}} = -0.027 \times \text{Temperature} + 2.808$$

$$\text{Biofilm Growth Rate}_{60-70^{\circ}\text{C}} = -0.015 \times \text{Temperature} + 2.072$$

In this study, it was found that the growth rate became zero between 35 and 40°C at the low temperature end and between 70 and 80°C at the high temperature end. For future studies, a more accurate estimate of the temperature limits for the growth of Geo1 could be achieved by more having data points (i.e. smaller temperature intervals).

5.4.2 CDC Reactor Runs: Anoxy2

Compared with Geo1, the growth range for Anoxy2 was narrower. Growth was limited to 50–60°C in 10% solids RSM. There was no growth from 40 to 60°C in 12 and 14% solids RSM shown on Figure 18 and Figure 19. There was also no growth at 40°C in 10% solids RSM.

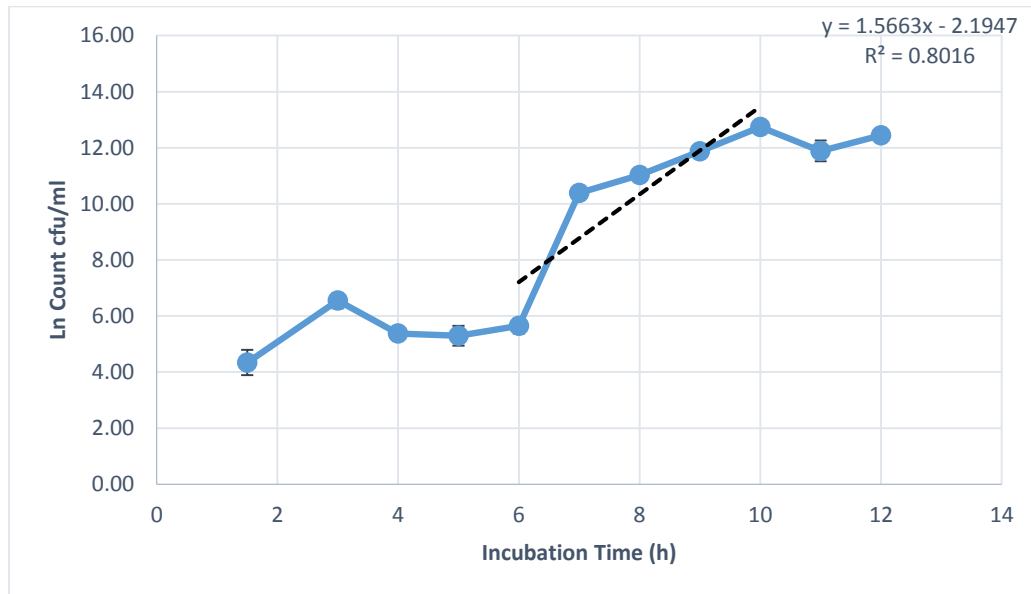


Figure 18: Biofilm growth curve for Anoxy2 at 50°C in 10% solids RSM.

Biofilm growth curve for Anoxy2 from the CDC reactor run at 50°C in 10% solids RSM for 12 h. The dashed line is the gradient of the log phase for calculating the maximum specific growth rate. The lag phase ends when the bacteria adapt to the environment and start to grow and enter log phase. The log phase starts when we can detect an increase in cell concentration in the suspension or on the coupon surface. Lag phase for 50°C = 6 h;

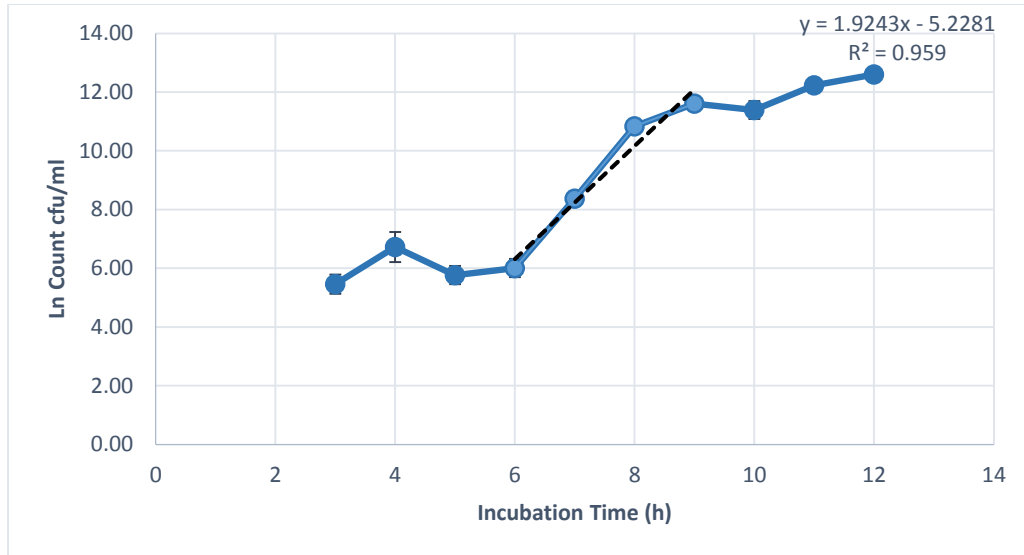


Figure 19: Biofilm growth curve for Anoxy2 at 60°C in 10% solids RSM.

Biofilm growth curve for Anoxy2 from the CDC reactor run at 60°C in 10% solids RSM for 12 h. The dashed line is the gradient of the log phase for calculating the maximum specific growth rate. The lag phase ends when the bacteria adapt to the environment and start to grow and enter log phase. The log phase starts when we can detect an increase in cell concentration in the suspension or on the coupon surface. Lag phase for 60°C = 6 h;

In 10% solids RSM, Anoxy2 grew faster at 60°C than at 50°C (comparing the gradients of two growth curves on Figure 18 and Figure 19). There was no growth at 40°C within 12 h. There was also no growth in 12 or 14% solids RSM.

Because of the lack of growth data in the factorial experiments, there was no model that could be used at this stage. However, two adjacent data points were joined to estimate growth within the range (Figure 20).

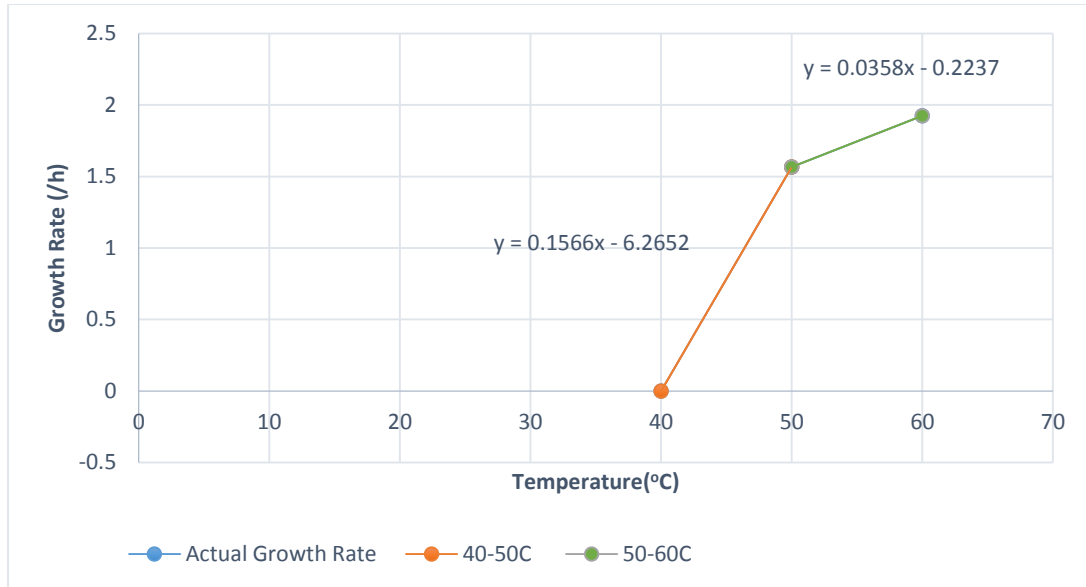


Figure 20: Estimated Anoxy2 biofilm growth rate equations based on actual growth.

Estimated biofilm growth rate equations for different temperature ranges based on the actual biofilm growth rates of Anoxy2 in 10% solids RSM. Equations were developed by joining two adjacent data together by a straight line.

The equations for calculating biofilm growth rate of Anoxy2 under 10% RSM based on different temperatures are:

$$\text{Biofilm Growth Rate}_{40-50^{\circ}\text{C}} = 0.1566 \times \text{Temperature} - 6.2652$$

$$\text{Biofilm Growth Rate}_{50-60^{\circ}\text{C}} = 0.0358 \times \text{Temperature} - 0.2237$$

5.5 Summary

The results from this preliminary study provided us with the extreme points for constructing first approximation growth response surfaces for the chosen isolates. Geo1 grew at 40–60°C in 10% solids RSM and at 50–60°C in 14% solids RSM; 18% solids was inhibitory. Anoxy2 grew only at 50–60°C in 10% solids RSM, with no growth beyond 10% total solids. Scott, Brooks, Rakonjac, Walker, & Flint (2007) determined that *G. stearothermophilus* occurs mostly in evaporators, whereas *A. flavithermus* occurs mainly in the preheating section. This was proven by the current

study: the growth range of *G. stearothersophilus*, in terms of both temperature and water activity, was wider than that of *A. flavithermus*, which allowed *G. stearothersophilus* to grow in a tougher environment, such as the evaporators.

Because of the discontinuous nature of the data, there was no readymade mathematical model that would fit them. However, an equation was generated by linking two adjacent data points to produce an indicative tool to estimate growth within the linked range.

6 Temperature-cycling Experiments

6.1 Outline

Temperature cycling is a potential novel technology for disrupting thermophile growth in the dairy industry. Previous studies have shown the potential of temperature cycling in controlling streptococci (Knight, Nicol, & McMeekin, 2004). The same concept may be able to control the growth of thermophilic bacilli. However, the success of this concept depends on setting the correct degree and frequency of temperature shift and this may need to vary depending on the growth limits of different strains. This chapter contains the layout of the temperature-cycling experiments.

The results from the temperature-cycling experiments for Geo1 are discussed in the following order.

- Thermocycling (sine wave):
 - 55–30°C; (Detailed data in Appendix 18 in the data CD)
 - 55–35°C. (Detailed data in Appendix 19 in the data CD)
- Thermospiking (square wave):
 - 55–30°C; (Detailed data in Appendix 20 in the data CD)
 - 55–35°C; (Detailed data in Appendix 21 in the data CD)

Investigations into the effect of preheating pipes on the growth of Geo1, the effect of temperature step changes on bacterial viability and the effect of cold shock on spore formation are discussed. The aim of the temperature-cycling experiments was to study the formation of biofilms of Geo1 under different temperature-cycling regimes.

6.2 Temperature-cycling Experiments

The aim of the temperature-cycling experiments was to investigate the possibility of implementing a temperature-cycling regime into the preheating section of a milk

manufacturing plant before the evaporators, to reduce thermophiles. All thermocycling and thermospiking experiments were done using 10% RSM (prepared from gamma-sterilized skim milk powder in sterile deionized water).

The purpose of temperature cycling was to use temperature changes to disrupt the growth of biofilms of these thermophiles. As these thermophiles can survive up to 65–70°C, temperature changes/spikes using the lower extremes of the growth range appear to be more efficient in controlling biofilm development and growth (Aplin & Flint, 2007).

Geo1 was chosen for this part of the study, because this isolate is likely to be more problematic to the dairy industry than Anoxy2 because of its survivability under a wider range of growth conditions.

Thermocycling refers to experiments with the temperature increasing and decreasing smoothly in a sine wave pattern. **Thermospiking** refers to experiments with the temperature increasing and decreasing sharply in a square wave pattern.

6.2.1. Temperature-cycling System

The temperature-cycling experiments were achieved using hexagonal-shaped stainless steel laboratory-scale reactors on a modified PCR machine (thermocycler) with a controlled temperature profile. The hexagonal reactors were made of 316L stainless steel with 2B surface finish especially for the study by Fonterra Research & Development Centre, Palmerston North, New Zealand.

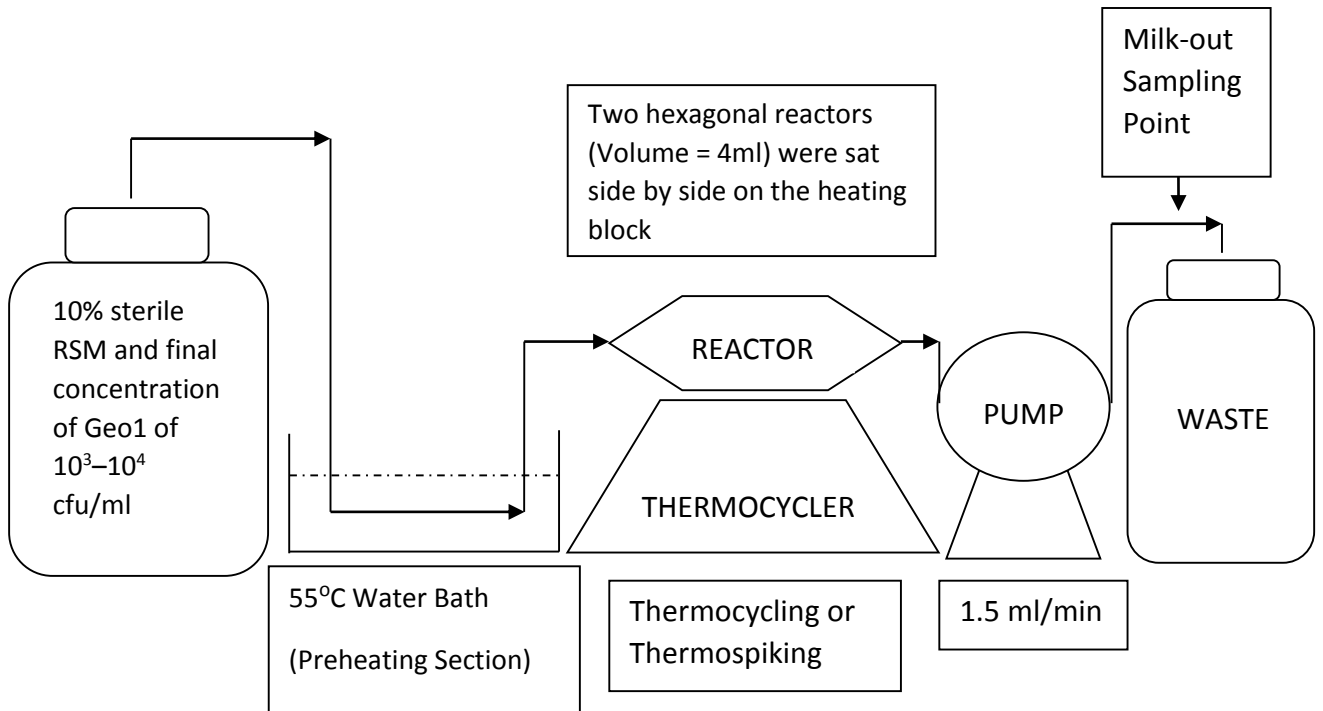


Figure 21: Experimental set-up of the thermocycler system.

Temperature-cycling system developed by Massey University for this study using custom-made stainless steel hexagonal reactors (two identical reactors sit side-by-side) and a modified thermocycler PCR machine. The volume of the hexagonal reactor is 4ml. The flow rate of the system was set to be 1.5ml/min.

The system was linked as indicated in Figure 21. The lid of the thermocycler (Techne PHC-3 PCR thermocycler, John Morris Scientific, Palmerston North, New Zealand) and the metal tube block were removed. Two reactors were arranged side by side on the heating block of the thermocycler with a layer of copper coated with silicone heat transfer compound (Unick Chemical Corp., Taiwan, China) sandwiched in between to enhance heat conductivity and transfer. Each outlet reactor pipe had a thermocouple inserted and linked to a digital thermometer, which was sealed with hot silicone glue, to monitor the temperature.

6.2.2. Experimental Procedures: Temperature Cycling

Sterile RSM (10% solids) was made according to Section 3.2.1. Geo1 culture was grown as described in Section 3.3.3. The RSM feed was inoculated as described in Section 3.3.4. The system was assembled aseptically, as shown in Figure 21

The flowrate used in the experiment was 1.5 ml/min to minimize planktonic growth within the system based on the doubling time of the bacteria (t_D) and the size of the reactor.

$$\text{Mean Residence Time} = \frac{\text{Volume of the system (ml)}}{\text{Flow rate of the system (ml/min)}}$$

$$\text{Mean Residence time} = \frac{4\text{ml}}{1.5\text{ml/min}} = 2.67 \text{ minutes} \ll t_D (18\text{minutes})$$

The thermocycler was programmed to ramp in either thermocycling mode or thermospiking mode according to the directions in Section 6.3 and Section 6.4. The milk-out sampling point was located before the milk stream went to waste. Inoculum and milk-in samples (milk entering the reactor) were taken at time 0. Milk-out samples (milk leaving the reactor) were taken every 2 h for the first 12 h and at the 24 h end point. For the milk flowing out of each of the two parallel reactors, 10 ml was sampled into separate 20 ml sterile glass bottles at each sampling time interval. A 100 μ l sample was plated on to each of triplicate TSA plates using the spiral plater. The plates were read after incubation at 55°C for 24 h.

6.2.3. Hexagonal Reactor Sampling

In all the temperature-cycling experiments, the hexagonal reactor surfaces were sampled at the end of the 24 h run, after each reactor had been rinsed with sterile TSB to wash off any loosely attached cells. Then the whole reactor (with lid taken off) was vortex mixed in a 100 ml bottle with 60 ml of sterile TSB and 20 g of sterile glass beads for 2 min on maximum speed. The TSB was plated on to triplicate TSA plates using spiral plater and incubated overnight at 55°C.

6.2.4. Cleaning Procedure

After the experiments, all the tubes and reservoirs were washed and sanitized using Trigene (Medichem, Barcelona, Spain) and were thoroughly rinsed with deionized

water. The hexagonal reactors were brushed with detergent (Pyroneg, Thermo Fisher Scientific, Scoresby, VIC, Australia) and then treated using the cleaning procedure for coupons (Section 3.4.2). Everything was then autoclaved at 121°C for 15 min before the next use.

6.3. Thermocycling (Sine Wave)

6.3.1. Thermocycler Calibration (Sine Wave)

The thermocycler was calibrated, so that a smooth heating wave with different periods of sine wave could be achieved.

Table 13: Thermocycler calibration to achieve sine wave heating

	Ramp Rate Setting = 6	Ramp Rate Setting = 4	Ramp Rate Setting = 2	Ramp Rate Setting = 1
Flowrate (ml/min)	1.5	1.5	1.5	1.5
Water Bath Preheater (°C)	55	55	55	55
Cycle Temperature (°C)	30–55–30	30–55–30	30–55–30	30–55–30
Heating Cycle Time (min) (from 30 to 55°C)	5	8.5	12	25
Cooling Cycle Time (min) (from 55 to 30°C)	5	8.5	12	25
Full Cycle Time (min) (Period)	10	17	24	50

The thermocycler PCR machine was calibrated using RSM to determine the setting for generating sine waves with periods of 10, 20 and 50 min.

6.3.2. Factorial Design of Thermocycling (Sine Wave) Experiments

The thermocycler was programmed to achieve sine waves with different periods as shown in Figure 22 and Table 14.

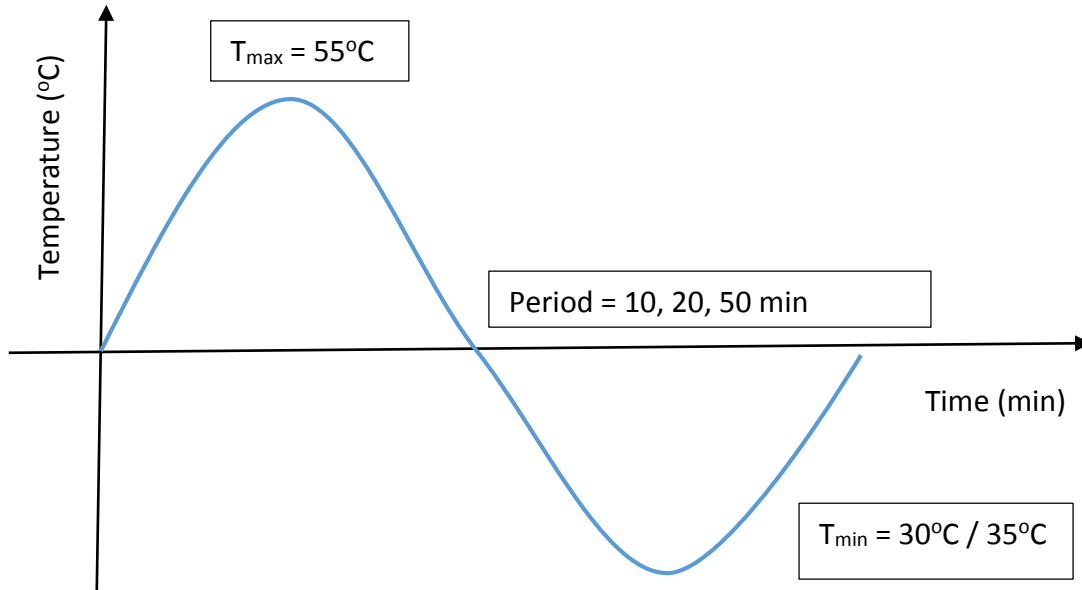


Figure 22: Thermocycling (sine wave) temperature profile.

The actual temperature curve from the milk runs conformed well to theoretical heating curve. The thermocycler was calibrated based on actual milk temperature measured by thermocouples in the exit stream. When the thermocycler was calibrated, they were calibrated based on the actual milk temperature. The thermocycler was modified so the heat transfer is maximized with heat transfer paste and insulation to prevent heat loss.

Table 14: Factorial design of thermocycling (sine wave) experiments for Geo1

Run No.	Temperature Difference (°C)	Period of Sine Wave (min)
1	55–30	50
2	55	Control, no ramping
3	55–30	20
4	55–30	10
5	55	Control, no ramping
6	55–35	50
7	55–35	10
8	55–35	20

Factorial design of the thermocycling (sine wave) experiments for Geo1 at different temperatures and periods of sine wave in 10% RSM.

6.3.3 Results and Discussion of Thermocycling (Sine Wave)

6.3.3.1 55–30°C Thermocycling Regime

Figure 23 shows the results from the Geo1 55–30°C thermocycling runs with different periods (10 min, 20min, 50min, and non-cycled control runs).

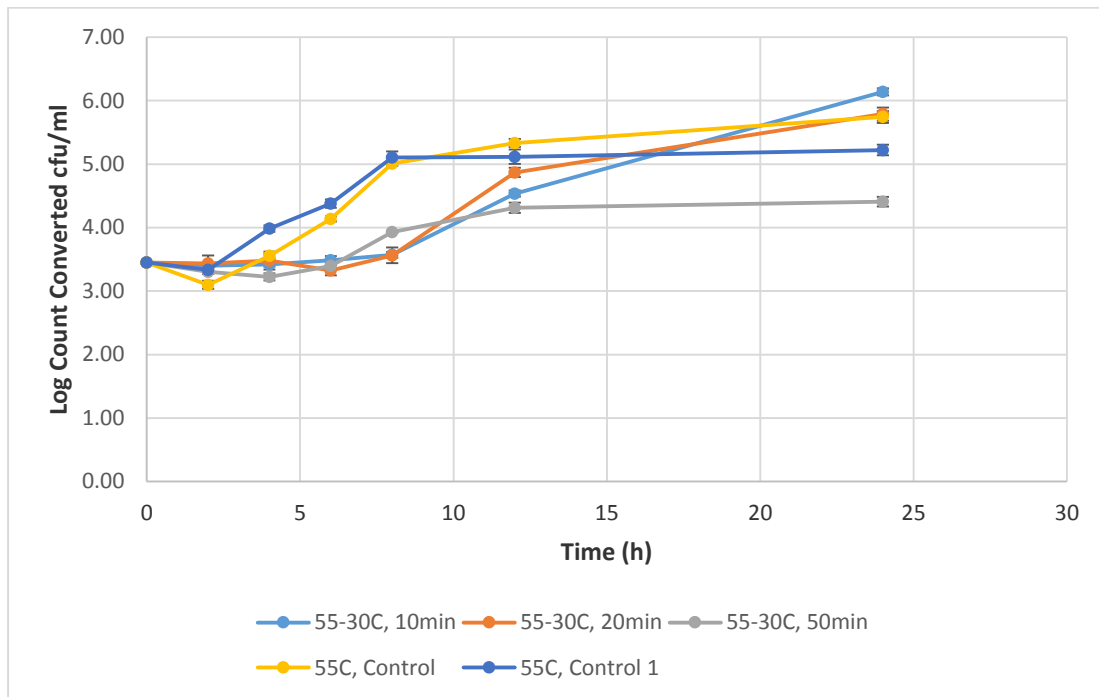


Figure 23: Geo1 thermocycling (sine wave) normalized data (55–30°C).

The bacterial counts in the milk-out samples of Geo1 for different sine wave periods of the 55–30°C thermocycling conditions for 24 h in 10% solids RSM; Y-axis = the log count of the milk-out sample (cfu/ml); X-axis = time (h). The different sine wave periods tested were 10, 20 and 50 min. (Detailed data in Appendix 18 in the data CD). The mean and standard deviation of triplicate plate readings of the same sampling point (3 replicates for each reactor, so 6 replicates per point) were calculated and converted into log counts then graphed above. The points on the graph are the mean of two independent reactors, reactor 1 and reactor 2. The raw data was normalized to the lowest T0 (milk-in) according to get the normalized data. +/- one SD was plotted as error bars.

Using this temperature shift, the lag phase was extended compared with non-cycled control runs (Figure 23). The non-cycled control runs had a 2 h lag phase whereas thermocycling at 30°C with sine wave periods of 10, 20 and 50 min resulted in lag phases of 8, 8 and 6 h respectively.

From the normalized growth data (Figure 23), in which the inoculum concentration for each run was the same, thermocycling at 30°C with a sine wave period of 50 min produced a reduction of 1 – 1.5 log in bacterial counts in the outflowing milk after 24 h. After 12 h, the counts for thermocycling with a sine wave period of 50 min were 1 log lower than for the control runs. Thermocycling at 30°C with sine wave periods of 10 and 20 min gave no reduction in the counts of thermophilic bacteria in the milk after 24 h compared with control runs.

6.3.3.2 55–35°C Thermocycling Regime

Figure 24 shows the results from the Geo1 55–35°C thermocycling runs with different periods (10 min, 20min, 50min, and non-cycled control runs).

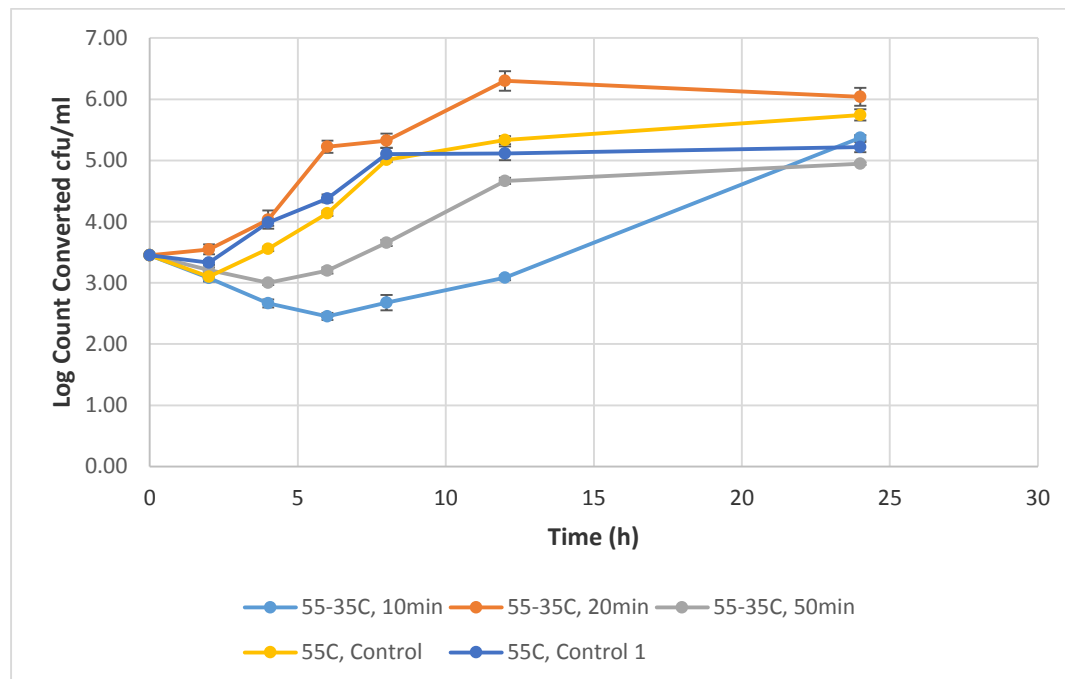


Figure 24: Geo1 thermocycling (sine wave) normalized data (55–35°C).

The bacterial counts in the milk-out samples of Geo1 for different sine wave periods of the 55–35°C thermocycling conditions for 24 h in 10% solids RSM; Y-axis = the log count of the milk-out sample (cfu/ml); X-axis = time (h). The different sine wave periods tested were 10, 20 and 50 min. (Detailed data in Appendix 19 in the data CD) The mean and standard deviation of triplicate plate readings of the same sampling point (3 replicates for each reactor, so 6 replicates per point) were calculated and converted into log counts then graphed above. The points on the graph are the mean of two independent reactors, reactor 1 and reactor 2. The raw data was normalized to the lowest T0 (milk-in) according to get the normalized data. +/- one SD was plotted as error bars.

Using this temperature shift, the lag phase was extended with sine wave periods of 10 and 50 min. The non-temperature-cycled control runs had a 2 h lag phase, whereas thermocycling at 35°C with sine wave periods of both 10 and 50 min resulted in a lag phase between 6 to 8 h.

Figure 24 shows that, when the inoculum concentration for each run was the same, thermocycling at 35°C with a sine wave period of 20 min gave no obvious reduction in bacterial counts in the outflowing milk after 24 h. However, with sine wave periods of 10 and 50 min, the bacterial counts in the outflowing milk were reduced by approximately 1 log during the lag phase and by 2 and 0.5 log respectively after 12 h.

6.3.3.3 Discussion on Thermocycling (Sine Wave) Regimes

From Figure 25 below, it can be seen that the growth curve patterns for thermocycling at 30 and 35°C were very different. There was an initial reduction in bacterial counts in the outflowing milk during the lag phase in the 35°C runs, whereas this phenomenon was not seen in the 30°C runs. The possible reason for this observation will be explained in Chapter 9.

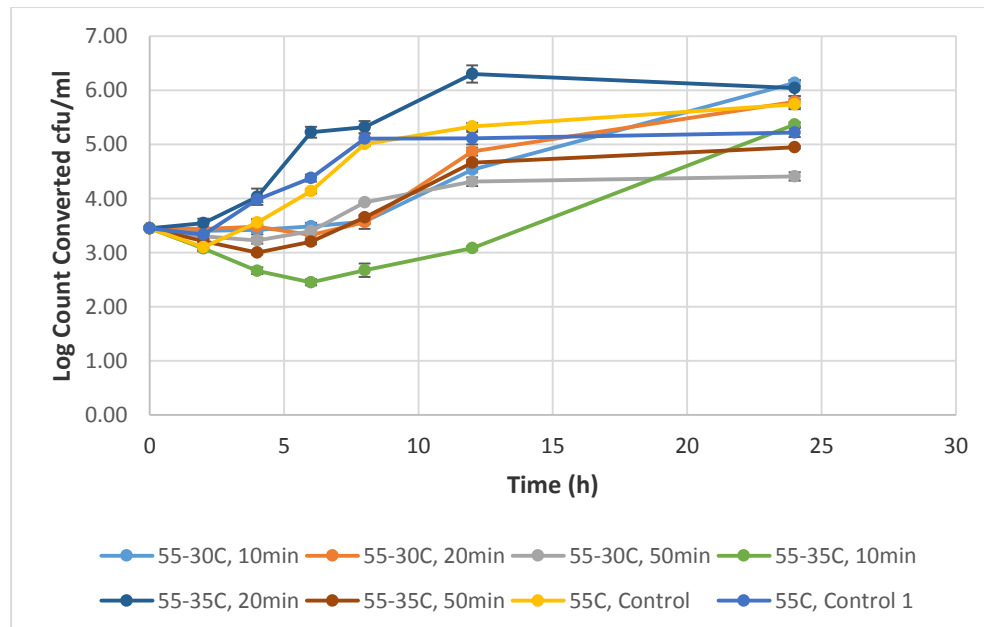


Figure 25: Summary graph of Geo1 thermocycling (sine wave) data.

The bacterial counts in the milk-out samples of Geo1 for different sine wave periods of the 55–35°C and 55–35°C thermocycling conditions for 24 h in 10% solids RSM; Y-axis = the log count of the milk-out

sample (cfu/ml); X-axis = time (h). The different sine wave periods tested were 10, 20 and 50 min. (Detailed data in Appendix 18 and 19 in the data CD). The mean and standard deviation of triplicate plate readings of the same sampling point (3 replicates for each reactor, so 6 replicates per point) were calculated and converted into log counts then graphed above. The points on the graph are the mean of two independent reactors, reactor 1 and reactor 2. The raw data was normalized to the lowest T0 (milk-in) according to get the normalized data. +/- one SD was plotted as error bars.

All thermocycling protocols except for the 10 and 20 min sine wave cycles at 55–35°C produced similar results. Thermocycling at 55–35°C with a sine wave period of 20 min had no effect compared with the control runs. Thermocycling at 55–35°C with a sine wave period of 10 min had the most obvious effect, with a prolonged lag phase and an initial decrease in bacterial counts. This regime may provide the dairy industry with better quality products during the first 12 h of manufacturing runs. An alternative regime would be 55–30°C with a sine wave period of 50 min, producing a shorter lag phase than for the 10 min cycle at these temperatures but resulting in a 1 – 1.5 log reduction in the final bacterial count after 24 h, suggesting that this regime could prolong the manufacturing run length.

6.4 Thermospiking (Square Wave)

6.4.1. Factorial Design of Thermospiking (Square Wave) Experiments

The thermocycler was programmed to achieve a square wave with variable spike times (Figure 26 and Table 15).

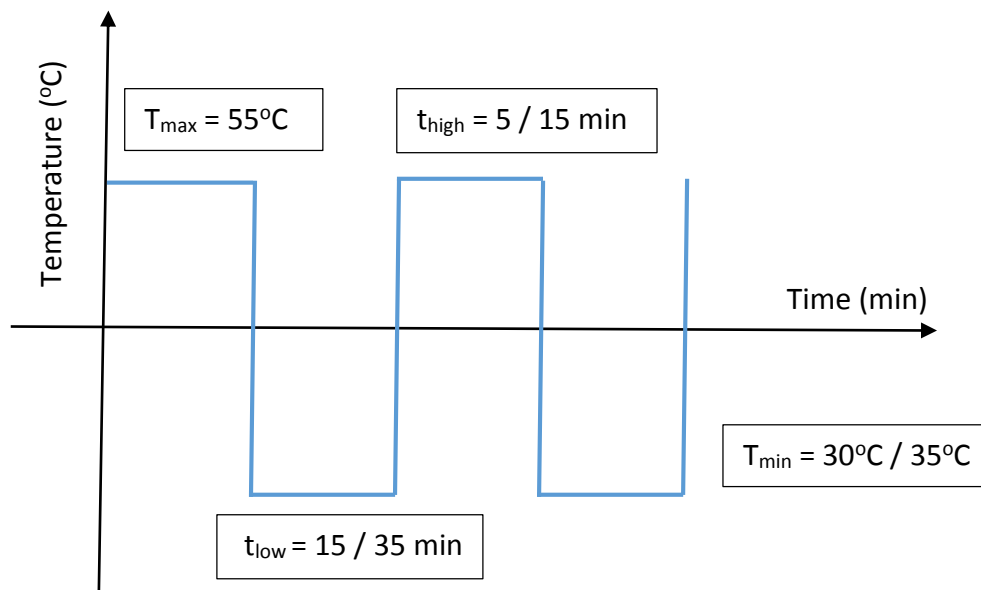


Figure 26: Thermospiking (square wave) temperature profile.

The actual temperature curve from the milk runs conformed well to theoretical heating curve. The thermocycler was calibrated based on actual milk temperature measured by thermocouples in the exit stream. When the thermocycler was calibrated, they were calibrated based on the actual milk temperature. The thermocycler was modified so the heat transfer is maximized with heat transfer paste and insulation to prevent heat loss.

Table 15: Factorial design of thermospiking (square wave) experiments for Geo1

Run No.	Temperature Diff. (°C)	t _{low} 30/35°C (min)	t _{high} 55°C (min)
1	55–30	15	5
2	55–30	35	15
3	55–35	35	15
4	55–35	35	5
5	55–35	15	5
6	55–35	15	15
7	55–30	15	15
8	55–30	35	5

Factorial design of the thermospiking (square wave) experiments for Geo1 at different temperatures and with different times spent at low and high temperatures in 10% RSM.

6.4.2 Results and Discussion of Thermospiking (Square Wave)

6.4.2.1 55–30°C Thermospiking Regime

Figure 27 shows the results from the Geo1 55–30°C thermospiking runs with different time periods spent at low temperature (30°C) and high temperature (55°C).

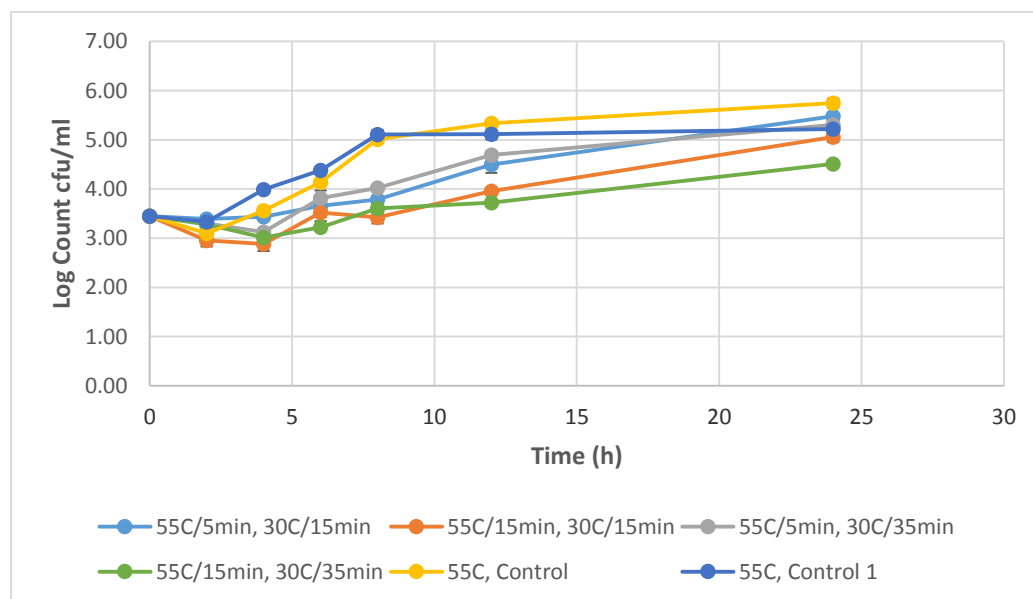


Figure 27: Geo1 thermospiking (square wave) normalized data (55–30°C).

The bacterial counts in the milk-out samples of Geo1 for thermospiking (square wave) conditions of 55–30°C for 24 h in 10% solids RSM; Y-axis = the log count of the milk-out sample (cfu/ml); X-axis = time (h). The data were normalized by shifting and converting on to the same scale using the lowest inoculum; for example, 55°C/5 min, 30°C/15 min = time spent at 55°C was 5 min and time spent at 30°C was 15 min, so that the period of the square wave was 20 min. (Detailed data in Appendix 20 in the data CD) The mean and standard deviation of triplicate plate readings of the same sampling point (3 replicates for each reactor, so 6 replicates per point) were calculated and converted into log counts then graphed above. The points on the graph are the mean of two independent reactors, reactor 1 and reactor 2. The raw data was normalized to the lowest T0 (milk-in) according to get the normalized data. +/- one SD was plotted as error bars.

The square wave regimes increased the lag phase from 2 to 4 h compared with the non-cycled control run. Other interesting observations from Figure 27 are summarised below.

- All the square wave regimes had some reduction in bacterial counts in the first 12 h.
- After 24 h, the counts were similar, except for the 55°C/15 min, 30°C/35 min run, which produced a < 1 log reduction compared with non-cycled control runs.
- The **55°C/5 min runs** (55°C/5 min, 30°C/15 min and 55°C/5 min, 30°C/35 min) had higher counts than the **55°C/15 min runs** (55°C/15 min, 30°C/15 min and 55°C/15 min, 30°C/35 min) throughout the first 12 h.
- After 12 h, the **55°C/5 min runs** (55°C/5 min, 30°C/15 min and 55°C/5 min, 30°C/35 min) had a 0.5 log reduction in bacterial counts, whereas the **55°C/15 min runs** (55°C/15 min, 30°C/15 min and 55°C/15 min, 30°C/35 min) had < 1.5 log reduction compared with the control run.
- The **30°C/15 min runs** (55°C/5 min, 30°C/15 min and 55°C/15 min, 30°C/15 min) had no obvious effect compared with the **30°C/35 min runs** (55°C/5 min, 30°C/35 min and 55°C/15 min, 30°C/35 min) throughout the 24 h of the run.

6.4.2.2 55–35°C Thermospiking Regime

Figure 28 shows the results from the Geo1 55–35°C thermospiking runs with different time periods spent at low temperature (35°C) and high temperature (55°C).

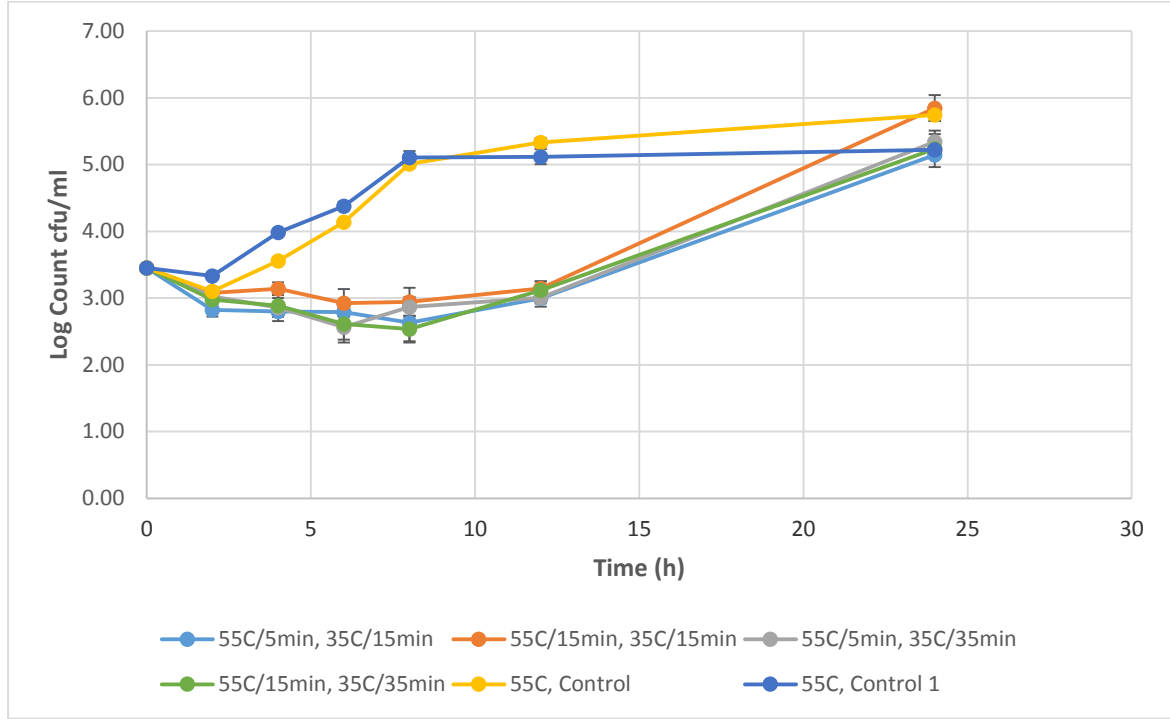


Figure 28: Geo1 thermospiking (square wave) normalized data (55–35°C).

The bacterial counts in the milk-out samples of Geo1 for thermospiking (square wave) conditions of 55–35°C for 24 h in 10% solids RSM; Y-axis = the log count of the milk-out sample (cfu/ml); X-axis = time (h). The data were normalized by shifting and converting on to the same scale using the lowest inoculum; for example, 55°C/5 min, 35°C/15 min = time spent at 55°C was 5 min and time spent at 35°C was 15 min, so that the period of the square wave was 20 min. (Detailed data in Appendix 21 in the data CD) The mean and standard deviation of triplicate plate readings of the same sampling point (3 replicates for each reactor, so 6 replicates per point) were calculated and converted into log counts then graphed above. The points on the graph are the mean of two independent reactors, reactor 1 and reactor 2. The raw data was normalized to the lowest T0 (milk-in) according to get the normalized data. +/- one SD was plotted as error bars.

The lag phase of bacterial growth was generally extended under different square wave regimes at 35°C. The non-cycled control runs had a 2 h lag phase whereas the square wave at 35°C produced a 12 h lag phase.

Other interesting observations from Figure 28 are summarised below.

- All square wave regimes produced a > 2 log reduction in bacterial counts after 12 h. This reduction was not seen after 24 h.
- The **55°C/5 min runs** (55°C/5 min, 35°C/15 min and 55°C/5 min, 35°C/35 min) had no obvious effect compared with the **55°C/15 min runs** (55°C/15 min, 35°C/15 min and 55°C/15 min, 35°C/35 min) throughout the 24 h run.
- The **35°C/15 min runs** (55°C/5 min, 35°C/15 min and 55°C/15 min, 35°C/35 min) had no obvious effect compared with the **35°C/35 min runs** (55°C/5 min, 35°C/35 min and 55°C/15 min, 35°C/35 min) throughout the 24 h run.

Square waves of 55–35°C showed a reduction in bacterial counts over the first 12 h of the run, but did not show an effect after 24 h. This meant that square wave regimes of 55–35°C may allow the industry to produce much better quality products than are achieved currently within the first 12 h. These regimes may not help to extend the run length because the counts at 24 h were similar to those for the non-cycled control.

6.4.2.3 Discussion on Thermospiking (Square Wave) Regimes

Figure 29 shows the results summary from the Geo1 thermospiking runs with different time periods spent at low temperature (30/35°C) and high temperature (55°C).

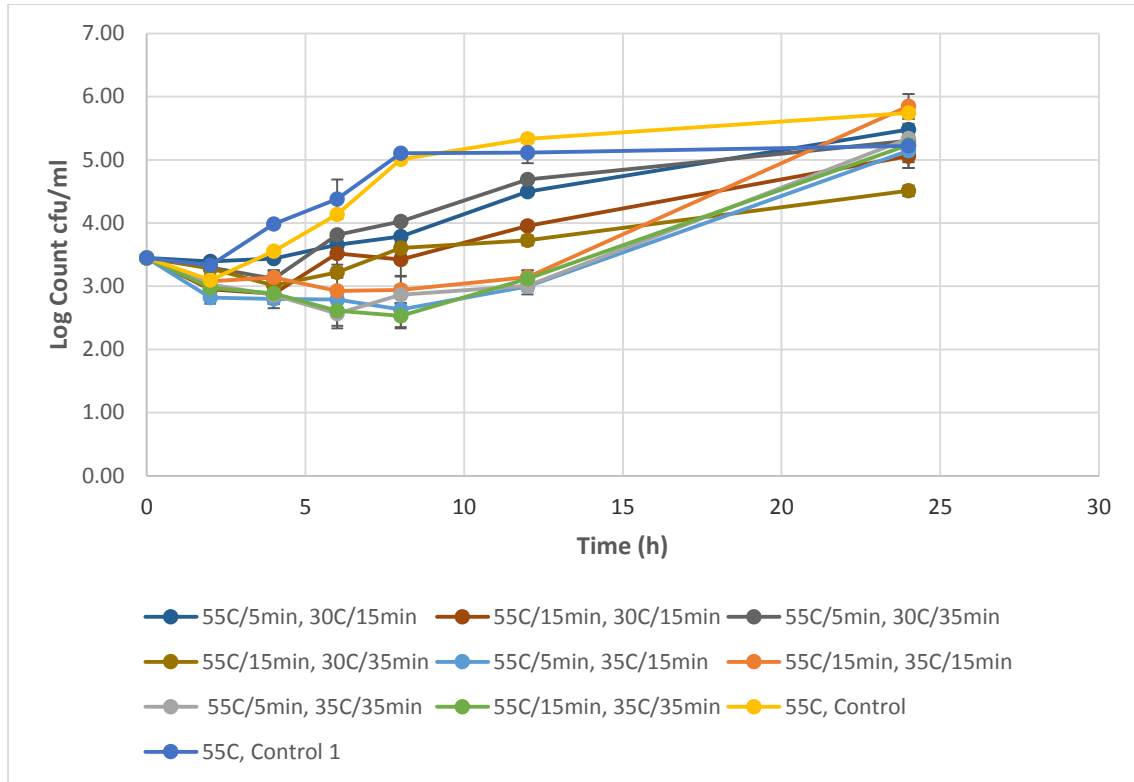


Figure 29: Summary graph of Geo1 thermospiking (square wave) data.

The bacterial counts in the milk-out samples of Geo1 for thermospiking (square wave) conditions of 55–30°C and 55–35°C for 24 h in 10% solids RSM; Y-axis = the log count of the milk-out sample (cfu/ml); X-axis = time (h). The data were normalized by shifting and converting on to the same scale using the lowest inoculum. (Detailed data in Appendix 20 and 21 in the data CD) The mean and standard deviation of triplicate plate readings of the same sampling point (3 replicates for each reactor, so 6 replicates per point) were calculated and converted into log counts then graphed above. The points on the graph are the mean of two independent reactors, reactor 1 and reactor 2. The raw data was normalized to the lowest T0 (milk-in) according to get the normalized data. +/- one SD was plotted as error bars.

The square wave regimes of 55–35°C (Figure 28) had different growth patterns from the square wave regimes of 55–30°C (Figure 27). The 55–35°C square wave regimes showed a 1 log reduction in bacterial counts from the initial inoculum during a 12 h lag phase and the bacterial counts were > 2 log less than for the control runs over the first 10–12 h of the run. The 55–30°C square wave regime produced a 0.5 - 1 log reduction compared with the control runs over the first 10–12 h of the run. All square wave runs produced lower counts than the control runs during the first 12 h.

The 55–35°C square wave regimes can prolong the lag phase from 2 to 12 h, whereas 55–30°C square wave regimes can prolong the lag phase to 4 h. The 55–35°C square

wave regimes reduced the bacterial counts in the prolonged lag phase, which would allow the dairy industry to produce better quality product during the first 12 h of a manufacturing run. The 55°C/15 min, 30°C/35 min square wave regime may have the potential to extend the manufacturing run time, with a < 1 log reduction after 24 h.

6.5. Biofilm Development in Temperature-cycling Experiments

The inner surfaces of the reactor chambers (without lids) of both upper and lower reactors were sampled after temperature cycling for 24 h. The densities of biofilm formation on these inner surfaces (cfu/cm²) after thermocycling experiments are given in Figure 30 and after thermospiking experiments are given in Figure 31.

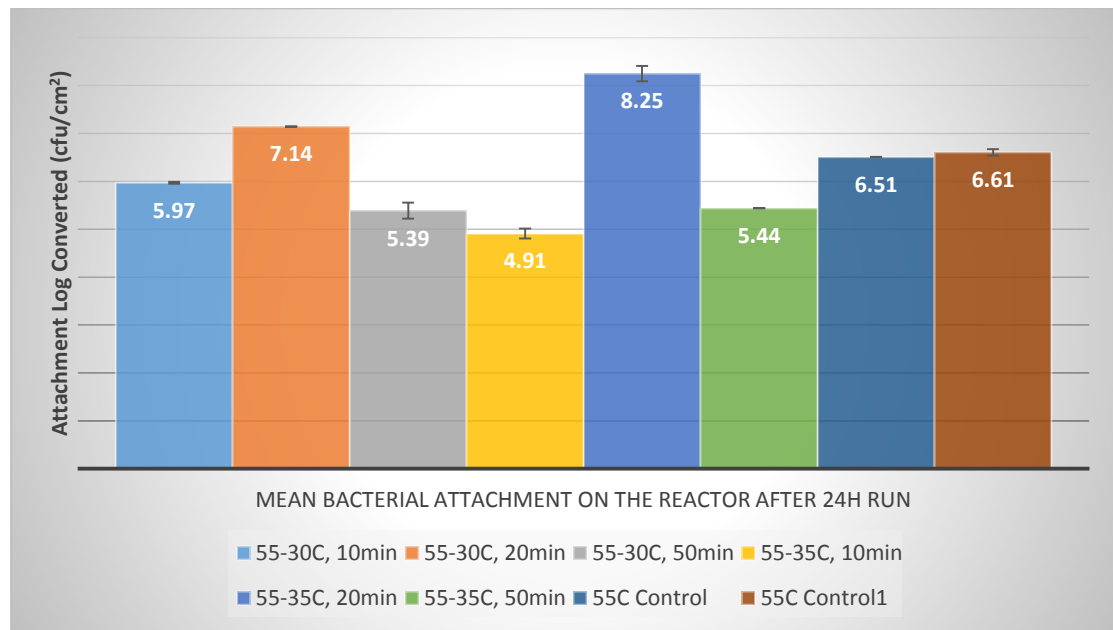


Figure 30: Bacterial attachment on the reactor after 24 h using thermocycling (sine wave).

Biofilm formed on the inner surfaces of the stainless steel reactors. The inner surfaces were sampled by dislodging the bacterial cells in 60 ml of TSB using glass beads and vortex mixing at maximum speed for 2 min. The bacterial concentration of the TSB was enumerated, normalized according to the lowest T₀ value then converted to the bacterial attachment cfu/cm². Mean and standard deviation of the attachment plotted. Bacterial concentration of the TSB (cfu/ml) is converted to attachment (cfu/cm²) = the concentration of the TSB x TSB volume / reactor surface area = Concentration x 60ml / 8cm² (Detailed data in Appendix 22 in the data CD) +/- one SD was plotted as error bars.

Thermocycling runs using a sine wave 35°C with a period of 10 min produced the best reduction in biofilm formation on the inner surfaces, with a 1.5 log reduction compared with the non-thermocycled control after 24 h. Thermocycling runs with a period of 50 min produced 1 log reduction. Those with a period of 20 min were similar to the control. The period of the sine wave was more important than the difference in temperature (55–35 °C or 55–30 °C). When Figure 30 was reorganized according to the different sine wave periods, the least biofilm formed on the reactor surface from thermocycling runs with a period of 10 min. There was less biofilm formed in thermocycling runs with a period of 50 min than in the control runs and the thermocycling runs with a period of 20 min.

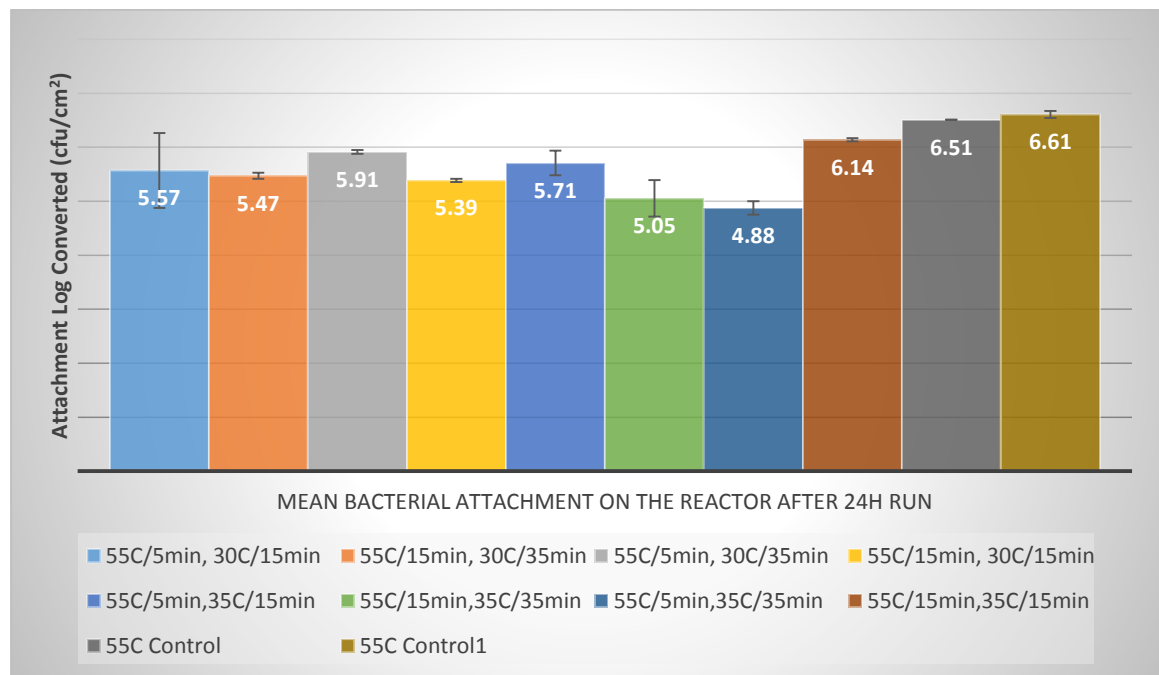


Figure 31: Bacterial attachment on the reactor after 24 h using thermospiking (square wave).

Biofilm formed on the inner surfaces of the stainless steel reactors. The inner surfaces were sampled by dislodging the bacterial cells in 60 ml of TSB using glass beads and vortex mixing at maximum speed for 2 min. The bacterial concentration of the TSB was enumerated, normalized according to the lowest T_0 value then converted to the bacterial attachment cfu/cm^2 . Mean and standard deviation of the attachment plotted. Bacterial concentration of the TSB (cfu/ml) is converted to attachment (cfu/cm^2) = the concentration of the TSB x TSB volume / reactor surface area = Concentration x 60ml / 8cm² (Detailed data in Appendix 23 in the data CD) +/- one SD was plotted as error bars.

The 55°C/5 min–35°C/35 min and 55°C/15 min–35°C/35 min square wave regimes produced a >1.5 log reduction in biofilm formation compared with the control after 24 h (Figure 31). The 55°C/15 min–30°C/15 min square waves produced a > 1 log reduction compared with the control.

Temperature cycling that produces a >1.5 log reduction in counts compared with the counts in the absence of temperature cycling offers a real advantage to a dairy manufacturing plant, enabling a longer run length while providing the potential for the product to remain within specification limits for thermophilic bacterial contamination.

6.6. Investigations of the Preheating Pipes

The thermocycling and thermospiking experiments were done using the ‘inoculation in the milk-in’ method. After the temperature-cycling experiments, the issue of the preheating section arose during discussion with the statistician Dr Robin Hankin (2013, personal communication). In each experiment, 60 cm lengths of silicone tubing were submerged in a water bath maintained at 55°C for 24 h. Thermocycling and thermospiking in the reactors were affected by biofilm formation in the preheating pipes. This biofilm formation will increase the bacteria in the reactor system. Therefore, this part of the study investigated the effect of biofilm formation in the preheating pipe on the thermocycling and thermospiking experiments. This effect was taken into consideration in the mathematical model developed later.

6.6.1. Experimental Procedures: Investigations of the Preheating Pipes

Sterile 10% solids RSM was prepared as described in Section 3.2.1. Geo1 culture was grown as described in Section 3.3.3. The RSM feed was inoculated as described in Section 3.3.4. The system was assembled aseptically as shown in Figure 21. The preheating section was directly connected to the pump without linking to the reactors and the PCR machine. The temperature of the water bath was maintained at 55°C throughout the 24 h period. Inoculum and milk-in samples were taken at time 0. The

entire 30 min of milk-out sample was collected and processed through a 24 h run. All samples were plated on to duplicate TSA plates using the spiral plater and were incubated overnight at 55°C before being read.

6.6.2. Results and Discussion: Investigations of the Preheating Pipes

The bacterial counts from the milk-out samples were plotted against time to visualize the effect of biofilm formation and bacterial attachment on to the preheating pipes over the 24 h run (Figure 32).

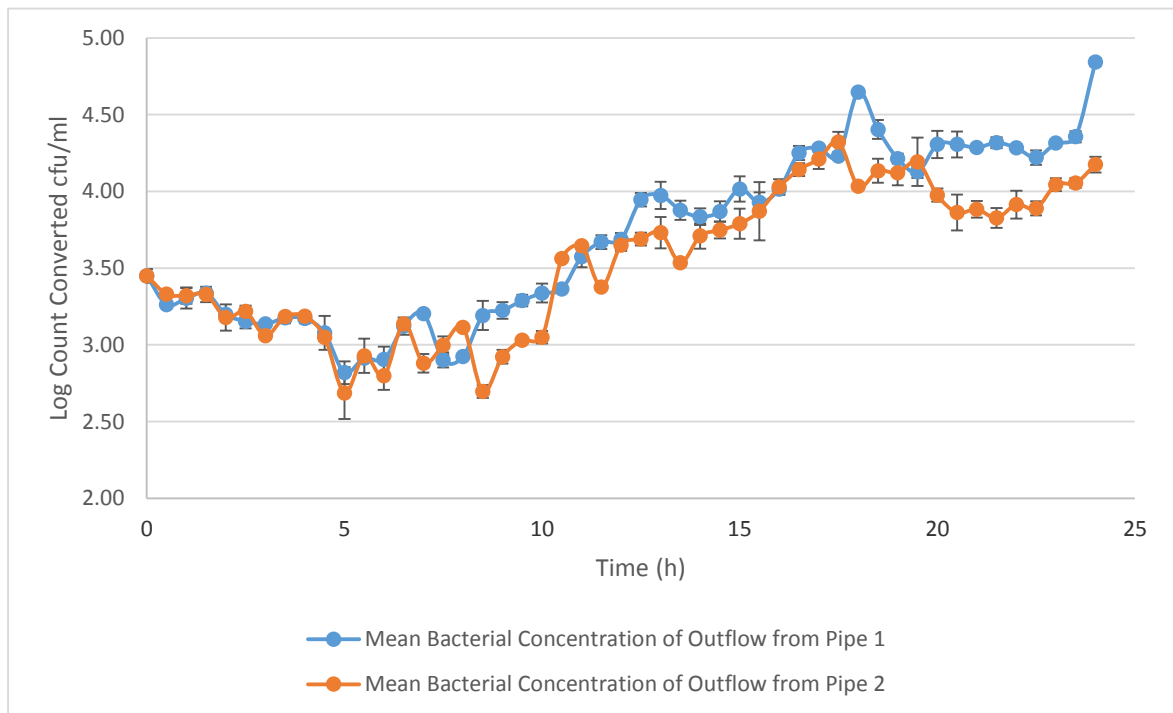


Figure 32: Preheating-pipe-only run for Geo1.

Bacterial counts in the milk-out samples of Geo1 using the preheating pipe (length = 60cm) only, which was maintained at 55°C for 24 h, and with 30 min sampling intervals. Y-axis = log count of the milk-out sample (cfu/ml); X-axis = time (h). The entire 30 min of each milk-out sample was collected and processed through a 24 h run. (Detailed data in Appendix 26 in the data CD) The mean and standard deviation of triplicate plate readings of the same sampling point (3 replicates for each reactor, so 6 replicates per point) were calculated and converted into log counts then graphed above. The points on the graph are the mean of two independent preheating pipes, pipe 1 and pipe 2. The raw data was normalized to the lowest T0 (milk-in) according to get the normalized data. +/- one SD was plotted as error bars.

The milk from the preheating pipes had a lag phase of around 10 h, a log phase of around 6 h and a stationary phase of around 8 h, with cell counts reaching a maximum of 6.5 log. There was a 0.5 log reduction in bacterial numbers during the lag phase. Compared with the inoculum, biofilm growth in the preheating pipes resulted in a 1–1.5 log increase in bacterial counts after 24 h, which would affect the thermocycling and thermospiking results. This biofilm growth in the preheating pipes needed to be considered and modelled before the biofilm growth in the reactor was modelled.

We debated whether the ‘inoculate milk’ method or the ‘inoculate reactor’ method should be used in the temperature-cycling experiments. These two methods offer different insights into biofilm development.

The ‘inoculate milk’ method starts with a known amount of bacteria in the incoming milk and sterile reactors and, to a certain extent, represents the situation in a dairy manufacturing plant; that is, the milk entering the manufacturing process will contain low numbers of bacteria and the plant surfaces can be assumed to be clean at the start of a manufacturing run. The measurable factors in the experiment are the outflowing milk and final counts on the reactors. The amount of biofilm development in the preheating pipe is unknown. This was not considered in earlier experiments (Aplin & Flint, 2007). The biofilm in the preheating pipe may affect the results of the experiment in the reactor. If the amount of bacteria released from the preheating pipe were known, it could be subtracted from the overall result.

An alternative method of performing these experiments is using an ‘inoculated reactor’ method, starting with a sterile milk feed and inoculated reactors. The incoming milk will be sterile, all growth will occur in the reactors and the milk coming out of the reactor will contain bacteria, reflecting the growth in the reactor. To make full use of this method, some knowledge of the amount of bacteria seeding the reactor surfaces is needed.

Since the ‘inoculated milk’ method was used in temperature-cycling experiments, the amount of bacteria released from the preheating pipe need to be modelled first before looking into the whole temperature-cycled reactor system.

6.7. Investigations of Effect of Temperature Step Changes on Bacterial Viability of Geo1

6.7.1. Experimental Procedures: Investigations of Temperature Step Changes on Bacterial Viability of Geo1

Sterile 10% RSM was prepared as described in Section 3.2.1. Geo1 culture was grown as described in Section 3.3.3. The RSM feed was inoculated as described in Section 3.3.4. The system was assembled aseptically as shown in Figure 21. The PCR machine was programmed to hold the temperature at 55°C for 24 h, followed by one step-down change (55°C to 30/35°C, ramp rate = maximum) and constant holding at 30/35°C for 24 h, and then one step-up change (30/35°C to 55°C, ramp rate = maximum) and constant holding at 55°C for 24 h. Inoculum and milk-in samples were taken at time 0. Milk-out samples were taken every 2 h for the first 12 h and then at 24 h. This sampling regime was repeated over 3 days (72 h).

6.7.2. Results and Discussion: Investigations of Temperature Step Changes on the Bacterial Viability of Geo1

Geo1 was inoculated onto the sterile inner chamber surface of the reactor and incubated for 1 hour prior to these following temperature cycling experiments. Sterile milk feed was used in this part of the experiment.

The aim of this part of the study was to investigate the effect of a single and long ‘temperature step change’ on the bacterial viability of Geo1. To understand the effect of temperature cycling on bacterial viability or biofilm behaviour, the thermospiking experiments were simplified to one step-up change and one step-down change. Each step change was extended to 24 h, which was long enough to see the behaviour of the bacteria after the stationary phase.

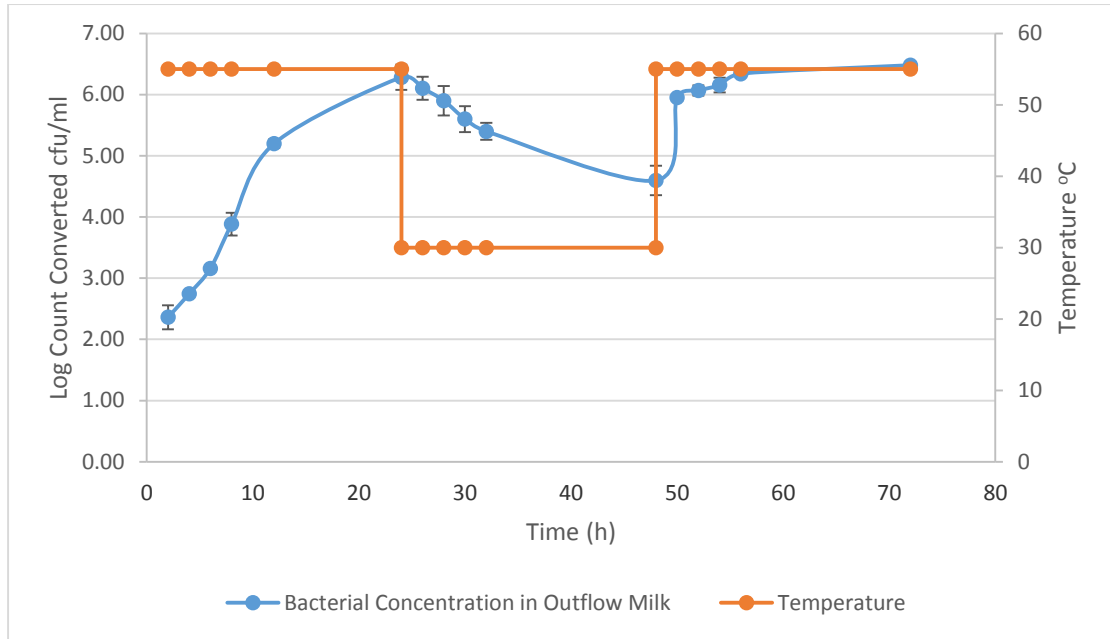


Figure 33: Temperature-cycling run for Geo1 with a 55–30–55°C temperature step change.

55–30–55°C temperature step change for Geo1 with a 24 h duration for each step and a total time of 72 h; Y-axis = log count of the milk-out sample (cfu/ml); X-axis = time (h). Mean bacterial concentration of outflowing milk from upper and lower reactors was plotted. One +/- standard deviation as plotted as error bar. (Detailed data in Appendix 24 in the data CD)

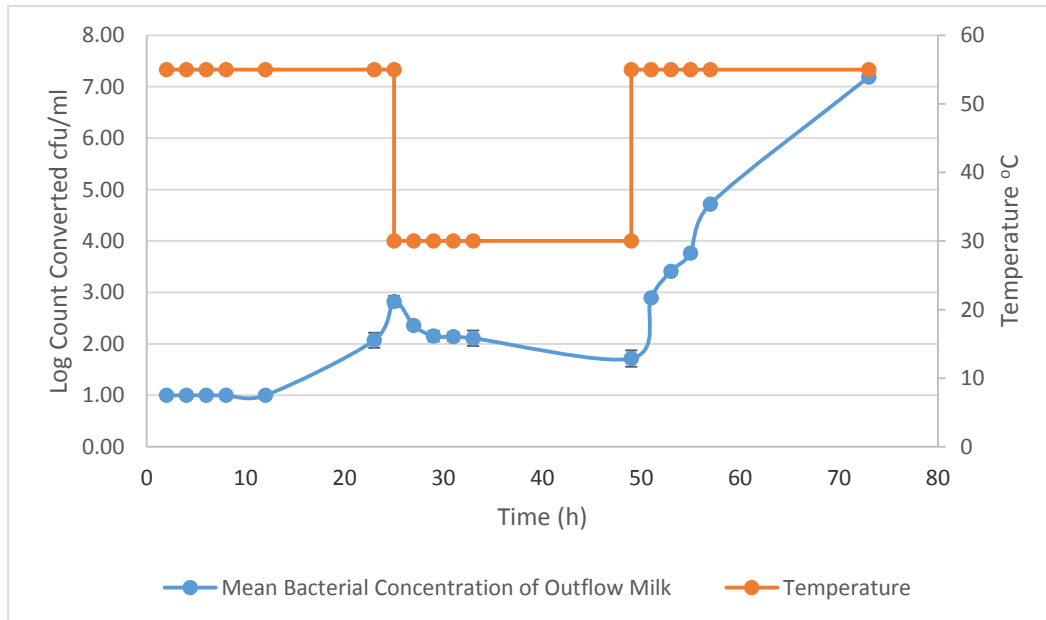


Figure 34: Temperature-cycling run for Geo1 with a 55–35–55°C temperature step change.

55–35–55°C temperature step change for Geo1 with a 24 h duration for each step and a total time of 72 h (one extra hour in the first step due to low growth was observed from first few hours); Y-axis = log count of the milk-out sample (cfu/ml); X-axis = time (h). Mean bacterial concentration of outflowing milk from upper and lower reactors was plotted. One +/- standard deviation as plotted as error bar.. (Detailed data in Appendix 25 in the data CD)

According to Figure 33 and 34, the decrease in temperature from 55 to 30/35°C resulted in a slow decrease in the bacterial counts in the outflowing milk. The increase in temperature from 30/35 to 55°C resulted in an increase in the bacterial counts in the outflowing milk with a very short lag phase. Thus, Geo1 was not damaged or killed during the decrease phase in temperature. It recovered and started to grow as soon as the temperature increased to the desired temperature range. Rice, Hamilton, & Camper (2000) also found that new bacterial cells needed to adapt to the new environment before growth, whereas cells existing in the system may not have this lag phase before the re-colonization process.

6.8 Impact of Cold Storage on Spores and Bacterial Counts

Spore-forming bacteria tend to sporulate when the growth conditions are unfavourable. Cold shock is one unfavourable condition that may influence spore formation, germination or the death of vegetative cells. Cold storage of the inoculated milk for the temperature-cycling experiments may have influenced the viability of the inoculum. The following experiment was designed to look at the viability of the total cell count and spores during cold storage.

6.8.1. Experimental Procedures: Impact of Cold Storage

RSM and Geo1 culture were prepared according to the instructions in Sections 3.3.3 and 3.2.1. The Geo1 culture (1 ml) was diluted in 9 ml of sterile TSB and then the whole 10ml was diluted in 1 L of 10% RSM (1:100) at 4 °C. The inoculated RSM was stored at 4°C for 24 h. The bacteria and spores were counted using TSA plates, at inoculum (after the first 1:10 dilution), T₀, T₂, T₄ and T₂₄ h. For the spore counts, the vegetative cells were killed by treating a 10 ml RSM sample at 100°C for 15 min before plating.

6.8.2. Results and Discussion: Impact of Cold Storage

The bacterial and spore counts of Geo1 at different sampling times were compared over the 24 h of cold storage in Table 16.

Table 16: Bacterial and spore counts of Geo1 during 24 h of cold storage

Geo1 Cold Shock Study	
Sample No.	Log cfu/ml
Inoculum in the milk T₀ Bacteria	5.59
Bacteria T₂	5.13
Bacteria T₄	5.15
Bacteria T₂₄	4.95
Inoculum in the milk T₀ Spore	3.34
Spore T₂	3.45
Spore T₄	3.76
Spore T₂₄	3.62

Bacterial and spore log counts of Geo1 were tested before (inoculum), during (at 2 and 4 h) and after (at 24 h) cold storage at 4°C over a 24 h period. (Detailed data in Appendix 27 in the data CD)

Both the bacterial counts and the spore counts were very stable during cold storage. Cold shock did not induce or enhance sporulation or germination. The bacteria in the cold milk at 4 °C did not show obvious reduction at 4 hours after storage and only had 0.5 log reduction over 24 h. Therefore, the quality of the milk in the reservoir could be regarded as being constant throughout the experiment. This information was very useful for later modelling work.

6.9 Summary

This chapter reports the results from various regimes of thermocycling and thermospiking. Thermocycling at 55–35°C with a period of 10 min and at 55–30°C with a period of 50 min influenced the length of the lag phase or reduced the bacterial counts in the lag phase or after 24 h. Thermospiking at 55–35°C produced different results in the prolonged lag phase compared with thermospiking at 55–30°C. Thermospiking at

55–35°C reduced the bacterial counts during the prolonged lag phase over the first 12 h. Thermospiking at 55°C/15 min, 30°C/35 min reduced the numbers of bacteria by 1 – 1.5 log after 24 h. This may have the potential to extend the manufacturing run time.

The preheating pipes had no effect on the contamination of milk for 12 h, but the effect became greater from 12 to 24 h. This effect needed to be considered in the mathematical modelling of the temperature-cycling results. As step changes of long duration did not kill or damage the bacterial cells, the results from the temperature cycling are likely to be the result of slowing the growth of the bacteria rather than killing the bacteria. As cold shock did not induce or enhance more spore production after 24 h, it is unlikely to have influenced the results in these experiments.

7 Mathematical Modelling of Preheating Section

7.1 Outline

To determine the effects of temperature cycling and to develop models for these effects, the influence of the preheating section on the results needed to be determined. The preheater data were modelled first. The model was constructed as follows.

- Basic theory: Logistic equation
- Mathematical model of the preheating pipes:
 - Mathematical model set-up
 - Assumptions of the mathematical model
 - Mathematical model development
 - Mathematical model optimization
 - Mathematical model justification

The aim was to develop a successful model that predicted the effect of preheating pipes on the reactor system based on bacteriological knowledge and a mathematical understanding.

7.2 Logistic Equation

The logistic equation was established in 1844–1845 by Pierre Francois Verhulst to model sigmoidal population growth (Weisstein, 2013). Sigmoidal population growth can be found in various areas including biology, economy, chemistry, ecology etc. The general logistic equation is:

Equation 7-1

$$P(t) = \frac{1}{1 + e^{-t}}$$

Where P is the population size

In 1925, the ‘law of population growth’ was derived from the general logistic equation by Alfred J. Lotka for modelling population growth in ecology (Weisstein, 2013).

Equation 7-2

$$\frac{dP}{dt} = rP\left(1 - \frac{P}{k}\right)$$

$r = \text{growth rate of the population};$

$k = \text{carrying capacity of the system};$

Equation 7-3

$$\frac{dP}{dt} = rP - \frac{rP^2}{k} = \text{growth} - \text{death}$$

At equilibrium, as the rate of change of the population is zero, the rate of death is equal to the rate of growth.

Equation 7-4

$$\frac{dP}{dt} = 0 \quad \text{so,} \quad rP = \frac{rP^2}{k}$$

Equation 7-5

$$\text{Therefore, } P = k$$

In other words, at equilibrium, the population size is equal to the carrying capacity of the system. Therefore, the unit of the carrying capacity is the same as that of the population. In our case, the carrying capacity has the same unit as the bacteria population, which is cfu.

7.3 Mathematical Modelling of Bacterial Growth in the Preheating Pipes

7.3.1 Mathematical Model Set-up

As shown in Figure 32, the bacterial counts in the outflow from the preheating pipes increased over 24 h, which was assumed to be due to biofilm formation within the pipes. This could potentially influence the results of thermocycling and thermospiking in the hexagonal reactors. Therefore, the mathematical model for the thermocycling and thermospiking systems needed to take account of the increase in bacteria in the preheating section.

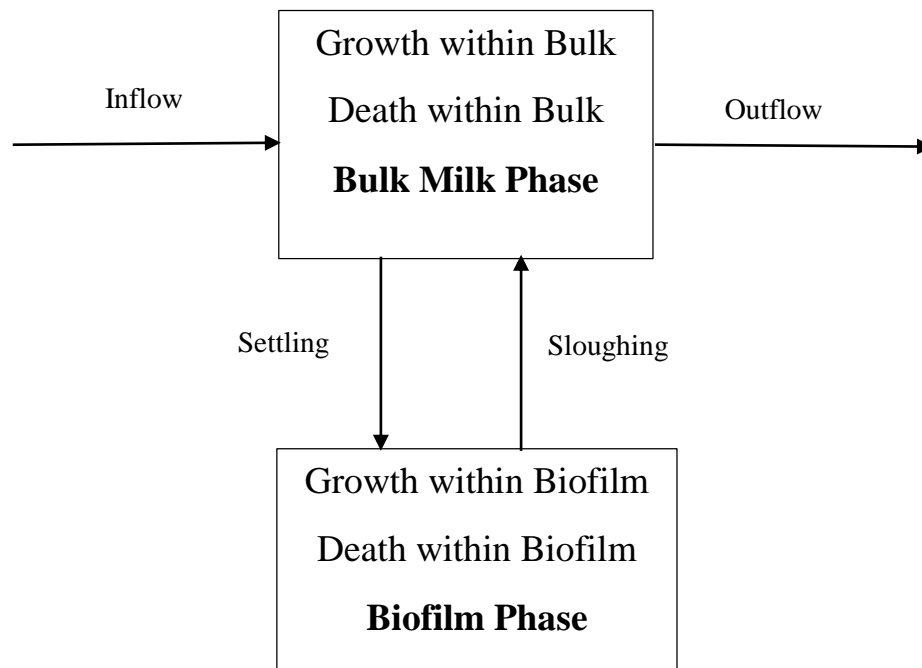


Figure 35: Schematic diagram of processes in the preheating pipes.

In the schematic diagram of the processes shown on Figure 35, there is bacterial interchange between the **bulk milk phase** and the **biofilm phase**. This is often called the biotransfer potential or more simply the release of bacteria from a biofilm into the surrounding medium. Bacterial attachment on to a substrate or an existing biofilm is

called **settling**, whereas bacterial detachment from the biofilm into the bulk milk stream is called **sloughing**.

The bacterial count in the **inflow** or incoming milk was determined using the known flowrate and the measured concentration of the bacteria in the inoculated milk. The **outflow** was sampled and the bacterial counts were measured at 30 min intervals throughout the 24 h run.

This model was designed to estimate the bacterial counts in the bulk milk phase and in the biofilm phase based on the average rate and bacterial change in these phases. *M* is defined as the bacterial counts in the bulk milk in the preheating pipe with units of cfu. *F* is defined as the bacterial counts in the biofilm on the preheating pipe walls with units of cfu.

7.3.2 Assumptions of the Mathematical Model

Several assumptions were made while constructing the mathematical model.

- **There is no growth in the bulk milk phase.**

The flowrate was set to 1.5 ml/min, which gave a residence time in the pipe of 11.3 min, which was shorter than the doubling time (18 min) of *Geo1*.

Equation 7-6

$$\text{Residence time} = \frac{\text{Capacity}_{\text{reactor}}}{\text{Flowrate}_{\text{system}}} \text{ (s or min)}$$

In this case,

Equation 7-7

$$\text{Residence time (minutes)} = \frac{\text{Volume}_{\text{Reactor}} \text{ (ml)}}{\text{Flowrate} \text{ (ml/min)}}$$

Equation 7–8

$$\text{Residence time (minutes)} = \frac{16.956\text{ml}}{1.5\text{ml/min}} \approx 11.3 \text{ minutes} < tD_{Geo1}$$

- **There is no death in either the bulk milk phase or the biofilm phase.**

As the temperature was maintained at the optimum growth temperature of 55°C, no death occurred in the 24 h experimental period.

- **The death term in the logistic growth equation is treated as ‘sloughing’. The ‘sloughing’ event is random.**

The ‘law of population growth’ equation describes the sigmoidal nature of the population growth. This sigmoidal growth is similar to our observed growth curve in Chapter 5. Bacterial growth has an exponential growth phase and an equilibrium stationary phase. The logistic growth equation was found to be the simplest model to fit this situation.

The only process that decreases the bacterial population is sloughing. Bacteria can slough off or detach from the biofilm as single cells or lumps of biomass. This term is the average rate for both forms of detachment. Thus, the death term in the logistic equation (Equation 7–3) was interpreted as the sloughing term. The ‘law of population growth’ equation describing the change in the biofilm population (rate of change in F) could be rewritten as:

Equation 7–9

$$\frac{dF}{dt} = \text{Growth within the Biofilm} - \text{Sloughing}$$

Therefore, the growth and sloughing terms are expressed as:

Equation 7–10

$$Growth = rF(cfu/s)$$

Equation 7–11

$$Sloughing = \frac{rF^2}{k_{pipe}} (cfu/s)$$

$r =$ growth rate of the biofilm (/s) based on $e - fold$ time (/s);

$k_{pipe} =$ carrying capacity of the biofilm on the pipe wall of the whole pipe (cfu);

- **The inflow is treated as a constant for each run.**

The inflow may vary from one run to another but will be constant throughout a single run. The inflow remains cold throughout the 24 h experimental period, which is unfavourable for the growth of thermophilic bacteria such as *Geo1*. Therefore, the inflow can be treated as a constant for each run. The rate of bacterial change in the **inflow** over time can be determined as shown below.

Equation 7–12

$$Inflow(cfu/s) = Incoming\ milk\ concentration\ (cfu/ml) \\ \times\ flowrate\ (ml/s)$$

- **Estimated M is not the measured outflow; it is proportional to the outflow.**

Outflow counts are the actual measurements from the experiment whereas M, which is predicted from the model, is only proportional to the outflow. The rate of bacterial change in the **outflow** is expressed as:

Equation 7–13

$$Outflow\ (cfu/s) = \frac{M(cfu) \times flowrate(ml/s)}{Volume_{pipe}(ml)}$$

7.3.3 Mathematical Model Development

The model is based on the logistic equation with modification (the ‘law of population growth’).

For the bulk milk phase, the rate of change in bacterial counts is affected only by the rates of the inflow, outflow, settling and sloughing processes because there is no growth in the bulk milk. Bacteria come into the pipe via the inflow and exit out of the pipe via the outflow. Bacteria in the bulk milk settle and attach on to the pipe wall and form a biofilm. In the later stage of the experiment, bacteria from the biofilm release back into the bulk milk stream. The rate of bacterial change in the bulk milk phase (the rate of change of M) over time (cfu/s) is expressed as:

Equation 7–14

$$\frac{dM}{dt} = \text{Inflow} - \text{Outflow} - \text{Settling} + \text{Sloughing}$$

For the biofilm phase, the rate of change in bacterial counts is influenced by the rate of the settling and sloughing processes as well as the rate of growth within the biofilm. Bacteria within the biofilm grow with time. The rate of change in bacterial counts in the biofilm phase (the rate of change of F) over time (cfu/s) is expressed as:

Equation 7–15

$$\frac{dF}{dt} = \text{Settling} - \text{Sloughing} + \text{Growth within Biofilm}$$

- **Growth Term**

In the ‘growth within the biofilm’ term, r represents the proportional increase in the population in one unit of time. The constant r can also be represented by the growth e-folding time ($t_{G,pipe}$, units of s). The growth e-folding time is defined as the time interval for exponential growth to increase by a factor of e ($e = 2.71$).

Equation 7–16

$$\text{Growth within biofilm} = rF \text{ (cfu/s)}$$

$$r = \text{growth rate of the biofilm based on } e - \text{fold growth} = \frac{1}{t_{G,pipe}}$$

e-Fold growth and **e-folding time** are used to describe the exponential growth phenomenon in the logistic growth equation. The e-folding time is the time interval for an exponential quantity of the population to increase by a factor of e. This term is used as the base analog to the doubling time t_D . Equation 7–17 is used to mathematically express the bacterial counts in a biofilm on the pipe walls (F) at time t with respect to the initial population F_0 :

Equation 7–17

$$F(t) = F_0 \times e^{rt} \text{ where } F_0 \text{ is the initial population;}$$

At the initial condition

Equation 7–18

$$t = 0, e^0 = 1, F = F_0$$

Equation 7–17 can also be rewritten as:

Equation 7–19

$$F(t) = F_0 \times e^{t/t_G}$$

After differentiation

Equation 7–20

$$\frac{dF}{dt} = F_0 \times \frac{1}{t_G} \times e^{t/t_G}$$

After rearrangement

Equation 7-21

$$\frac{dF}{dt} = \frac{1}{t_G} \times F_0 \times e^{t/t_G}$$

After substituting Equation 7-19 into Equation 7-21

Equation 7-22

$$\frac{dF}{dt} = \frac{F}{t_{G,pipe}} = \text{Growth within Biofilm (unit is cfu/s)}$$

- **Settling Term**

A similar approach can be used for the **settling** term. The settling e-folding time (t_0) is used. The settling term describes the process of the decrease in the numbers of bacteria in the bulk milk as they leave to form a biofilm. Therefore, the settling term in relation to the rate of change in M should be negative.

Equation 7-23

$$\text{Settling} = -\alpha M$$

$$\alpha = \text{settling rate of the bacteria based on } e - \text{fold settling time} = \frac{1}{t_{0,pipe}}$$

The e-fold settling rate and the e-folding settling time are used because

Equation 7-24

$$M(t) = M_0 \times e^{-\alpha t} \text{ where } M_0 \text{ is the initial population;}$$

At the initial condition

Equation 7–25

$$t = 0, e^o = 1, M = M_0$$

Equation 7–24 can also be rewritten as:

Equation 7–26

$$M(t) = M_0 \times e^{-t/t_0}$$

After differentiation

Equation 7–27

$$\frac{dM}{dt} = M_0 \times \left(-\frac{1}{t_0}\right) \times e^{-t/t_0}$$

After rearrangement

Equation 7–28

$$\frac{dM}{dt} = \left(-\frac{1}{t_0}\right) \times M_0 \times e^{-t/t_0}$$

After substituting Equation 7–26 into Equation 7–28

Equation 7–29

$$\frac{dM}{dt} = -\frac{M}{t_{0,pipe}} = \textit{Settling process in relation to Bulk Milk Phase (unit: cfu/s)}$$

The rate of settling is negative in relation to the bulk milk phase because it describes bacteria leaving the bulk milk. However, this settling term becomes positive when it describes the increase in bacteria forming the biofilm phase.

Equation 7–30

$$\frac{dM}{dt} = \frac{M}{t_{0,pipe}} = \textit{Settling process in relation to Biofilm Phase (unit: cfu/s)}$$

- **Sloughing Term**

After substituting the e-folding growth rate r from Equation 7–16 into Equation 7–11, the sloughing term is expressed as:

Equation 7–31

$$\text{Sloughing} = \frac{rF^2}{k_{\text{pipe}}} = \frac{F^2}{k_{\text{pipe}} \times t_{G,\text{pipe}}} \text{ (cfu/s)}$$

The inflow term is derived in Equation 7–12. The outflow term is derived in Equation 7–13. The growth term is derived in Equation 7–22. The settling term in relation to the bulk milk phase is derived in Equation 7–29. The settling term in relation to the biofilm phase is derived in

Equation 7–30. The sloughing term is derived in Equation 7–31. As all terms describe the rate of a process, they all have units of cfu/s. The volume and the area are properties of the system, i.e. the preheating pipe.

After substituting in all the terms, the two main process equations (Equation 7–14 and Equation 7–15) can be rewritten as:

Rate of Change of Bacterial Counts in the Bulk Milk Phase (the rate of change in M):

Equation 7–32

$$\begin{aligned} \frac{dM}{dt} &= \text{Inflow} - \text{Outflow} - \text{Settling} + \text{Sloughing} \\ &= (\text{Milk conc}_{\text{inflow}} \times \text{Flowrate}) - \left(\frac{M \times \text{Flowrate}}{\text{Volume}_{\text{pipe}}} \right) - \left(\frac{M}{t_{0,\text{pipe}}} \right) \\ &\quad + \left(\frac{F^2}{k_{\text{pipe}} \times t_{G,\text{pipe}}} \right) \end{aligned}$$

Rate of Change of Bacterial Counts in the Biofilm Phase (the rate of change in F):

Equation 7–33

$$\begin{aligned} \frac{dF}{dt} &= \textit{Settling} - \textit{Sloughing} + \textit{Growth} \\ &= \left(\frac{M}{t_{0,pipe}}\right) - \left(\frac{F^2}{k_{pipe} \times t_{G,pipe}}\right) + \left(\frac{F}{t_{G,pipe}}\right) \end{aligned}$$

7.3.4 Mathematical Model Optimization

The statistical software ‘R’ (version 2.15.3, developed by the Institute of Statistics and Mathematics of Wirtschaftsuniversit ät Wien, Vienna, Austria) was used in this part of the study. Equation 7–32 and Equation 7–33 were rewritten into the language for R (Appendix 5) and were optimized (Appendix 6).

The ultimate goal was to determine the ‘best’ parameters ($t_{0,pipe}$, $t_{G,pipe}$ and k_{pipe}), which would allow the model to fit the measured data. This goal was achieved by the following process.

- The model is rewritten into ‘R’ language. After inserting different values for each of the parameters, the output of the model is the estimated M and F values for each time interval.
- The measured outflow data are converted into M values using Equation 7–13.
- ‘R’ calculates the difference between the converted M data and the estimated M values from the model and returns this difference as badness (lack of fit).

Equation 7–34

$$Total\ Badness = \sum \frac{(Estimation - Observation)^2}{Estimation}$$

- Optimization minimizes this badness value by inserting different values for the three unknown parameters using an iteration process.

After the optimization process, the best values for these parameters were:

Equation 7–35

$$t_{0,pipe} = settling\ e - folding\ time = 4.853 \times 10^4\ s$$

Equation 7–36

$$t_{G,pipe} = growth\ e - folding\ time = 6.473 \times 10^3\ s$$

Equation 7–37

$$k_{pipe} = carrying\ capacity\ of\ the\ biofilm\ on\ the\ pipe\ wall = 4.067 \times 10^8\ cfu$$

7.3.5 Justification of the Mathematical Model

From the CDC reactor experiments, in 10% solids RSM, the growth rate of the biofilm for Geo1 was 1.47/h at 50°C and 1.20/h at 60°C. The growth rate at 55°C was 1.60/h.

The $t_{G,pipe}$ calculated by R can be converted back to the maximum specific growth rate (/h) and the doubling time (t_D , h). The e-folding time is 1.44 times ($1/\ln 2$) the doubling time.

Equation 7–38

$$t_D = t_{G,pipe} \div \frac{1}{\ln 2} \approx 4486\ seconds \approx 1.25\ hour$$

Equation 7–39

$$Doubling\ growth\ rate = \frac{\ln 2}{t_D} \approx 0.56\ /h$$

The estimated maximum specific growth rate calculated from above equations based on estimated $t_{G,pipe}$ from R was lower than the actual observed growth rate for the Geo1 biofilm from CDC reactor experiment. This reduction in biofilm growth rate may have been caused by the change in the environment; for example, the behaviour of attachment to silicone tubes may differ from that to stainless steel coupons.

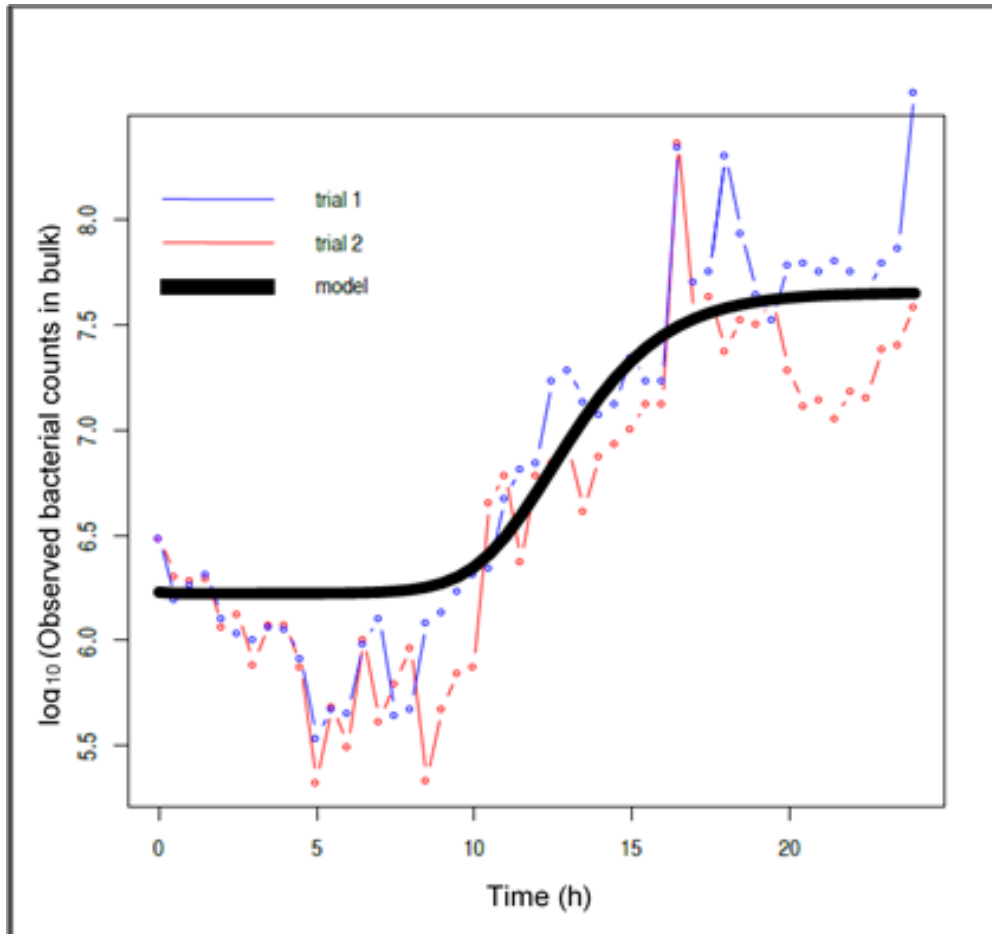


Figure 36: Preheating-pipe-only model: estimated versus actual bacterial counts in the bulk milk phase along time scale.

Milk-out sampled from the preheating pipe experiment for Geo1 in a 55°C water bath for 24 h. Black line is the estimated bacterial counts in the bulk milk phase from R using the best parameters. Dots linked by blue and red lines are the actual bacterial counts in the bulk milk phase from two independent pipe-only experiments, trial 1 and trial 2. Y-axis is the log converted bacterial count readings (cfu); X-axis = time (s). The observed bacterial counts in the bulk milk phase converted from the observed bacterial concentration of the bulk milk phase (cfu/ml) to have the same unit of cfu as the output from the model M. The converted data is expressed in log₁₀ form and the conversion formula is: $\log_{10}(\text{observed concentration of the bulk milk phase} \times \text{Volume of the pipe}) = \log_{10}(\text{observed concentration of the bulk milk phase}) + \log(\text{Volume of the pipe})$;

Figure 36 shows that this model provided a reasonable first approximation of the actual growth in the preheating pipe. This model predicted growth with lag, log and stationary phases of similar lengths to those observed. However, the reduction in bacterial count in the lag phase was not predicted as well as a few outliers in the stationary phase. Figure 38 shows that this model and logistic growth theory can be used to feed into the coupon reactor model to take account of the changes in the counts in the incoming milk.

7.4 Summary

A mathematical model for the preheating pipes was developed in this chapter. The model accurately predicted the duration and the level of the logarithmic and stationary growth phases. However, it could not predict the reduction in bacterial counts in the lag phase. As the parameters in this model were optimized, estimates from this model could be fed into the reactor model as the bacterial concentration in the incoming milk.

8 Mathematical Modelling of Temperature Cycling

8.1 Outline

Once the model for the preheating pipes had been developed, the output from that model could be used as the estimated bacterial concentration in the incoming milk into the reactor. Therefore, the mathematical model for the reactor section was developed as follows.

- Mathematical model set-up
- Growth rate, temperature and time relationship
- Assumptions of the mathematical model
- Mathematical model development
- Mathematical model justification
- Use of the mathematical model

The aim was to develop a successful model based on the knowledge learnt from the development of the preheating pipe model and the experimental data.

8.2 Mathematical Model Set-up

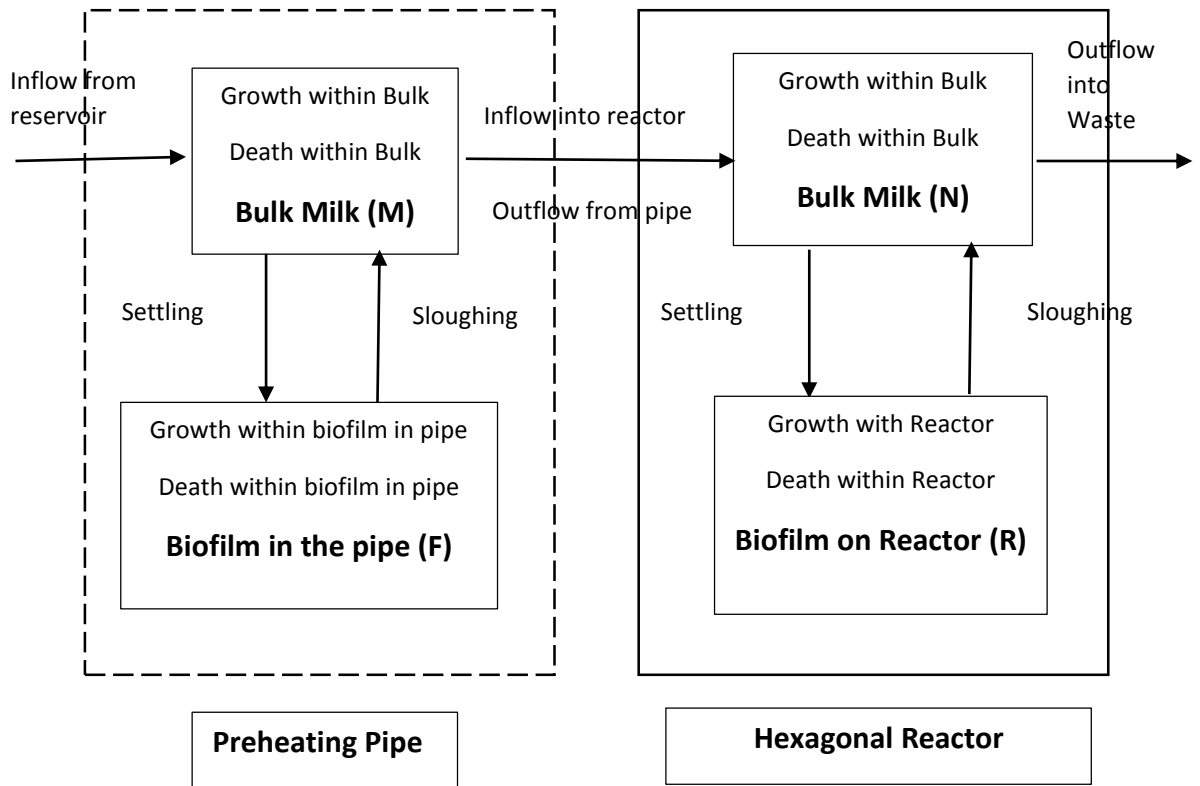


Figure 37: Schematic diagram of process in preheating pipe and hexagonal reactor.

The dashed-line box is the preheating pipe section, whereas the solid-line box is the reactor section. M is the bacterial counts in the bulk milk phase in the preheating pipe section with units of cfu. F is the bacterial counts in the biofilm phase in the preheating pipe section with units of cfu. N is the bacterial counts in the bulk milk phase in the reactor section with units of cfu. R is the bacterial counts in the biofilm phase in the reactor section with units of cfu.

Figure 37 shows the compartments of the reactor system. It consists of two parts. The first part, the preheating pipe section, was discussed in Chapter 7. This chapter describes the model for the whole system. There is interchange of bacteria between the bulk milk phase and the biofilm phase in the hexagonal reactors. Bacterial attachment from the bulk milk stream on to the biofilm is called $\text{Settling}_{\text{reactor}}$ whereas bacterial detachment from the biofilm into the bulk milk stream is called $\text{Sloughing}_{\text{reactor}}$. $\text{Inflow}_{\text{reactor}}$ of the hexagonal reactor is the outflow of the preheating pipe. $\text{Outflow}_{\text{reactor}}$ was sampled and measured throughout the 24 h run.

This model was designed to estimate the bacterial counts in the bulk milk phase (N) and the bacterial counts in the biofilm phase (R) in the reactor section based on the average rates of bacterial change in these sections. The units for both N and R are cfu.

8.3 Biofilm Growth Rate, Temperature and Time Relationship

To predict the biofilm growth rate at any specific time during the experiment, growth rate versus temperature and temperature versus time relationship functions needed to be constructed. Then the predicted biofilm growth rate could be used to predict the growth e-folding time t_G for any specific given time.

- ***Growth Rate versus Temperature Relationship***

Geobacillus species are classified as moderate thermophiles (Bergey's Manual Trust, 2009). Previous studies have shown that reference strains can grow at 42–68°C (Ratkowsky, Lowry, McMeekin, Stokes, & Chandler, 1983). In our study, Geo1 was a wild strain that was isolated from milk powder. Its growth range was wider than that of the reference strain reported in the literature (Bergey's Manual Trust, 2009); it had the ability to grow at above 70°C and below 40°C.

The biofilm growth rate was also studied at 35 and 70°C in addition to the temperatures used in the CDC reactor runs (Chapter 5). Determining the growth rates at different temperatures is important in developing models for temperature cycling, results shown on Figure 38 below.

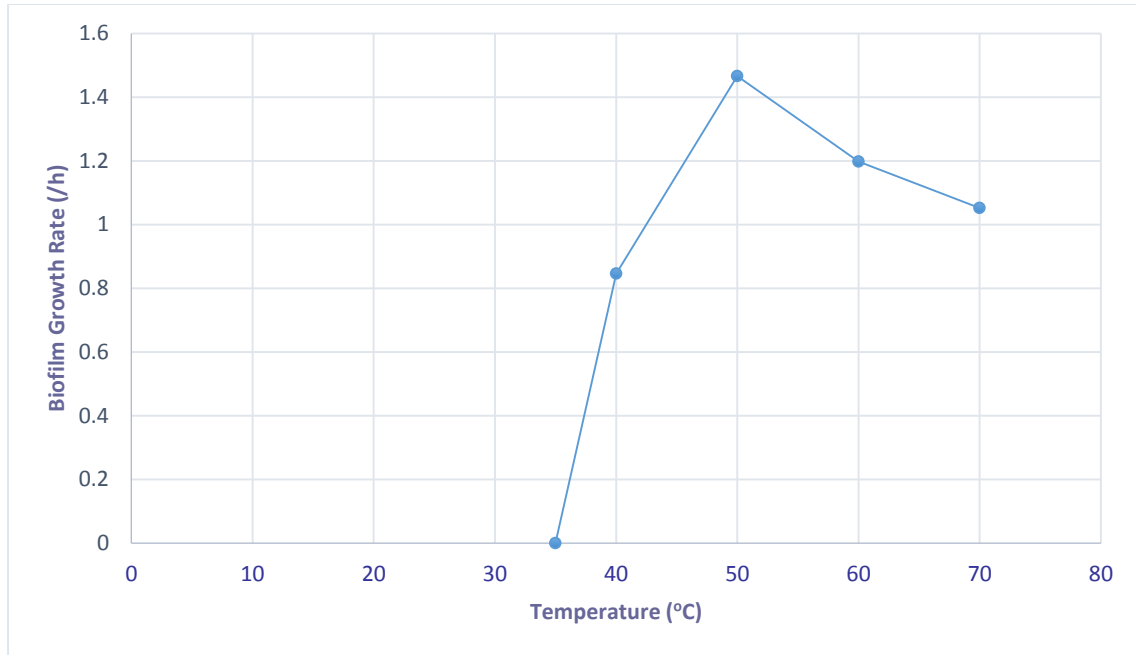


Figure 38: Geo1 biofilm growth rate versus temperature relationship in 10% RSM.

Biofilm growth rate of Geo1 at different temperatures in the CDC reactors and 10% RSM. Y-axis = maximum specific biofilm growth rate calculated at the corresponding temperature from the CDC reactor results (/h); X-axis = temperature (°C).

From Figure 38, biofilm did not develop at below 35°C. The biofilm development rate decreased when the temperature was increased from 50 to 60°C. The optimum growth temperature of Geo1 was between 50 and 60°C, based on the literature and planktonic growth rate experiments (Ratkowsky, Lowry, McMeekin, Stokes, & Chandler, 1983).

As there was no biofilm development at either 35 or 30°C (Figure 38), the difference in the results (prolonged lag phase and initial reduction in bacterial counts of the outflowing milk in the lag phase) for the temperature-cycling experiments between 30°C (Section 6.4.2.1) and 35°C (Section 6.4.2.2) could not be explained. Originally, it was thought that the biofilm growth rates at 30 and 35°C could be different and that this might explain the variability of the temperature-cycling results. The possible explanation for this observation will be discussed later in Chapter 9.

The results in Table 18 were used in the statistics package R to construct a function that could determine the specific growth rate at various temperatures and times in the temperature-cycling experiments (Appendix 9).

Table 17: Geo1 maximum specific biofilm growth rate versus temperature relationship in 10% RSM

Temperature (°C)	Maximum Specific Biofilm Growth Rate (/h)
35	1×10^{-6} (no growth, measured using CDC reactor, in 36 h)
40	0.8465
50	1.4661
60	1.1977
70	1.0520
80	1×10^{-6} (no growth, estimated from planktonic growth, in 24 h)

Maximum specific biofilm growth rates of Geo1 at different temperatures in 10% solids RSM. The planktonic growth rate at 80°C was estimated from the preliminary test for the CDC reactor runs: ‘testing boundary conditions’ results. A very small result (1×10^{-6} /h) was given to the no-growth situations because the model required an actual number as a divider.

- **Temperature versus Time Relationship (Appendix 8)**

In the **sine wave experiments (thermocycling)**, the temperature and time relationship was expressed as in Equation 8–1 to calculate the temperature at any specific given time point during the thermocycling experiments; T_{max} is the maximum temperature and T_{min} is the minimum temperature, time is in units of s and period is in units of min.

Equation 8–1

Temperature at any given time

$$= \left(\frac{T_{min} + T_{max}}{2} \right) - \left(\frac{T_{max} - T_{min}}{2} \right) \times \cos\left(\frac{2\pi \times time}{period \times 60} \right)$$

In the **square wave experiments (thermospiking)**, the temperature and time relationship was constructed using a ‘modulus’ (in R terminology, %% is used for the

modulus of the integer division) to calculate the temperature at any specific given time point during the thermospiking experiments. ‘Modulus’ is defined as the ‘remainder’ of integer division. The given time is divided by the sum of times spent at high (t_{high}) and low (t_{low}) temperatures (period of one cycle). If the remainder is larger than the time at high temperature, then the given time point should be on the low temperature. If the remainder is smaller than the time at high temperature, then the given time point should be on the high temperature. Therefore, using R language, the above statements can be expressed using a true or false decision. An output value of 1 is given to the true statement, whereas an output value of 0 is given to the false statement.

Equation 8–2

if Modulus of 'specific time / ($t_{high} + t_{low}$)' < t_{high} , it is true, 1

Equation 8–3

if Modulus of 'specific time / ($t_{high} + t_{low}$)' > t_{high} , it is false, 0

Then, if the statement is true, the temperature at a specific given time is equal to the high temperature (T_{max} , expressed as $T_{min} + \text{difference between } T_{max} \text{ and } T_{min}$). If the statement is false, the temperature at a specific given time is equal to the low temperature (T_{min} , expressed as $T_{min} + 0$). Thus, the temperature at a specific given time is described as follows:

Equation 8–4

Temperature at any given time = $T_{min} + (T_{max} - T_{min}) \times (1 \text{ or } 0)$

For example, in the thermospiking run at 55°C/15 min, 35°C/35 min, to calculate the temperature at 2.8 h (168 min):

$$\text{Modulus of } \frac{168 \text{ min}}{15 \text{ min} + 35 \text{ min}} = 18 \text{ min} > t_{high}, \text{ it is false, } 0;$$

$$\text{Temperature at } 2.8 \text{ h} = 35^{\circ}\text{C} + (55^{\circ}\text{C} - 35^{\circ}\text{C}) \times 0 = 35^{\circ}\text{C}$$

Therefore, the temperature at 2.8 h is on the low temperature part of the cycle. In contrast, in the same thermospiking experiment, the temperature at 2.6 h (156 min) is:

$$\text{Modulus of } \frac{156 \text{ min}}{15 \text{ min} + 35 \text{ min}} = 6 \text{ min} < t_{\text{high}}, \text{ it is true, } 1;$$

$$\text{Temperature at } 2.6 \text{ h} = 35^{\circ}\text{C} + (55^{\circ}\text{C} - 35^{\circ}\text{C}) \times 1 = 55^{\circ}\text{C}$$

8.4 Assumptions of the Mathematical Model

All assumptions in Chapter 7 held. Some additional assumptions were made before construction of this model.

- **The bacteria in the system react instantaneously to temperature changes.**

There is definitely a lag time before the growth rate adapts when bacteria are exposed to temperature changes; however, the length of the lag is unknown (Rice, Hamilton, & Camper, 2000). As this model was only a first approximation, it was assumed that bacteria have an instantaneous response to temperature changes.

- **The bacterial attachments in the metal reactors and the silicone preheating pipe are similar.**

It is known that both silicone pipes and stainless steel (316L with 2B finish) are hydrophobic materials; however, no data on the actual hydrophobicity of each were available. Therefore, it was assumed that silicone pipes and stainless steel have similar surface properties. Hence, the bacterial

attachments in the metal reactors and in the silicone preheating pipes were assumed to be similar.

- **A cosine function is used instead of a sine function.**

In the experiments, the thermocycler was started and heated to the maximum temperature T_{\max} (55°C) before counting the first cycle. A cosine function was used instead of a sine function because the sine function starts at the centre temperature, which is half of the sum of T_{\max} and T_{\min} .

- **A very small number, rather than zero, was used for the growth rate ($1 \times 10^{-6}/\text{h}$) in the ‘no-growth’ situations.**

In this model, the growth rate was used as a divider. A ‘not a number’ signal results if the growth rate is zero. Therefore, a very small number that would not influence the estimation was used.

- **Bacteria attach from the bulk milk phase on to the surface at constant velocity.**

It was assumed that the bacterial attachment process does not involve acceleration, as described in Figure 39.

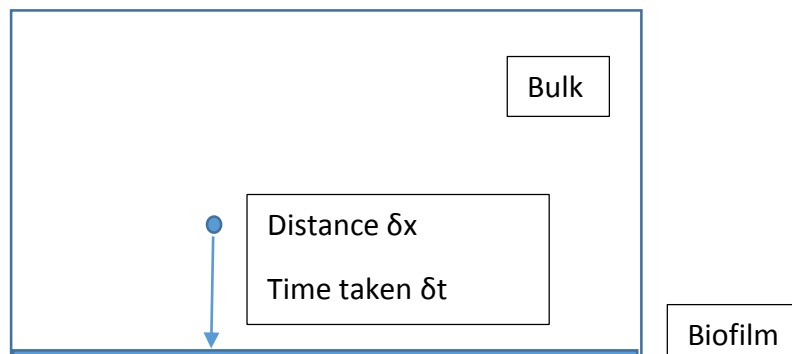


Figure 39: Settling of bacteria from the bulk phase on to the biofilm.

The dot represents the settling of a single bacterium.

The distance that bacteria travel before reaching the biofilm is δx and time taken is δt . N represents the number of bacteria in the bulk phase in the reactor (cfu). The volume and the area are properties of the system, i.e. the preheating pipe or the reactor. The number of bacteria settling is proportional to the number of bacteria in the bulk phase. Settling decreases the number of bacteria in the bulk phase. From the bulk phase point of view, the settling term is negative.

Equation 8-5

$$\text{Change in Bacteria due to Settling} = - \frac{\delta x \times \text{Area} \times N}{\text{Volume}}$$

The settling velocity is defined by the distance and the time taken to travel that distance. Therefore, this relationship is written as:

Equation 8-6

$$\text{Distance } \delta x = \text{Velocity} \times \delta t$$

After replacing the distance term

Equation 8-7

$$\text{Change in Bacteria due to Settling} = - \frac{\delta t \times \text{Velocity} \times \text{Area} \times N}{\text{Volume}}$$

After rearrangement

Equation 8-8

$$\text{Bacteria settled} = -N \times \left(\frac{\text{Area}}{\text{Volume}} \right) \times \text{Velocity} \times \delta t$$

After differentiation

Equation 8–9

$$\frac{dN}{dt} = -N \times \left(\frac{Area}{Volume} \right) \times Velocity$$

The settling term can also be described using the settling e-folding time t_0 , as in Section 7.3.3.

Equation 8–10

$$N = N_0 \times e^{-t/t_0}$$

After differentiation

Equation 8–11

$$\frac{dN}{dt} = -\frac{1}{t_0} \times (N_0 \times e^{-t/t_0})$$

The bracketed term in Equation 8–11 can be replaced with Equation 8–10:

Equation 8–12

$$\frac{dN}{dt} = \left(-\frac{1}{t_0} \right) \times N$$

Therefore, these two different expressions (Equation 8–9 and Equation 8–12) can be linked to establish the relationship between velocity and the settling e-folding time t_0 .

Equation 8–13

$$-N \times \left(\frac{Area}{Volume} \right) \times Velocity = \left(-\frac{1}{t_0} \right) \times N$$

After cancelling terms

Equation 8–14

$$\left(\frac{Area}{Volume}\right) \times Velocity = \frac{1}{t_0}$$

After rearrangement

Equation 8–15

$$Velocity = \frac{Volume}{Area \times t_0} (cm/s)$$

Equation 8–16

$$t_0 = \frac{Volume/Area}{Velocity} (s)$$

The volume and area parameters are specific for the system. Therefore

Equation 8–17

$$t_{0,preheating\ pipe} = \frac{Volume_{pipe}/Area_{pipe}}{Velocity} (s)$$

Equation 8–18

$$t_{0,reactor} = \frac{Volume_{reactor}/Area_{reactor}}{Velocity} (s)$$

- **The carrying capacities of the preheating pipe and the reactor differ only because of the difference in surface area.**

As it was assumed that silicone pipes and stainless steel have similar surface properties, the carrying capacity k of the pipe could be modified and used

to calculate the carrying capacity k of the stainless steel reactors. Also, it was assumed that this term does not change with changes in temperature.

Equation 8–19

$$k_{pipe} = \text{carrying capacity per unit area} \times Area_{pipe} (cfu)$$

Equation 8–20

$$k_{reactor} = \text{carrying capacity per unit area} \times Area_{reactor} (cfu)$$

Therefore, the carrying capacity of the reactor can be rewritten using the known k_{pipe} term:

Equation 8–21

$$k_{reactor} = \frac{k_{pipe} \times Area_{reactor}}{Area_{pipe}} (cfu)$$

8.5 Mathematical Model Development

The basis for this model was to use a similar approach and a similar logistic equation to those in Section 7.3.3 and to link the preheating pipe model with the reactor model.

In the base model, the rate of change of the bacterial counts in the bulk milk phase (N) can be expressed as the net result of the rates of all processes in the schematic diagram in Figure 35, with units for all terms of cfu/s:

Equation 8–22

$$\frac{dN}{dt} = Inflow_{reactor} - Outflow_{reactor} - Settling_{reactor} + Sloughing_{reactor}$$

The rate of change of the bacterial counts in the biofilm on the reactors (R) can be expressed as the net result of the rates of all processes in the schematic diagram in Figure 35, with units for all terms of cfu/s:

Equation 8–23

$$\frac{dR}{dt} = \text{Settling}_{reactor} - \text{Sloughing}_{reactor} + \text{Growth}_{reactor}$$

- ***Inflow Term***

The inflow to the reactor is the outflow from the preheating pipe, which is linked with the estimated output bacterial counts in the bulk milk phase of the pipe model (M, cfu).

Equation 8–24

$$\text{Outflow concentration} = \frac{M}{\text{Volume}_{pipe}} (\text{cfu/ml})$$

Equation 8–25

$$\text{Inflow}_{reactor} = \text{Outflow Concentration} \times \text{Flowrate} (\text{cfu/s})$$

Equation 8–26

$$\text{Inflow}_{reactor} = \frac{M \times \text{Flowrate}}{\text{Volume}_{pipe}} (\text{cfu/s})$$

- ***Outflow Term***

The outflow from the reactor is related to the bacterial counts in the bulk milk phase in the reactor section (N) and the dimensions of the reactor.

Equation 8–27

$$\text{Outflow}_{reactor} = \frac{N \times \text{Flowrate}}{\text{Volume}_{reactor}} (\text{cfu/s})$$

- **Settling Term**

From Chapter 7 and the assumptions, it is known that the process of settling on to the reactor is related to the settling e-folding time.

Equation 8–28

$$t_{0,reactor} = \frac{Volume_{reactor} / Area_{reactor}}{Velocity} (s)$$

Equation 8–29

$$Settling_{reactor} = \frac{N}{t_{0,reactor}} = \frac{Velocity \times Area_{reactor} \times N}{Volume_{reactor}} (cfu/s)$$

- **Sloughing Term**

According to the modified logistic equation, the sloughing term can be used to replace the death term (Section 7.3.2) and becomes:

Equation 8–30

$$Sloughing_{reactor} = \frac{R^2}{k_{reactor} \times t_{G,reactor}} (cfu/s)$$

As

Equation 8–31

$$k_{reactor} = \frac{k_{pipe} \times Area_{reactor}}{Area_{pipe}} (cfu)$$

Then

Equation 8–32

$$Sloughing_{reactor} = \frac{R^2 \times Area_{pipe}}{k_{pipe} \times Area_{reactor} \times t_{G,reactor}} (cfu/s)$$

- **Growth Term**

The $t_{G,reactor}$ term is calculated using a separate file within R containing the growth, temperature and time relationship function (Section 8.3). The growth term is expressed as:

Equation 8–33

$$Growth_{reactor} = \frac{R}{t_{G,reactor}} (cfu/s)$$

The **inflow**_{reactor} term is derived in Equation 8–26. The **outflow**_{reactor} term is derived in Equation 8–27. The **settling**_{reactor} term is derived in Equation 8–29. The settling term is negative with respect to the bulk milk phase and is positive with respect to the biofilm phase. The **sloughing**_{reactor} term is derived in Equation 8–32. The **growth**_{reactor} term is derived in Equation 8–33. As all terms describe the rate of a certain process, all have units of cfu/s. Replacing all the terms, the base models (Equation 8–22 and Equation 8–23) become:

Rate of Change of the ‘Bacterial Counts in the Bulk Milk Phase (N)’:

Equation 8–34

$$\begin{aligned} \frac{dN}{dt} &= Inflow_{reactor} - Outflow_{reactor} - Settling_{reactor} + Sloughing_{reactor} \\ &= \left(\frac{M \times Flowrate}{Volume_{pipe}} \right) - \left(\frac{N \times Flowrate}{Volume_{reactor}} \right) - \left(\frac{Velocity \times Area_{reactor} \times N}{Volume_{reactor}} \right) \\ &\quad + \left(\frac{R^2 \times Area_{pipe}}{k_{pipe} \times Area_{reactor} \times t_{G,reactor}} \right) \end{aligned}$$

Rate of Change of the ‘Bacterial Counts of the Biofilm in the Reactor Phase (R)’:

Equation 8–35

$$\begin{aligned} \frac{dR}{dt} &= Settling_{reactor} - Sloughing_{reactor} + Growth_{reactor} \\ &= \left(\frac{Velocity \times Area_{reactor} \times N}{Volume_{reactor}} \right) - \left(\frac{R^2 \times Area_{pipe}}{k_{pipe} \times Area_{reactor} \times t_{G,reactor}} \right) + \left(\frac{R}{t_{G,reactor}} \right) \end{aligned}$$

8.6 Justification of the Mathematical Model

The statistical package R was used to construct this model. All the parameters configured from the earlier ‘pipe-only model’, the settings and the model equations from the ‘reactor model’, the growth rate, temperature and time function and the observed growth rate data were input to the package and the program was run (Appendix 7). The output data were the estimated bacterial counts (cfu) in the bulk phase (N) and in the biofilm on the reactor (R) over time at different sampling intervals. The output dataset included estimations of the following.

- **M** (estimated bacterial counts in the bulk milk phase using the pipe-only model).
- **F** (estimated bacterial counts in the biofilm phase on the pipe using the pipe-only model).
- **N** (estimated bacterial counts in the bulk milk phase using the reactor model).
- **R** (estimated bacterial counts in the biofilm phase on the reactor using the reactor model).

To visualize whether or not this reactor model estimation was close to actual, N values needed to be converted into the outflow concentration of bacteria using the known reactor volume. Then, these converted values were transformed to \log_{10} and compared with actual observed milk-out readings. The volume of the hexagonal reactor was 4 ml. N values were the output of the R programming of the model.

Equation 8–36

$$N_{Converted} = \frac{N}{Volume_c} = \frac{Estimated\ N\ from\ model\ output}{4ml} (cfu/ml)$$

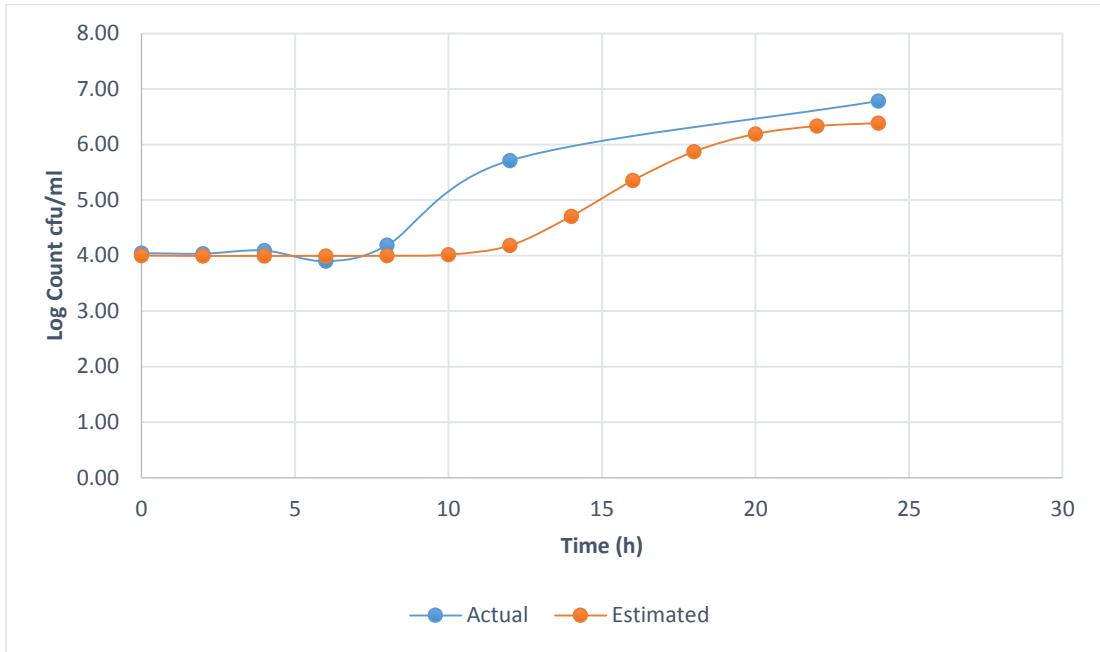


Figure 40: Estimated versus actual growth (sine wave, 20 min, 55–30°C).

Comparison between the estimated outflow bacterial concentration in the bulk phase using the reactor model and the actual outflow bacterial concentration (cfu/ml) for thermocycling at 55–30°C with a sine wave period of 20 min in 10% RSM. (Detailed data in Appendix 33 in the data CD)

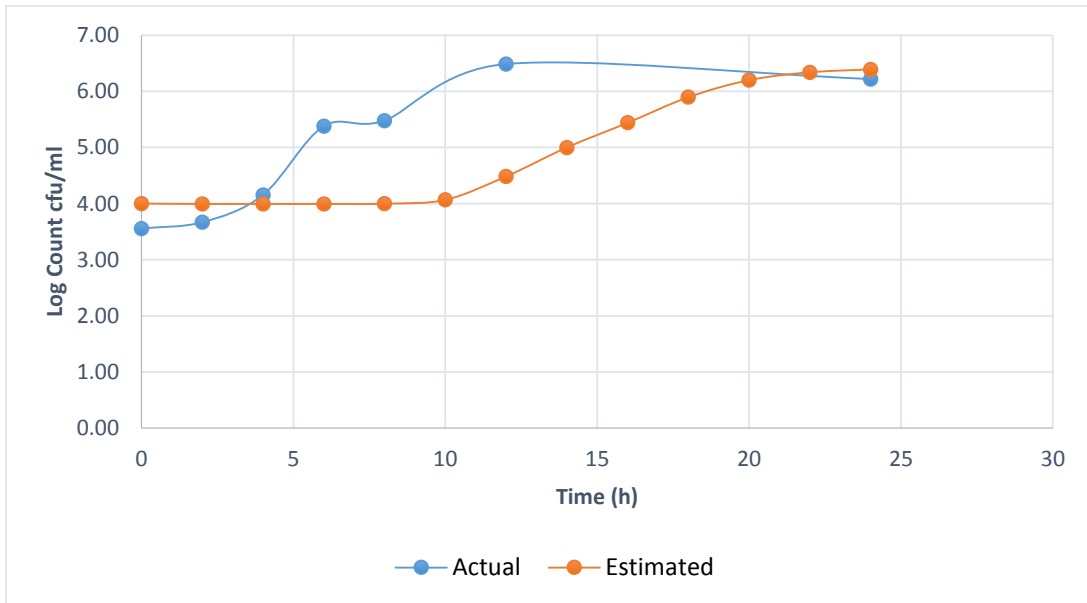


Figure 41: Estimated versus actual growth (sine wave, 20 min, 55–35°C).

Comparison between the estimated outflow bacterial concentration in the bulk phase using the reactor model and the actual outflow bacterial concentration (cfu/ml) for thermocycling at 55–35°C with a sine wave period of 20 min in 10% RSM. (Detailed data in Appendix 33 in the data CD)

This model estimation was closer to the actual readings for thermocycling at 55–30°C/20min (Figure 40) than for thermocycling at 55–35°C/20min (Figure 41). Also,

this model predicted the final concentration of bacteria in the outflow after 24 h. The model was more accurate in the later stages of growth than in the earlier stages because it did not predict the reduction in bacterial counts in the outflow during the lag phase in the 35°C experiments. It also overestimated the length of the lag phase.

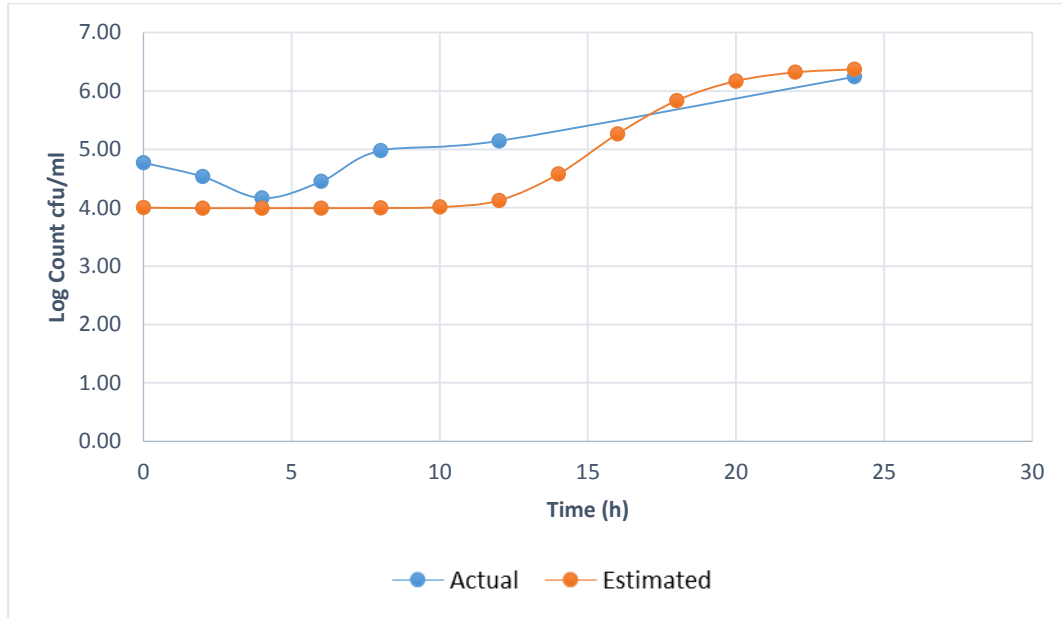


Figure 42: Estimated versus actual growth (square wave, 55–30°C).

Comparison between the estimated outflow bacterial concentrations in the bulk phase using the reactor model and the actual outflow bacterial concentration (cfu/ml) for square wave thermospiking at 55°C/15 min, 30°C/35 min in 10% RSM. (Detailed data in Appendix 33 in the data CD)

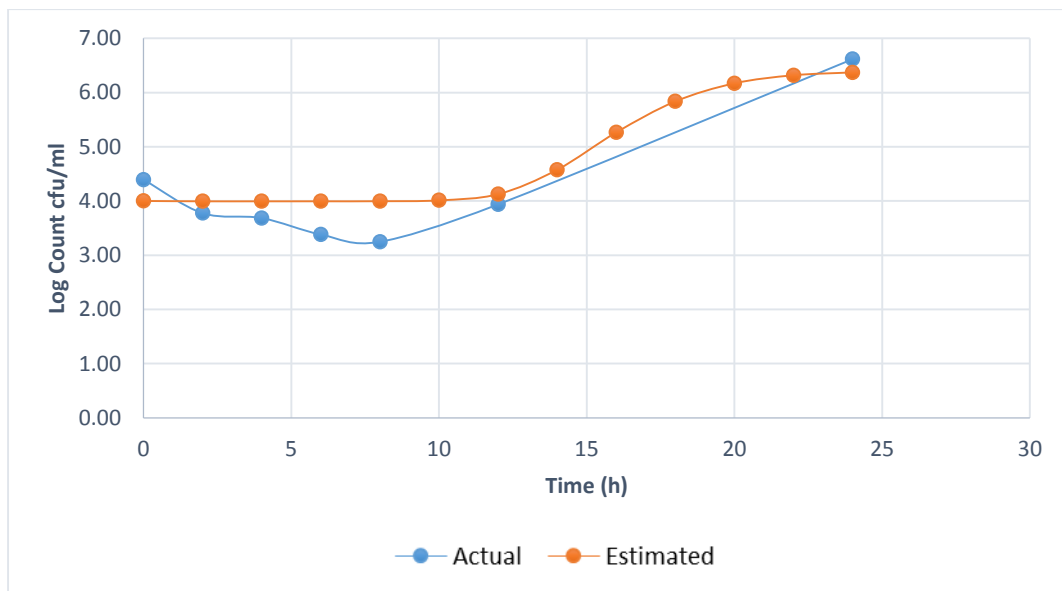


Figure 43: Estimated versus actual growth (square wave, 55–35°C).

Comparison between the estimated outflow bacterial concentration in the bulk phase using the reactor model and the actual outflow bacterial concentration (cfu/ml) for square wave thermospiking at 55°C/15 min, 35°C/35 min in 10% RSM. (Detailed data in Appendix 33 in the data CD)

In the square wave regimes, this model predicted the final output concentration of the bulk milk phase after 24 h well, results shown on Figure 42 for 55–30°C and Figure 43 for 55–35°C. It did not predict the reduction in bacterial counts in the outflow during the lag phase, especially at 35°C. It predicted the lengths of each phase of bacterial growth very closely.

This model predicted the general behaviour of bacterial attachment in this system. It was a reasonable first approximation for the temperature-cycling experiments. It predicted the general growth behaviour of the bacteria in the temperature-cycling experiments and the duration of each phase, i.e. the lag phase, the log phase and the stationary phase of the bacteria outflowing from the temperature-cycled reactors. It represent the growth and stationary phase well, but not the initial lag phase. The actual process is more complex than we currently modelled. The model provides some of insights of what is going on, the model can be expanded in the future after more work. The logistic equation is used widely to predict populations in ecology and biology. It is a simple and robust model based on the logistic growth theory of populations in nature, but was not discussed in a biofilm modelling review (Wanner et al., 2006).

However, there is some debate about this model.

- **The predicted output (predicted N) was not smooth.**

Because of the assumption of an instantaneous response of the bacteria, the predicted output was not smooth. It did not represent the actual behaviour of the bacteria during the experiment because of a lag in the reaction of bacteria to temperature changes. The frequent appearance of peaks, which may have been driven by the temperature cycling or by the frequent sampling intervals (1 min) of the model (Figure 44), was not observed or achieved (compared with 2h sampling intervals of the model, Figure 45).

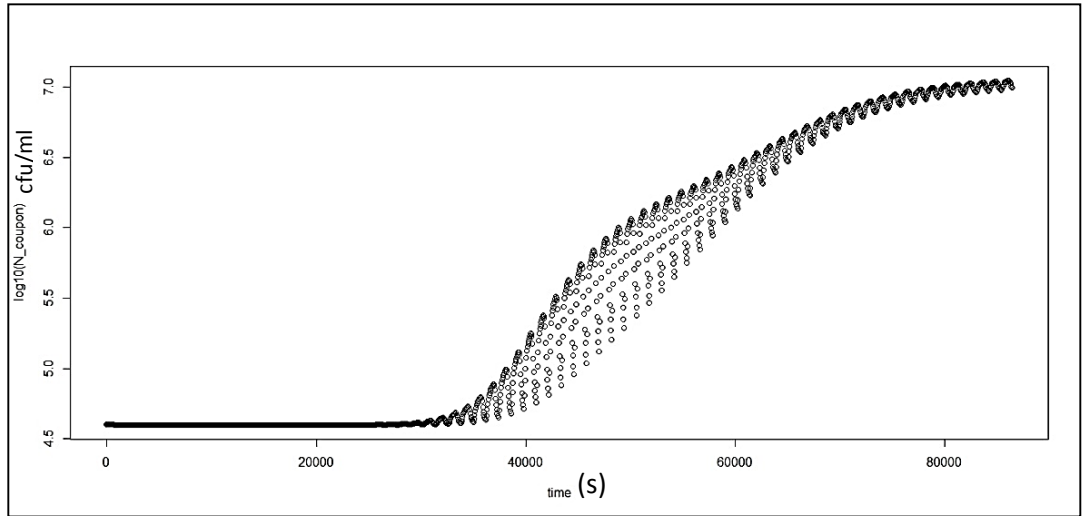


Figure 44: Output graph from R: estimated N_{reactor} (sampling interval: 1 min).

Output graph from R program: estimated bacterial counts in the outflowing bulk milk phase N_{reactor} ; thermocycling of Geo1 at 55–35°C with a sine wave period of 20 min and a sampling interval of **1 min** for 24 h, plotted using a logarithmic scale. Y-axis = log bacterial counts of the outflowing milk (cfu); X-axis = time (s).

This mismatch between the simulations and the experimental outputs was due to the fine resolution/high frequency responses of the simulations. The experimental protocols need to be refined to achieve better resolution of the experimental outputs.

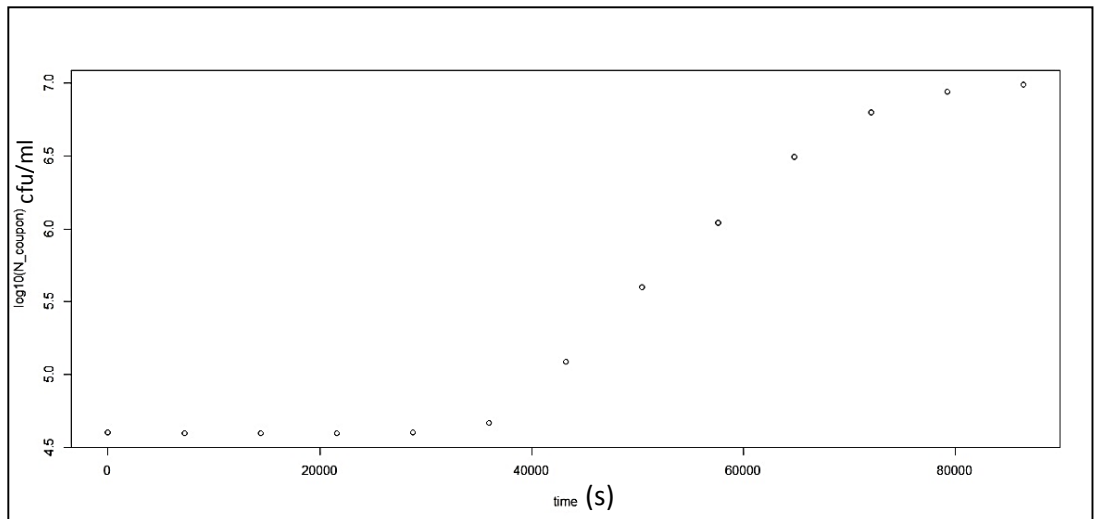


Figure 45: Output graph from R: estimated N_{reactor} (sampling interval: 2 h).

Output graph from R program: estimated bacterial counts in the outflowing bulk milk phase N_{reactor} ; thermocycling of Geo1 at 55–35°C with a sine wave period of 20 min and a sampling

interval of **2 h** for 24 h, plotted using a logarithmic scale. Y-axis = log bacterial counts of the outflowing milk (cfu); X-axis = time (s).

- **The observed different growth curves from the temperature-cycling experiments at 30 and 35°C could not be explained.**

No growth was predicted at either 30 or 35°C. The biofilm growth rates at both these temperatures were the same ($1 \times 10^{-6}/\text{h}$). Thus, the predictions, which were made on the basis of biofilm growth rates, were the same.

However, the growth curves from the thermospiking experiments at 30°C (Section 6.4.2.1, Figure 27) and 35°C (Section 6.4.2.2, Figure 28) were different. The 35°C runs had a prolonged lag phase and an initial reduction in the bacterial counts in the outflowing milk during the lag phase, which were not seen in the 30°C runs. This model does not reflect or explain these differences.

The factors causing these differences in the growth curves are unclear. It is not known whether the cells were lysing, sporulating, germinating or dying, because the reactors could not be opened aseptically and reassembled during the experiments. The attachment process and the development of a biofilm are more complicated than we thought and predicted under cycling conditions.

However, some hypotheses can be made to address these differences. One possible explanation is the ‘maintenance energy’ (Pirt, 1965), which is defined as the energy used by bacteria to survive and live rather than to reproduce any new materials or grow. From this theory, the observed growth yield (Y) can be expressed as

Equation 8–37

Y

$$= \frac{\text{Certain Amount of the Organism}}{\text{Amount of Energy Substrate}_{\text{growth}} + \text{Amount of Energy Substrate}_{\text{maintenance}}}$$

It can be seen that the amount of maintenance energy used at high rates of growth (high observed growth yield) is a very small proportion of the total energy requirement, whereas it becomes a very important factor at low rates of growth (low observed growth yield) (Pirt, 1965).

Pirt later developed the observed growth yield, as given in Equation 8–38, where μ is the maximum specific growth rate of the organism and Y_G is the ‘true growth yield’ (when the maintenance energy = 0, all the energy is consumed for the synthesis of new materials).

Equation 8–38

$$1/Y = \text{maintenance energy coefficient}/\mu + 1/Y_G$$

In the temperature-cycling experiments, the maintenance energy coefficient of the two temperatures (30 and 35°C) and the maintenance energy for each temperature may have been different. Although the maximum specific growth rate was very small at both temperatures, the observed growth yield for each temperature could still have been different.

Another possible explanation is that 35°C might induce more attachment/settling than 30°C. From the model and the data, it can be seen that, during the prolonged lag phase in the thermospike experiments, the bacterial counts in the bulk milk phase decreased over time, which meant that the rate of change of bacterial counts was negative.

Equation 8–39

$$\frac{dN}{dt} = \text{Inflow}_{\text{reactor}} - \text{Outflow}_{\text{reactor}} - \text{Settling}_{\text{reactor}} + \text{Sloughing}_{\text{reactor}} < 0$$

Therefore, the net rate of bacteria flowing out of the bulk milk phase was greater than the net rate of bacteria flowing into the bulk milk phase:

Equation 8–40

$$Inflow_{reactor} + Sloughing_{reactor} < Outflow_{reactor} + Settling_{reactor}$$

Equation 8–41

$$\left(\frac{M \times Flowrate}{Volume_{pipe}} \right) + \left(\frac{R^2 \times Area_{pipe}}{k_{pipe} \times Area_{reactor} \times t_{G,reactor}} \right) < \left(\frac{N \times Flowrate}{Volume_{reactor}} \right) + \left(\frac{Velocity \times Area_{reactor} \times N}{Volume_{reactor}} \right)$$

M is the bacterial counts in the bulk milk phase in the preheating pipe flowing into the reactor; as it is small at the beginning of the experiment, the inflow term is small. N is the bacterial counts in the bulk milk phase in the reactor; as it is also small at the beginning of the experiment, the outflow term is also small. R is the bacterial counts in the biofilm phase on the surface of the reactor. As the occupation sites are not full and the bacterial counts in the biofilm phase are smaller than the carrying capacity at the beginning of the experiment, the sloughing term is small. Therefore, settling is the important dominating process towards bacterial reduction during the prolonged lag phase.

This could also be explained by the 35°C being in a range where metabolism was continuing perhaps in an unbalanced manner, resulting in more overall damage than cycling to 30°C, where metabolism was more seriously reduced. Exposing bacteria to the unfavourable conditions would result unbalanced metabolism during bacterial growth hence reduce bacterial growth yield (Brooks & Meers, 1973).

- **The ‘scale-up effect’ was not considered in this model.**

This model was designed using a mono-culture system in laboratory reactors. Dairy manufacturing plants have more complicated processes than this model, with more than one thermophilic culture within the milk feed. The ‘scale-up effect’ was not considered in this model. The model needs to be validated using a pilot plant to determine whether the predictions still hold.

- **This model was validated using only 10% milk solids with the *Geobacillus* species (Geo1).**

The growth of this *Geobacillus* species in 14% and 18% solids RSM needs to be tested further to gain more understanding of the growth/temperature relationship, prior to using this model.

- **There were some mathematical defects in the model that need to be improved in the future.**

The parameters for the ‘reactor model’ were not optimized because of the complexity of the temperature changes. The parameters $t_{0,reactor}$, $t_{G,reactor}$ and $k_{reactor}$ need to be optimized for each experimental condition, which may be very difficult and will require more data (Robin Hankin, 2013, personal communication). It was assumed that the carrying capacity of the reactor did not change with changes in temperature. The settling velocity was unique to the system geometry and there may be differences with different species of microorganism or different temperatures. No consideration was given to different surface properties of different materials.

Also, in the real manufacturing environment, particles travel in different flow conditions result boundary layers. The velocity decrease or becomes unstable within boundary layers in different flow types. The different flow types (laminar flow or turbulent flow) and flow conditions will influence the particle / bacteria travel or adhere in the pipe, which needs very complex partial differential equations to estimate fully (Robin Hankin, 2013, personal communication).

- **A preheating pipe does not exist in dairy manufacturing plants.**

The reactors was to represent conditions and experimental similarities of the preheaters in the dairy manufacturing conditions. The silicone preheating

pipes, as known as preheating section, acts as preheater for the reactor system. The silicone pipes are to preheat milk entering the reactor, otherwise the heating / cooling time is too long to get any meaningful results. The preheating pipes, as used in this study, do not exist in real manufacturing plants (no preheater needed before preheater). This study is not simulating the manufacturing plants, however, it provides an analogy to the plant and study the effect and application of temperature-cycling technology onto dairy isolates.

8.7 Use of the Mathematical Model

This model is very simple to use under laboratory conditions. To implement it in an actual dairy process, the reactor model needs to be validated using pilot plant trials. The outcome and the assumptions need to be tested to determine whether the conclusions of this reactor model still hold. After validation in the pilot plant, the model may be used in manufacturing plants as a prediction tool by changing the parameters in the model. The area and the volume can be changed easily.

The maximum temperature, the minimum temperature and the period of the wave need to be provided in the thermocycling (sine wave) system. The maximum temperature, the minimum temperature, the time spent at maximum temperature and the time spent at minimum temperature need to be provided in the thermospiking (square wave) system. The model can be programmed to give predictions on the bacterial counts of the product and in the output stream at the desired frequency, i.e. hourly or half-hourly. It can be programmed to give feedback on the run automatically.

This model is an indicative tool that provides a first approximation to modelling the biofilm behaviour of Geo1, *Geobacillus stearothermophilus* in a flowing, heated system. As it was designed based on simulation of simplified and idealized processes

in the manufacturing plant rather than on what actually occurs in the plant, there are some limitations in applying this model to real manufacturing situations. Some validation work is needed.

8.8 Summary

Mathematical models for the bulk milk phase side and the biofilm side of the reactor system were developed. This model predicted the general behaviour of Geo1 bacteria under different temperature-cycling regimes. However, there are some limitations with the use of this model, such as the mono-culture laboratory system.

9 Final Discussion and Conclusions

9.1 Mathematical Model for Prediction of the Growth of Geo1

Ratkowsky, Lowry, McMeekin, Stokes, & Chandler (1983) designed a model for predicting planktonic bacterial growth over a range of temperatures, where T_{\min} and T_{\max} are the minimum and maximum growth temperatures in Kelvin, and c and b are the constants determined using Gauss–Newton curve fitting.

$$\log\left(1 - \frac{\sqrt{\text{growth}}}{b(T - T_{\min})}\right) = c(T - T_{\max})$$

In the current study, to construct the temperature versus growth relationship, we decided to use a linear regression approach and to connect adjacent temperature points. This approach overcame the complexity of the mathematics in the model and kept the robustness of the model without losing prediction power (Robin Hankin, 2013, personal communication).

“We spoke about a more sophisticated interpolation method than the piecewise linear interpolation that we used in the model. In my opinion, such sophisticated schemes are inadvisable on several grounds. Firstly, they are not robust as mis-predictions do occur. Secondly, it is extremely difficult, both mathematically and bacteriologically, to incorporate prior information about growth range into the models. Thirdly, the mathematical form of such growth curves is poorly suited to such techniques.” (Robin Hankin, 2013, personal communication)

Some processes in this current pipe and reactor model were simplified; they can be expanded and studied in more detail in the future. Boundary layers and diffusion could be included in the calculation of attachment (de Jong, te Giffel, & Kiezebrink, 2002).

Also other models use partial differential equations to take account of particles moving along the system (Wanner et al., 2006). The main advantage of this current model was its simplicity and robustness. It simplified the processes in the system down to inflow, outflow, settling, sloughing and growth, and was designed using measured data. The estimation process was done automatically using the R program. The current model did not involve complicated terms and constants or expensive computer programs. As a first approximation, its simplicity and controllability were maintained without loss of the power of prediction (Robin Hankin, 2013, personal communication).

However, when this model is applied to the real manufacturing environment, additional processes and their effects on the overall thermophile count and biofilm formation will need to be considered.

- **Spores**

Spore-forming bacteria form endospores when the growth conditions are not favourable. The spores then germinate back into the vegetative cell form. The spore count increases after preheating and during the evaporation process, when the total solids increase from 13 to 48% (Scott, Brooks, Rakonjac, Walker, & Flint, 2007). Sporulation, which occurs 9 h into a milk powder manufacturing plant run, contributes all the spores within the manufacturing system (i.e. the spores are not from raw milk or contamination) (Scott, Brooks, Rakonjac, Walker, & Flint, 2007).

If the current reactor model is to be used in the evaporation process, sporulation and germination will affect the overall thermophile count in the biofilm and the final product. Additional terms taking account of the effect sporulation and germination processes could be added into the reactor model based on data collected from factories and various manufacturing processes, such as % of cells in the sporulation / germination processes.

- **Foulant/cleaning residues**

Thermophilic bacteria attach more rapidly on to pre-fouled surfaces than on to un-fouled stainless steel (Hinton, Trinh, Brooks, & Manderson, 2002) with spores predominating in the foulant. Spores from the foulant may be released to recontaminate the clean plant or the product stream during processing (Marshall, 1994) (Scott, Brooks, Rakonjac, Walker, & Flint, 2007).

- **Inoculum level in the raw milk**

The inoculum level in the temperature-cycling experiment (approximately 10^4 cfu/ml) was much higher than inoculum level in the raw milk feed (approximately 10 cfu/ml) in the realistic manufacturing situations (Scott, Brooks, Rakonjac, Walker, & Flint, 2007). The inoculum level in the model, which is the Inflow term can be changed according to the inoculum level in the raw milk feed. The model needs to be tested against such change whether the change in inoculum level will affect the prediction. If the inoculum level is lower in the temperature-cycling run, it may result a longer lag phase and even greater potential to run plant for longer than currently indicated by this study.

9.2 Effectiveness of Temperature Cycling

Knight, Nicol, & McMeekin (2004) were the first to report the effect of temperature cycling on the control of dairy biofilms by either interrupting exponential growth or preventing cell attachment to surfaces. The mechanism of temperature cycling used in the present study was the same as that of Knight, Nicol, & McMeekin (2004), involving shifting thermophilic bacteria out of the growth temperature zone on a regular basis to disrupt biofilm formation or exponential growth. There were some differences between the two studies. The Knight group used pilot-scale experiments, whereas we used laboratory-scale experiments. The Knight group proposed applying a temperature wave

to the regenerative section of the plate heat exchanger, whereas we proposed applying temperature waves and spikes to the heating section of the plate heat exchanger.

Exponential growth can be delayed through an extended lag phase or can be shortened through cell death (Knight, Nicol, & McMeekin, 2004). In the present study, with an industry isolate of *Geobacillus*, Geo1, a longer lag phase and a reduced exponential growth phase compared with a control, non-cycled system were produced, as has been reported previously (Aplin & Flint, 2007) (Knight, Nicol, & McMeekin, 2004).

In a previous study using the same system (Aplin & Flint, 2007), thermocycling at 30–50°C over a 20 min cycle was effective in controlling thermophilic bacteria for up to 14 h in a reactor using skim milk. In the current study, thermocycling at 30–55°C over a 20 min cycle was not effective against *G. stearothermophilus* (Geo1). However, thermocycling at 30–55°C over a 50 min cycle gave a 1.5 log reduction after 24 h. Thermocycling at 35–55°C over a 10 min cycle extended the lag phase to up to 12 h. This differed from the previous study, and may be explained by strain differences or differences in the experimental set-up such as the maximum temperature. More information is needed through sampling more points over the 12–24 h period.

9.3 Application of Temperature Cycling in the Dairy Industry

It has been shown that different species of thermophilic bacteria predominate in different zones or areas in milk powder manufacturing plants (Scott, Brooks, Rakonjac, Walker, & Flint, 2007). *Geobacillus* species are dominant in evaporators, whereas *Anoxybacillus* is found in the preheating section. The total thermophile count and the spore count increased during the preheating section before the evaporator and in evaporator passes 1 and 2, indicating possible sites for vegetative cell growth and sporulation. Plate heat exchangers and evaporators provide a large surface area for thermophile attachment and biofilm development, under suitable growth conditions.

The current study produced a model and temperature-cycling regimes to control growth and biofilm development of *Geobacillus stearothermophilus*. In the future, temperature-cycling experiments on *Anoxybacillus* and mixed species will be required. In the meantime, some hypotheses can be made based on the growth of *Anoxybacillus*.

The *Anoxybacillus* strain in this study, Anoxy2, had a narrower temperature range for biofilm formation than Geo1; biofilm development was restricted to 50–60°C in 10% RSM in the CDC reactor (grew faster at 60°C than at 50°C). For planktonic growth, Anoxy2 grew slowly at 40°C and 65–70°C in 10–15% RSM.

The optimum growth temperature for Anoxy2 is between 60 and 65°C based on Ratkowsky, Lowry, McMeekin, Stokes, & Chandler (1983). Anoxy2 had a slightly longer doubling time (23 min) than Geo1 (19 min). To shift Anoxy2 out of the suitable temperature zone for growth, the temperature-cycling regimes can be either 65–30°C or 65–35°C. Raising the temperature above the optimal growth temperature may have less effect since these thermophiles can survive up to 70°C. Also, holding at any higher temperature can cause detrimental effect to product quality. Some adaptation of the thermospiking regimes may be possible, such as increasing the time spent at high temperature from 15 to 20 min to maintain the heating efficiency of the heat exchanger while maintaining the effect of the temperature cycle in controlling the growth of thermophilic bacteria.

If this proposed scheme can control the growth of and biofilm development of Anoxy2 successfully (with reductions in the thermophile count and biofilm development in the reactors), the next stage will be to apply this to a biofilm of mixed thermophile species. Geo 1 has wider tolerance in temperature and water activity than Anoxy2, so there are the possibilities that these two targeted control bacteria may be controlled by one temperature-cycling scheme, which was tested to control Geo1 successfully.

Suggestions to the Industry about Different Regimes

When biofilm formation after 24 h and bacterial concentrations in the outflowing milk from different thermocycling and thermospiking regimes were compared, four different options gave successful control of Geo1. Successful control was defined as providing a noticeable reduction (i.e. a reduction of > 1 log cfu/ml) in bacterial counts after 24 h, because of a prolonged lag phase, and a reduction in biofilm formation.

Table 18: Options for successful temperature-cycling regimes controlling Geo1

Option	Regime	Reduction after 24 h in Outflowing Milk Concentration (cfu/ml)	Reduction after 12 h in Outflowing Milk Concentration (cfu/ml)	Lag Phase Length (h)	Reduction in Biofilm Formation (cfu/cm²)
1	55–35°C, 10 min	No reduction	2 log	12	1.6 log
2	55–30°C, 50 min	1 – 1.5 log	1 log	6	1 log
3	55°C/15 min –35°C/35 min	No reduction	> 2 log	12	1.5 log
4	55°C/15 min –30°C/35 min	< 1 log	< 1.5 log	4	1 log

Options 1 and 2 are thermocycling regimes, whereas Options 3 and 4 are thermospiking regimes; 10 min and 50 min are the period of the sine wave; 15 min in the thermospiking regimes is the time spent at the maximum temperature, 55°C; 35 min in the thermospiking regimes is the time spent at the minimum temperature, 30 or 35°C.

Options 2 and 4 have the most potential to extend the run length when Geo1 is present, because of the reduction in bacterial concentration in the outflowing milk after 24 h. Options 1 and 3 produced a greater reduction in bacterial concentration in the outflowing milk after 12 h, which means that the plant could produce better quality product within the first 12 h of a manufacturing run.

The effect of the temperature wave in Options 1 and 3 was reduced after the first 12 h. The lag phase was shorter and there was less reduction in the number of bacteria in the milk and the biofilm within the first 12 h for Options 2 and 4 compared with Options 1

and 3. However, the effect of controlling thermophile growth lasted for longer for Options 2 and 4 than for Options 1 and 3.

The reason for the differences between the different cycling regimes is not known. One possible explanation is that the maintenance energies for bacterial survival at 30 and 35°C are different and the settling rates at 30 and 35°C are different, as discussed in Section 8.6. Another possible explanation is different sporulation/germination at the two temperatures. If the vegetative cells start to sporulate, which is irreversible beyond certain stages, counts are higher after some storage time, however, no further growth can occur until the mature spores are heat activated (Pirt, 1975) (Young & Fitz-James, 1959). Spores, not vegetative cells, predominate in foulant (Scott, Brooks, Rakonjac, Walker, & Flint, 2007). It is not known whether the reduction in culturable thermophilic bacteria seen in the temperature-cycling experiments was due to cells dying or cells in a transition stage towards spore formation.

Advantages and Disadvantages of Temperature Cycling

Temperature cycling is a novel technology for disrupting thermophile growth in the dairy industry.

Temperature cycling may offer some economic benefits to the dairy industry. From previous laboratory and pilot plant studies, temperature cycling reduces streptococci in cheese (Knight, Nicol, & McMeekin, 2004). The present trial extended this concept for the control of thermophilic bacilli. If this concept works, it promises economic benefits to the dairy industry through reduced time needed for cleaning, increased plant capacity through longer run lengths, reduced cleaning costs and improved product quality. Large overhead costs to modify current manufacturing plants are not required (Knight, Nicol, & McMeekin, 2004). As this process does not subject milk to severe conditions or hazardous chemicals, the quality of the final products should not be affected.

However, there are arguments against the use of temperature cycling. Repeated temperature cycling may select a subpopulation, more tolerant of the fluctuating

metabolism and may gradually lose its effect. Exposing these thermophilic bacteria to temperature cycling (spore-inducing conditions or not) will encourage sporulation, producing a more heat-resistant and chemically resistant population (Traag, Pugliese, Eisen, & Losicka, 2013).

The present models have not been tested in a pilot plant or a production plant, and there may be some issues in the scale-up of the process. Validation and optimization for different manufacturing plants may be needed. Scale-up from the laboratory scale to industrial production may not be linear and may not achieve the same bacterial reduction (Aplin & Flint, 2007) (Knight, Nicol, & McMeekin, 2004). The temperature-cycling process implemented in the preheating plate heat exchanger section may result in colder milk entering the evaporators. Thus, more energy or steam input may be required to achieve normal evaporation. The cost and the efficiency of implementing temperature cycling need to be justified (Knight, Nicol, & McMeekin, 2004).

Where to Implement this New Temperature Cycling Technology?

There are two main sites for the development of biofilms of thermophilic bacteria in milk powder manufacturing plants, which cause noticeable increases in thermophilic bacteria and spore counts in the outflowing product. These are the plate heat exchanger before the evaporators and the first two passes of the evaporators (Scott, Brooks, Rakonjac, Walker, & Flint, 2007).

The preheating plate heat exchanger before the evaporators is a suitable site for implementing temperature cycling, as it is easy to set up and is unlikely to affect the operation of the evaporator. The shifts in temperature will change the temperature profile of the heat exchanger so that no one section is continuously under ideal conditions for thermophilic bacterial growth (Knight, Nicol, & McMeekin, 2004).

Implementing temperature cycling in evaporator passes 1 and 2 is less feasible because of the impact on the subsequent evaporation process. Temperature-cycled evaporation

would not be as efficient as non-temperature-cycled evaporation; if the milk stream is subjected to lower temperatures than the current evaporation temperature, more steam input through later effects of the evaporators may be needed to achieve the same amount of evaporation as under standard conditions.

Another possible site at which to introduce a temperature cycle may be the preheating heat exchanger or pasteurizer before separation. There are many different configurations for a dairy manufacturing plant, particularly around the separation process. Most separators run at temperatures $< 38^{\circ}\text{C}$ to avoid the growth of thermophilic bacteria and the production of thermophilic spores. Temperature cycling around separation may be another way to avoid thermophile growth and optimize the separation of cream and skim milk.

Recommendations to the Dairy Industry

From the results of the factorial experiments with the CDC reactor, the conditions for biofilm growth of two strains of thermophilic bacilli isolated from milk powder were determined. *G. stearothermophilus* grew at $40\text{--}70^{\circ}\text{C}$ in milk with 10–14% solids. *A. flavithermus* grew at $50\text{--}60^{\circ}\text{C}$ in milk with 10% solids. Unfortunately, there was no readymade mathematical model that would fit the growth rate curves for these bacteria. Ideally, more data are needed to produce a more refined mathematical model to estimate the biofilm growth rate of these thermophilic bacilli. In the meantime, we recommend that the biofilm growth rate at a certain temperature within the above range be calculated using the equation constructed from two adjacent data points (Figure 17).

TOOLBOX 1: Equations for calculating the biofilm growth rate of Geo1 in different temperature ranges.

***Geobacillus stearothermophilus* (Geo1) equations:**

$$\text{Biofilm Growth Rate}_{35-40^{\circ}\text{C}} = 0.1693 \times \text{Temperature} - 5.9255$$

$$\text{Biofilm Growth Rate}_{40-50^{\circ}\text{C}} = 0.062 \times \text{Temperature} - 1.6319$$

$$\text{Biofilm Growth Rate}_{50-60^{\circ}\text{C}} = -0.0268 \times \text{Temperature} + 2.8081$$

$$\text{Biofilm Growth Rate}_{60-70^{\circ}\text{C}} = -0.0146 \times \text{Temperature} + 2.0719$$

TOOLBOX 2: Equations for calculating the biofilm growth rate of Anoxy2 in different temperature ranges.

***Anoxybacillus flavithermus* (Anoxy2) equations:**

$$\text{Biofilm Growth Rate}_{40-50^{\circ}\text{C}} = 0.1566 \times \text{Temperature} - 6.2652$$

$$\text{Biofilm Growth Rate}_{50-60^{\circ}\text{C}} = 0.0358 \times \text{Temperature} - 0.2237$$

Two successful mathematical models were generated from this study. The preheating pipe model offered some insight into biofilm formation and the attachment of dairy thermophiles. Logistic theory was the foundation for both the preheating pipe model and the full reactor model. These two models could estimate biofilm growth with a known level of incoming thermophilic bacteria under constant or cycling temperatures.

9.4 Suggestions for Future Work

The following questions provide some guideline for future work.

- **What occurred during the initial decrease in bacteria in the outflowing milk? What caused this decrease?**

There was a decrease, which reached > 1 log/ml, in the bacterial counts in the outflowing milk in the thermospiking experiments at 35°C, for which there is currently no explanation.

There are several possible explanations. The decrease in cells released in the milk may have been due to cells attaching to the walls of the preheating pipe or the reactor walls. These thermophiles can attach on to stainless steel in as little as 30 s (Flint, Brooks, Bremer, Walker, & Hausman, 2002). If the attachment sites are not fully occupied, these thermophiles could continue to attach before the biofilm starts to develop and to release bacteria. Another possibility is that vegetative cells entering the new environment of the reactor may start to sporulate and therefore be in a state that cannot be cultured (Pirt, 1975) (Young & Fitz-James, 1959). Death and lysis may also occur in the early stages.

To investigate this early stage of the thermocycling experiments, reactors that enable regular sampling of the biofilm (e.g. Robbins devices or tube reactors) are needed. The laboratory equipment used in this trial could not be opened for analysis during the experiments. A reactor with removable coupons or sections would enable the biofilm to be examined at different stages during an experiment (Flint, Palmer, Bloemen, Brooks, & Crawford, 2001). A full set of the bacterial and spore counts on coupons and in the

outflowing milk would provide a more complete picture of the state of the thermophilic bacteria at this early stage of temperature cycling. Microscopy could also be used to determine the proportion of spores as well as of live and dead cells.

- **What happened during the 12–24 h period of the temperature-cycling experiments?**

More points from the 12–24 h period should be sampled to obtain a complete analysis of growth over this period.

- **How long can the effects of temperature cycling be maintained?**

Both models from this study predict that temperature cycling will be effective for at least 24 h. Trials beyond 24 h will enable the limits of temperature cycling to be determined.

- **The growth curves for Geo1 exposed to sine and square wave temperature cycling at 30 and 35°C were noticeably different. What would cause this difference? Why did 35°C produce a much longer lag phase than 30°C?**

In the 34 h runs in the CDC reactor, there was no growth at either 30 or 35°C. Some possible explanations are that 35°C may enhance the sporulation process, that the maintenance energies for bacterial survival at 30 and 35°C may be different and that the settling processes or the settling rates at 30 and 35°C may be different, as discussed in Sections 8.6 and 9.1.

Another possible explanation may be that the activity of key enzymes is disrupted during the temperature cycling. Cell death at the start of sporulation may be stimulated by temperature cycling. These possibilities need to be investigated through enzyme profiling or microscopy.

- **What happens in mixed cultures of *Geobacillus* and *A. flavithermus*?**

In the CDC reactor factorial runs, *A. flavithermus* (Anoxy2) had a much narrower temperature range for growth and a narrower total solids range than *G. stearothermophilus* (Geo1). Anoxy2 grew only at 10% solids at 50 and 60°C. A more complete dataset is needed to determine the growth rates of *A. flavithermus* at different temperatures. This will allow the limits for temperature cycling for Anoxy2 to be set. *A. flavithermus* is found mainly in the preheater of a milk powder manufacturing plant, where the milk is less concentrated than later in the manufacturing process (Scott, Brooks, Rakonjac, Walker, & Flint, 2007).

The growth of mixed species of thermophilic bacteria, and the design and testing of temperature cycling for these mixed populations may be important for controlling thermophilic bacteria in dairy manufacturing plants in which both species are present. This is to be expected as both species were found in the milk powder used for this study, especially in the evaporators (Scott, Brooks, Rakonjac, Walker, & Flint, 2007). What needs to be confirmed is whether both species are likely to grow together as biofilms in the manufacturing plant or whether they grow in different sections of the plant. This will be important in applying the appropriate temperature-cycling regimes to the corresponding parts of the manufacturing plant.

- **How do the models generated in this trial relate to dairy manufacturing plant?**

Some validation work and modifications may be needed to implement this temperature-cycling technology in a dairy manufacturing process. This model is designed only for mono-cultures in a specific laboratory system. However, it can be modified to suit a manufacturing plant using the same logistic growth equation but with different parameters. As the 'scale-up effect' was not considered in this project, pilot plant trials will be necessary.

- **Can flow cytometry be used in conjunction with this model to monitor the effect of temperature cycling with close to real-time results?**

Flow cytometry could be used to determine the incoming milk counts within a short period of time. This could then be used in the model to estimate the run time and the quality of the final product (counts in the outflowing milk). An estimate of cleaning residual biofilm/foulant from the previous run will also play an important role in estimates of run time. This may be difficult to estimate by flow cytometry as the number of viable cells remaining after cleaning is likely to be very low.

- **Would partial differential equations provide better models than ordinary differential equations, to take into account spatial differences in bacterial growth along the pipe?**

The current models were designed using ordinary differential equations with the assumption of uniform biofilm growth. In manufacturing plants, the growth along pipes and equipment will vary depending on conditions such as temperature. To take account of these differences and for more accurate estimates, partial differential equations could be used instead of ordinary differential equations. Partial differential equations will take a particle travelling through various zones into consideration. However, partial differential equations and the associated optimization are more complex than ordinary differential equations. The robustness of the model might be reduced for only a small increase in predictive power.

- **How would the oscillations in data and sloughing-off of cells from the biofilm affect the predictive models for temperature cycling?**

It was assumed that 'sloughing' from the biofilm into the bulk stream was random and non-periodic. Thus, these models did not consider possible oscillations in the data (Parker, Flint, & Brooks, 2003). Periodic or continuous sloughing-off of biofilms of these bacteria and the timing of

these events need to be determined. Some additional terms may need to be added into the model to predict this oscillating behaviour.

- **Can the parameters in the reactor model be optimized?**

All the parameters in the pipe-only model were optimized and fed into the reactor model. Because the reactor model is made up of a series of ordinary differential equations, it is complex and optimization of the parameters in the reactor model, such as $T_{G,reactor}$, $T_{0,reactor}$ and $k_{reactor}$, is difficult (Tjoa & Biegler, 1991).

- **Are there any mathematical assumptions that need to be confirmed to develop a refined model?**

It was assumed that the pipe and the reactor will share the same carrying capacity per unit area and will differ only because of their different geometries. The carrying capacity in the preheating pipe (k_{pipe}) was optimized for 55°C. Whether carrying capacities will differ under variable temperature-cycling conditions needs to be tested.

Also, it was assumed that the settling velocities of the bacteria on to pipes and reactors are the same, irrespective of their geometric properties. Are there any other factors that may influence the settling velocity?

The biofilm in the preheating tube is considered to be a uniform structure. However, there is the possibility of considering spatial differences in any future model using partial differential equations.

9.5 Conclusions

Two thermophilic bacilli – *G. stearothermophilus* (Geo1) and *A. flavithermus* (Anoxy2) – were isolated from skim milk powder. Experiments done on these two typical dairy thermophilic bacilli aimed to provide some guidelines for their control through engineering a thermal disruptive technology. As no appropriate model to describe the growth of these bacteria was available, a new model was developed.

In the thermocycling and thermospiking experiments with Geo1, there were regimes that either prolonged the lag phase or reduced the bacterial counts during the lag phase, or resulted in a reduced number of bacteria over 24 h. These regimes have the potential to extend the length of a manufacturing run in a milk processing plant. In summary:

- **Thermocycling at 55–35°C with a sine wave period of 10 min** had the greatest effect in prolonging the lag phase and producing an initial decrease in bacterial counts during the lag phase. This regime would offer the industry better quality products for up to 12 h of manufacture.
- **Thermocycling at 55–30°C with a sine wave period of 50 min** produced a short lag phase and a 1 – 1.5 log reduction in the number of thermophilic bacteria in the product for up to 24 h, which would have the potential to prolong the total run time for milk powder manufacture.
- **Square wave thermospiking at 55–35°C** prolonged the lag phase from 2 to 12 h, whereas that at 55–30°C prolonged the lag phase to 4 h. Square wave thermospiking at 55–35°C would allow the industry to produce much better quality product in the first 12 h. of manufacture. That at 55°C/15 min and 30°C/35 min has the potential to ensure run lengths of at least 24 h.

Models for estimating the development of biofilms of Geo1 and the numbers of bacteria in the outflowing milk from experimental reactors were developed. Models generated from this study were based on mass balances, process equations and the modified logistic growth equation. The rates of change in bacterial counts in the bulk milk phase (dM/dt) and the biofilm phase (dF/dt) were expressed as the rates of different processes within the system:

$$\frac{dM}{dt} = \text{Inflow} - \text{Outflow} - \text{Settling} + \text{Sloughing}$$

$$\frac{dF}{dt} = \text{Settling} - \text{Sloughing} + \text{Growth}$$

These equations were rewritten using the statistical package R, including all the known variables.

Rate of Change of Bacterial Counts in the Preheating Pipe Bulk Milk Phase (M):

$$\frac{dM}{dt} = \text{Milk conc}_{inflow} \times \text{Flowrate} - \frac{M \times \text{Flowrate}}{\text{Volume}_{pipe}} - \frac{M}{t_{0,pipe}} + \frac{F^2}{k_{pipe} \times t_{G,pipe}}$$

Rate of Change of Bacterial Counts in the Biofilm on the Preheating Pipe (F):

$$\frac{dF}{dt} = \frac{M}{t_{0,pipe}} - \frac{F^2}{k_{pipe} \times t_{G,pipe}} + \frac{F}{t_{G,pipe}}$$

The parameters in the pipe model were optimized using the automatic system in the R program.

$$t_{0,pipe} = \text{settling e - folding time} = 4.853 \times 10^4 \text{ s}$$

$$t_{G,pipe} = \text{growth e - folding time} = 6.473 \times 10^3 \text{ s}$$

$$k_{pipe} = \text{carrying capacity of the biofilm on the pipe wall} = 4.067 \times 10^8 \text{ cfu}$$

The optimized parameters were fed into the pipe model to generate the estimated concentration of bacteria in the outflow from the pipe of the preheating section into the reactor model.

Rate of Change of Bacterial Counts in the Bulk Milk Phase in the Reactor (N):

$$\frac{dN}{dt} = \frac{M \times \text{Flowrate}}{\text{Volume}_{\text{pipe}}} - \frac{N \times \text{Flowrate}}{\text{Volume}_{\text{reactor}}} - \frac{\text{Velocity} \times \text{Area}_{\text{reactor}} \times N}{\text{Volume}_{\text{reactor}}} + \frac{R^2 \times \text{Area}_{\text{pipe}}}{k_{\text{pipe}} \times \text{Area}_{\text{reactor}} \times t_{G,\text{reactor}}}$$

Rate of Change of Bacterial Counts in the Biofilm on the Reactor Surfaces (R):

$$\frac{dR}{dt} = \frac{\text{Velocity} \times \text{Area}_{\text{reactor}} \times N}{\text{Volume}_{\text{reactor}}} - \frac{R^2 \times \text{Area}_{\text{pipe}}}{k_{\text{pipe}} \times \text{Area}_{\text{reactor}} \times t_{G,\text{reactor}}} + \frac{R}{t_{G,\text{reactor}}}$$

These models need to be scaled up to pilot-plant-scale trials and validated before being implemented in manufacturing plants. To the author's knowledge, these models are robust and simpler to use and understand than published models. These models can be modified for *Anoxybacillus* species or mixed species for the control of thermophilic bacteria in dairy manufacturing plants.

References

- Alfa Laval/Tetra Pak (1995). *Dairy Processing Handbook*. Lund, Sweden: Tetra Pak Processing Systems.
- Aplin, J., & Flint, S. H. (2007). *Temperature disruption to prevent bacterial growth*. Palmerston North, New Zealand: Fonterra Co-operative Group Limited.
- Baier, R. E. (1980) Substrata influences on the adhesion of micro-organisms and their resultant new surface properties. In: *Adsorption of Micro-Organisms to Surface* (edited by G. Bitton & K.S. Marshall), pp. 59–104. New York, US: Wiley Interscience.
- Bacillus Genetic Stock Center (2001). *Catalog of Strains: The Genus Geobacillus. Introduction and Strain Catalog* (7th Edition, Volume 3). Retrieved from <http://www.bgsc.org/catalogs/Catpart3.pdf>.
- Bergey's Manual Trust (2009). *Bergey's Manual for Systematic Bacteriology* (2nd Edition, Volume 3). *The Firmicutes*. New York, NY, USA: Springer.
- Bremer, P. J., Fillery, S., & McQuillan, A. J. (2006). Laboratory scale clean-in-place (CIP) studies on the effectiveness of different caustic and acid wash steps on the removal of dairy biofilms. *International Journal of Food Microbiology*, 106, 254–262.
- Breyers, J. D., & Ratner, J. P. (2004). Bioinspired implant materials befuddle bacteria. *ASM News*, 70, 232–237.
- Brooks, J. D., & Flint, S. H. (2008a). Biofilms in the food industry: problems and potential solutions. *International Journal of Food Science & Technology*, 43, 2163–2176.
- Brooks, J. D., & Flint, S. H. (2008b). *Technology in Industry Fellowship Proposal: Modelling dairy biofilms for targeted control of thermophilic bacteria*. Palmerston North, New Zealand: Department of Food Technology, Massey University.
- Brooks, J. D., & Meers, J. L. (1973). The Effect of Discontinuous Methanol Addition on the Growth of a Carbon-limited Culture of *Pseudomonas*. *Microbiology*, 77(2), 513-519.
- Burgess, S. A., Brooks, J. D., Rakonjac, J., Walker, K. M., & Flint, S. H. (2009). The formation of spores in biofilms of *Anoxybacillus flavithermus*. *Journal of Applied Microbiology*, 107, 1012–1018.

- Centers for Disease Control and Prevention (2009) *CDC Reactor Manual*. Atlanta, GA, USA: Centers for Disease Control and Prevention.
- Coquet, L., Cosette, P., Junter, G. A., Beucher, E., Saiter, J. M., & Jouenne, T. (2002). Adhesion of *Yersinia ruckeri* to fish farm materials: influence of cell and material surface properties. *Colloids and Surfaces B: Biointerfaces*, 26, 373–378.
- Costerton, J. W. (1999). Introduction to biofilm. *International Journal of Antimicrobial Agents*, 11, 217–221.
- Costerton, J. W., & Wilson, M. (2004). Introducing biofilms. *Biofilms*, 1, 1–4.
- Costerton, J. W., Stewart, P. S., & Greenberg, E. P. (1999). Bacterial biofilms: a common cause of persistent infections. *Science*, 284, 1318–1322.
- Cunningham, A. B., Lennox, J. E., & Ross, R. J. (2011). Chapter 1: Introduction to biofilms. Retrieved from *The Biofilms Hypertextbook*: <http://www.hypertextbookshop.com/biofilmbook/v004/r003/contents/chapters/chapter001/chapter.html>.
- Davies, D. G., & Geesey, G. G. (1995). Regulation of the alginate biosynthesis gene *algC* in *Pseudomonas aeruginosa* during biofilm development in continuous culture. *Applied and Environmental Microbiology*, 61, 860–867.
- Davies, D. G., Parsek, M. R., Pearson, J. P., Iglewski, B. H., Costerton, J. W., & Greenberg, E. P. (1998). The involvement of cell-to-cell signals in the development of a bacterial biofilm. *Science*, 280, 295–298.
- de Jong, P., te Giffel, M. C., & Kiezebrink, E. A. (2002). Prediction of the adherence, growth and release of microorganisms in production chains. *International Journal of Food Microbiology*, 74, 13–25.
- Djordjevic, D., Wiedmann, M., & McLandsborough, L. A. (2002). Microtiter plate assay for assessment of *Listeria monocytogenes* biofilm formation. *Applied and Environmental Microbiology*, 68, 2950–2958.
- Donlan, R. M., & Costerton, J. W. (2002). Biofilms: survival mechanisms of clinically relevant microorganisms. *Clinical Microbiology Reviews*, 15, 167–193.
- Duncan-Hewitt, W. C. (1990). Nature of the hydrophobic effect. In: *Microbial Cell Surface Hydrophobicity* (edited by R. J. Doyle & M. Rosenberg), pp. 39–73. Washington, DC, USA: American Society for Microbiology.
- Flint, S. H. (1998). *Formation and control of biofilms of thermo-resistant streptococci on stainless steel*. PhD Thesis. Palmerston North, New Zealand: Department of Food Technology, Massey University.

- Flint, S. H., & Brooks, J. D. (2001). Rapid detection of *Bacillus stearothermophilus* using impedance-splitting. *Journal of Microbiological Methods*, 44, 205–208.
- Flint, S. H., & Hartley, N. (1996). A modified selective medium for the detection of *Pseudomonas* species that cause spoilage of milk and dairy products. *International Dairy Journal*, 6, 223–230.
- Flint, S., Bremer, P. J., & Brooks, J. D. (1997). Biofilms in dairy manufacturing plant – description, current concerns and methods of control. *Biofouling*, 11, 81–97.
- Flint, S. H., Brooks, J. D., & Bremer, P. J. (1997a). The influence of cell surface properties of thermophilic streptococci on attachment to stainless steel. *Journal of Applied Microbiology*, 83, 508–517.
- Flint, S. H., Brooks, J. D., & Bremer, P. J. (1997b). Use of the Malthus conductance growth analyser to determine numbers of thermophilic streptococci on stainless steel. *Journal of Applied Microbiology*, 83, 335–339.
- Flint, S. H., Brooks, J. D., & Bremer, P. J. (2000). Properties of the stainless steel substrate, influencing the adhesion of thermo-resistant streptococci. *Journal of Food Engineering*, 43, 235–242.
- Flint, S. H., Brooks, J. D., Bremer, P., Walker, K. M., & Hausman, E. (2002). The resistance to heat of thermo-resistant streptococci attached to stainless steel in the presence of milk. *Journal of Industrial Microbiology and Biotechnology*, 28, 134–136.
- Flint, S. H., Drocourt, J. L., Walker, K. M., Stevenson, B., Dwyer, M., Clarke, I., & McGill, D. (2006). A rapid, two-hour method for the enumeration of total viable bacteria in samples from commercial milk powder and whey protein concentrate powder manufacturing plants. *International Dairy Journal*, 16, 379–384.
- Flint, S. H., Palmer, J., Bloemen, K., Brooks, J. D., & Crawford, R. (2001). The growth of *Bacillus stearothermophilus* on stainless steel. *Journal of Applied Microbiology*, 90, 151–157.
- Flint, S. H., van den Elzen, H., Brooks, J. D., & Bremer, P. J. (1999). Removal and inactivation of thermo-resistant streptococci colonising stainless steel. *International Dairy Journal*, 9, 429–436.
- Flint, S. H., Ward, L. J. H., & Walker, K. M. (2001). Functional grouping of thermophilic *Bacillus* strains using amplification profiles of the 16S–23S internal spacer region. *Systematic and Applied Microbiology*, 24, 539–548.
- Foster, C. L., Britten, M., & Green, M. L. (1989). A model heat-exchange apparatus for the investigation of fouling of stainless steel surfaces by milk I. Deposit formation at 100 °C. *Journal of Dairy Research*, 56, 201–209.

- Hall-Stoodley, L., & Stoodley, P. (2002). Developmental regulation of microbial biofilms. *Current Opinion in Biotechnology*, 13, 228–233.
- Herigstad, B., Hamilton, M., & Heersink, J. (2001). How to optimize the drop plate method for enumerating bacteria. *Journal of Microbiological Methods*, 44, 121–129.
- Hermansson, M. (1999). The DLVO theory in microbial adhesion. *Colloids and Surfaces B: Biointerfaces*, 14, 105–119.
- Hinton, A. R., Trinh, K. T., Brooks, J. D., & Manderson, G. J. (2002). Thermophile survival in milk fouling and on stainless steel during cleaning. *Food and Bioproducts Processing*, 80, 299–304.
- Iversen, C., & Forsythe, S. (2004). Isolation of *Enterobacter sakazakii* and other Enterobacteriaceae from powdered infant formula milk and related products. *Food Microbiology*, 21, 771–776.
- Jenkinson, H. F., & Lappin-Scott, H. M. (2001). Biofilms adhere to stay. *Trends in Microbiology*, 9, 9–10.
- Jeurnink, T. J. M., & de Kruif, K. G. (1995). Calcium concentration in milk in relation to heat stability and fouling. *Netherlands Milk and Dairy Journal*, 49, 151–165.
- Kaiser, D. (1996). Bacteria also vote. *Science*, 272, 1598–1599.
- Kharazmi, A., Giwerzman, B., & Højby, N. (1999). Robbins device in biofilm research. *Methods in Enzymology*, 310, 207–215.
- Kirtley, S. A., & McGuire, J. (1989). On differences in surface constitution of dairy product contact materials. *Journal of Dairy Science*, 72, 1748–1753.
- Klausen, M., Heydorn, A., Ragas, P., Lambertsen, L., Aaes-Jørgensen, A., Molin, S., & Tolker-Nielsen, T. (2003). Biofilm formation by *Pseudomonas aeruginosa* wild type, flagella and type IV pili mutants. *Molecular Microbiology*, 48, 1511–1524.
- Kleerebezem, M., Quadri, L. E., Kuipers, O. P., & de Vos, W. M. (1997). Quorum sensing by peptide pheromones and two-component signal-transduction systems in Gram-positive bacteria. *Molecular Microbiology*, 24, 895–904.
- Knight, G. C., Nicol, R. S., & McMeekin, T. A. (2004). Temperature step changes: a novel approach to control biofilms of *Streptococcus thermophilus* in a pilot plant-scale cheese-milk pasteurisation plant. *International Journal of Food Microbiology*, 93, 305–318.
- Kokare, C. R., Chakraborty, S., Khopade, A. N., & Mahadik, K. R. (2009). Biofilm: importance and applications. *Indian Journal of Biotechnology*, 8, 159–168.

- Lewis, M. J., & Heppell, N. J. (2000). *Continuous Processing of Foods: Pasteurization and UHT Sterilization*. Gaithersburg, MD, USA: Aspen Publishers.
- Lichtman, J. W., & Conchello, J. A. (2005). Fluorescence microscopy. *Nature Methods*, 2, 910–919.
- Lindsay, D., Brözel, V. S., & von Holy, A. (2005). Spore formation in *Bacillus subtilis* biofilms. *Journal of Food Protection*, 68, 860–865.
- Marshall, K. C. (1994). Microbial adhesion in biotechnological processes. *Current Opinion in Biotechnology*, 5, 296–301.
- McCoy, W. F., Bryers, J. D., Robbins, J., & Costerton, J. W. (1981). Observations of fouling biofilm formation. *Canadian Journal of Microbiology*, 27, 910–917.
- McGuire, J., & Kirtley, S. A. (1989). On surface characterization of materials targeted for food contact. *Journal of Food Science*, 54, 224–226.
- Misumi (1994). *Surface Roughness*. JIS B 0601 (1994). Retrieved from Misumi USA: http://us.misumi-ec.com/pdf/press/us_12e_pr1257.pdf.
- Mittelman, M. W. (1998). Structure and functional characteristics of bacterial biofilms in fluid processing operations. *Journal of Dairy Science*, 81, 2760–2764.
- Mosteller, T. M., & Bishop, J. R. (1993). Sanitizer efficacy against attached bacteria in a milk biofilm. *Journal of Food Protection*, 56, 34–41.
- Muller-Steinhagen, H., & Zhao, Q. (1997). Investigation of low fouling surface alloys made by ion implantation technology. *Chemical Engineering Science*, 52, 3321–3332.
- Nazina, T. N., Tourova, T. P., Poltarau, A. B., Novikova, E. V., Grigoryan, A. A., Ivanova, A. E., Lysenko, A. M., Petrunyaka, V. V., Osipov, G. A., Belyaev, S. S., & Ivanov, M. V. (2001). Taxonomic study of aerobic thermophilic bacilli: descriptions of *Geobacillus subterraneus* gen. nov., sp. nov. and *Geobacillus uzenensis* sp. nov. from petroleum reservoirs and transfer of *Bacillus stearothermophilus*, *Bacillus thermocatenulatus*, *Bacillus thermoleovorans*, *Bacillus kaustophilus*, *Bacillus thermodenitrificans* to *Geobacillus* as the new combinations *G. stearothermophilus*, *G. th.* *International Journal of Systematic and Evolutionary Microbiology*, 51, 433–446.
- Palmer, J., Flint, S. H., & Brooks, J. D. (2007). Bacterial cell attachment, the beginning of a biofilm. *Journal of Industrial Microbiology and Biotechnology*, 34, 577–588.

- Parkar, S. G., Flint, S. H., & Brooks, J. D. (2003). Physiology of biofilms of thermophilic bacilli – potential consequences for cleaning. *Journal of Industrial Microbiology and Biotechnology*, 30, 553–560.
- Parkar, S. G., Flint, S. H., & Brooks, J. D. (2004). Evaluation of the effect of cleaning regimes on biofilms of thermophilic bacilli on stainless steel. *Journal of Applied Microbiology*, 96, 110–116.
- Pereni, C. I., Zhao, Q., Liu, Y., & Abel, E. (2006). Surface free energy on bacterial retention. *Colloids and Surfaces B: Biointerfaces*, 48, 143–147.
- Picioreanu, C., & Van Loosdrecht, M. C. (2002). A mathematical model for initiation of microbiologically influenced corrosion by differential aeration. *Journal of the Electrochemical Society*, 149, B211–B223.
- Picioreanu, C., Van Loosdrecht, M. C. M., & Heijnen, J. J. (1998). Mathematical modeling of biofilm structure with a hybrid differential-discrete cellular automaton approach. *Biotechnology and Bioengineering*, 58, 101–116.
- Picioreanu, C., Van Loosdrecht, M. C. M., & Heijnen, J. J. (2000a). A theoretical study on the effect of surface roughness on mass transport and transformation in biofilms. *Biotechnology and Bioengineering*, 68, 355–369.
- Picioreanu, C., Van Loosdrecht, M. C. M., & Heijnen, J. J. (2000b). Effect of diffusive and convective substrate transport on biofilm structure formation: a two-dimensional modeling study. *Biotechnology and Bioengineering*, 69, 504–515.
- Picioreanu, C., Van Loosdrecht, M. C. M., & Heijnen, J. J. (2000c). Modelling and predicting biofilm structure, In: *Community Structure and Co-operation in Biofilms* (edited by D. G. Allison, P. Gilbert, H. M. Lappin-Scott & M. Wilson), pp. 129–166. Cambridge, England: Cambridge University Press.
- Picioreanu, C., Van Loosdrecht, M. C. M., & Heijnen, J. J. (2001). Two-dimensional model of biofilm detachment caused by internal stress from liquid flow. *Biotechnology and Bioengineering*, 72, 205–218.
- Pikuta, E., Lysenko, A., Chuvilskaya, N., Mendrock, U., Hippe, H., Suzina, N., Nikitin, D., Osipov, G., & Laurinavichius, K. (2000). *Anoxybacillus pushchinensis* gen. nov., sp. nov., a novel anaerobic alkaliphilic, moderately thermophilic bacterium from manure, and description of *Anoxybacillus flavithermus* comb. nov. *International Journal of Systematic and Evolutionary Microbiology*, 50, 2109–2117.
- Pirt, S. J. (1965). The maintenance energy of bacteria in growing cultures. *Proceedings of the Royal Society of London Series B*, 163, 224–231.
- Pirt, S. J. (1975). *Principles of Microbe and Cell Cultivation*. New York, NY, USA: Halsted Press.

- Price, D. L., Sawant, A. D., & Ahearn, D. G. (1991). Activity of an insoluble antimicrobial quaternary amine complex in plastics. *Journal of Industrial Microbiology*, 8, 83–90.
- Ratkowsky, D. A., Lowry, R. K., McMeekin, T. A., Stokes, A. N., & Chandler, R. E. (1983). Model for bacterial culture growth rate throughout the entire biokinetic temperature range. *Journal of Bacteriology*, 154, 1222–1226.
- Reichert, P., & Wanner, O. (1997). Movement of solids in biofilms: significance of liquid phase transport. *Water Science and Technology*, 36, 321–328.
- Rice, A. R., Hamilton, M. A., & Camper, A. K. (2000). Apparent surface associated lag time in growth of primary biofilm cells. *Microbial Ecology*, 41, 8–15.
- Rijnaarts, H. H. M., Norde, W., Bouwer, E. J., Lyklema, J., & Zehnder, A. J. B. (1995). Reversibility and mechanism of bacterial adhesion. *Colloids and Surfaces B: Biointerfaces*, 4, 5–22.
- Rittmann, B. E., Pettis, M., Reeves, H. W., & Stahl, D. A. (1999). How biofilm clusters affect substrate flux and ecological selection. *Water Science and Technology*, 39, 99–105.
- Rittmann, B. E., & S áez, P. B. (2004). Improved pseudoanalytical solution for steady-state biofilm kinetics. *Biotechnology and Bioengineering*, 32, 379–385.
- Ronimus, R. S., Parker, L. E., Turner, N., Poudel, S., Rueckert, A., & Morgan, H. W. (2003). A RAPD-based comparison of thermophilic bacilli from milk powders. *International Journal of Food Microbiology*, 2644, 1–17.
- Rueckert, A., Ronimus, R. S., & Morgan, H. W. (2004). A RAPD-based survey of thermophilic bacilli in milk powders from different countries. *International Journal of Food Microbiology*, 96, 263–272.
- Sasahara, K. C., & Zottola, E. A. (1993). Biofilm formation by *Listeria monocytogenes* utilizes a primary colonizing microorganism in flowing systems. *Journal of Food Protection*, 56, 1022–1028.
- Schaule, G., Griebe, T., & Flemming, H.-C. (2000). Steps in biofilm sampling and characterization in biofouling cases. In: *Biofilms, Investigative Methods and Applications* (edited by H.-C. Flemming, U. Szewzyk & T. Griebe), pp. 1–21. Lancaster, PA, USA: Technomic.
- Scott, S. A., Brooks, J. D., Rakonjac, J., Walker, K. M. R., & Flint, S. H. (2007). The formation of thermophilic spores during the manufacture of whole milk powder. *International Journal of Dairy Technology*, 60, 109–117.
- Seale, R. B., Flint, S. H., McQuillan, A. J., & Bremer, P. J. (2008). Recovery of spores from thermophilic dairy bacilli and effects of their surface characteristics on

- attachment to different surfaces. *Applied and Environmental Microbiology*, 74, 731–737.
- Sharma, M., & Anand, S. K. (2002). Biofilms evaluation as an essential component of HACCP for food/dairy processing industry – a case. *Food Control*, 13, 469–477.
- Silley, P., & Forsythe, S. (1996). Impedance microbiology—a rapid change for microbiologists. *Journal of Applied Bacteriology*, 80, 233–243.
- Silyn-Roberts, G., & Lewis, G. (1997). A technique in confocal laser microscopy for establishing biofilm coverage and thickness. *Water Science and Technology*, 36, 117–124.
- Sinde, E., & Carballo, J. (2000). Attachment of *Salmonella* spp. and *Listeria monocytogenes* to stainless steel, rubber and polytetrafluorethylene: the influence of free energy and the effect of commercial sanitizers. *Food Microbiology*, 17, 439–447.
- Stoodley, P., Dodds, I., Boyle, J. D., & Lappin-Scott, H. M. (1999). Influence of hydrodynamics and nutrients on biofilm structure. *Journal of Applied Microbiology*, 85(Suppl. 1), 19S–28S.
- Stoodley, P., Sauer, K., Davies, D. G., & Costerton, J. W. (2002). Biofilms as complex differentiated communities. *Annual Review of Microbiology*, 56, 187–209.
- Sutherland, I. W. (2001). Biofilm exopolysaccharides: a strong and sticky framework. *Microbiology*, 147, 3–9.
- Sy-Lab (2009). *Manual for BacTrac 4300*. Sy-Lab, Vienna, Austria.
- Tamime, A. Y. (2008). *Cleaning-in-Place: Dairy, Food and Beverage Operations* (3rd Edition). Oxford, England: Blackwell Publishing.
- Tang, X., Flint, S. H., Brooks, J. B., & Bennett, R. J. (2008). Factors affecting the attachment of micro-organisms isolated from ultrafiltration and reverse osmosis membranes in dairy processing plants. *Journal of Applied Microbiology*, 107, 443–451.
- Teixeira, P., Lopes, Z., Azeredo, J., Oliveira, R., & Vieira, M. J. (2005). Physico-chemical surface characterization of a bacterial population isolated from a milking machine. *Food Microbiology*, 22, 247–251.
- The Gale Group Inc. (2003). *Acridine Orange*. Retrieved from Encyclopedia.com: <http://www.encyclopedia.com/doc/1G2-3409800010.html>.
- Tjoa, I. B., & Biegler, L. T. (1991). Simultaneous solution and optimization strategies for parameter estimation of differential-algebraic equation systems. *Industrial & Engineering Chemistry Research*, 30(2), 376–385.

- Toyoda, I., Schreier, P. J. R., & Fryer, P. J. (1994). A computational model for reaction fouling from whey protein solutions. In: *Proceedings of Fouling and Cleaning in Food Processing*, pp. 222–229. Cambridge, England.
- Traag, B. A., Pugliese, A., Eisen, J. A., & Losicka, R. (2013). Gene Conservation among Endospore-Forming Bacteria Reveals Additional Sporulation Genes in *Bacillus subtilis*. *Journal of Bacteriology*, 195(2), 253–260.
- Trachoo, N., & Brooks, J. D. (2005). Attachment and heat resistance of *Campylobacter jejuni* on *Enterococcus faecium* biofilm. *Pakistan Journal of Biological Sciences*, 8, 599–605.
- Tyler Research (2009). *Low Pressure Devices*. Retrieved from <http://www.tylerresearch.com/low-pressure-devices/>.
- Urmenyi, A. M., & Franklin, A. W. (1961). Neonatal death from pigmented coliform infection. *Lancet*, 11, 313–315.
- Van Houdt, R., Aertsen, A., Jansen, A., Quintana, A. L., & Michiels, C. W. (2004). Biofilm formation and cell-to-cell signalling in Gram-negative bacteria isolated from a food processing environment. *Journal of Applied Microbiology*, 96, 177–184.
- Visser, J., & Jurnink, Th. J. M. (1997). Fouling of heat exchangers in the dairy industry. *Experimental Thermal and Fluid Science*, 14, 407–424.
- Wanner, O., Eberl, H. J., Morgenroth, E., Noguera, D. R., Picioreanu, C., Rittmann, B. E. & Van Loosdrecht, M. C. M. (2006). *Mathematical modeling of biofilms*. Scientific and Technical Report No. 18. London, England: IWA Publishing.
- Weisstein, E. (2013). *Logistic Equation*. Retrieved from Wolfram MathWorld: <http://mathworld.wolfram.com/LogisticEquation.html>.
- Williams, C. M., Richter, C. S., Mackenzie, J. M., & Shih, J. C. (1990). Isolation, identification, and characterization of a feather-degrading bacterium. *Applied and Environmental Microbiology*, 56, 1509–1515.
- Xavier, J. B., Picioreanu, C., & Van Loosdrecht, M. C. (2005). A framework for multidimensional modelling of activity and structure of multispecies biofilms. *Environmental Microbiology*, 7, 1085–1103.
- Young, I. E., & Fitz-James, P. C. (1959). Chemical and morphological studies of bacterial spore formation II. Spore and parasporal protein formation in *Bacillus cereus* var. *Alesti*. *Journal of Biophysical and Biochemical Cytology*, 6, 483–498.
- Zhao, Q. (2004). Effect of surface free energy of graded Ni–P–PTFE coatings on bacterial adhesion. *Surface and Coatings Technology*, 185, 199–204.

- Zhao, Q., & Liu, Y. (2006). Modification of stainless steel surfaces by electroless Ni–P and small amount of PTFE to minimize bacterial adhesion. *Journal of Food Engineering*, 72, 266–272.
- Zhao, Q., Liu, Y., & Wang, C. (2005). Development and evaluation of electroless Ag–PTFE composite coatings with anti-microbial and anti-corrosion properties. *Applied Surface Science*, 252, 1620–1627.
- Zhao, Q., Liu, Y., Wang, C., Wang, S., & Muller-Steinhagen, H. (2005). Effect of surface free energy on the adhesion of biofouling and crystalline fouling. *Chemical Engineering Science*, 60, 4858–4865.
- Zottola, E. A. (1994). Microbial attachment and biofilm formation: a new problem for the food industry? *Food Technology*, 48, 107–114.

Appendices

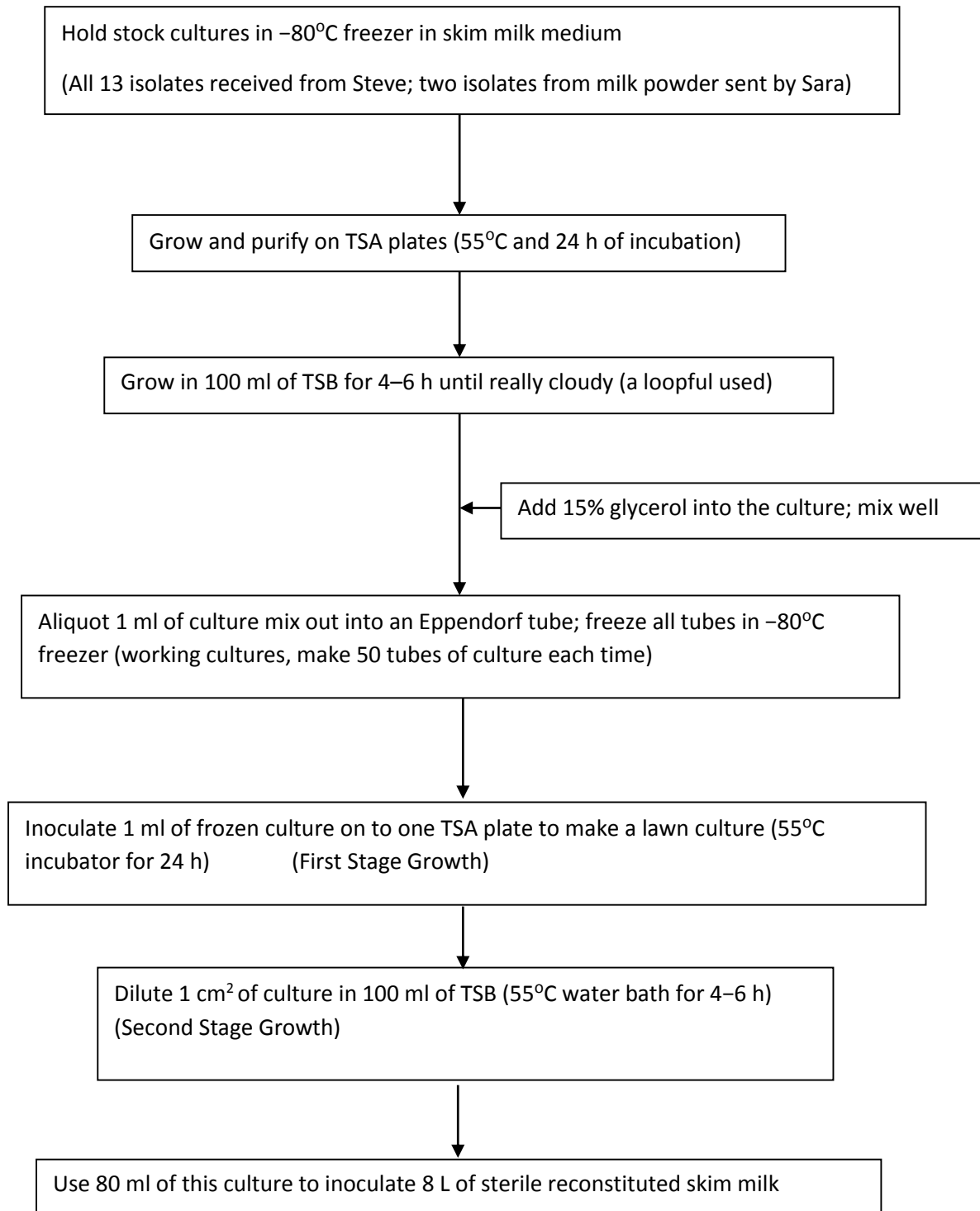
Only appendices used in text are included here. Additional appendices of analysed data for specific experiments are included in attached CD.

Appendix 1: Hexagonal Reactor Developed by Massey University and Fonterra



Appendix 2: Culture Management System

1. Culture Management System Currently Used



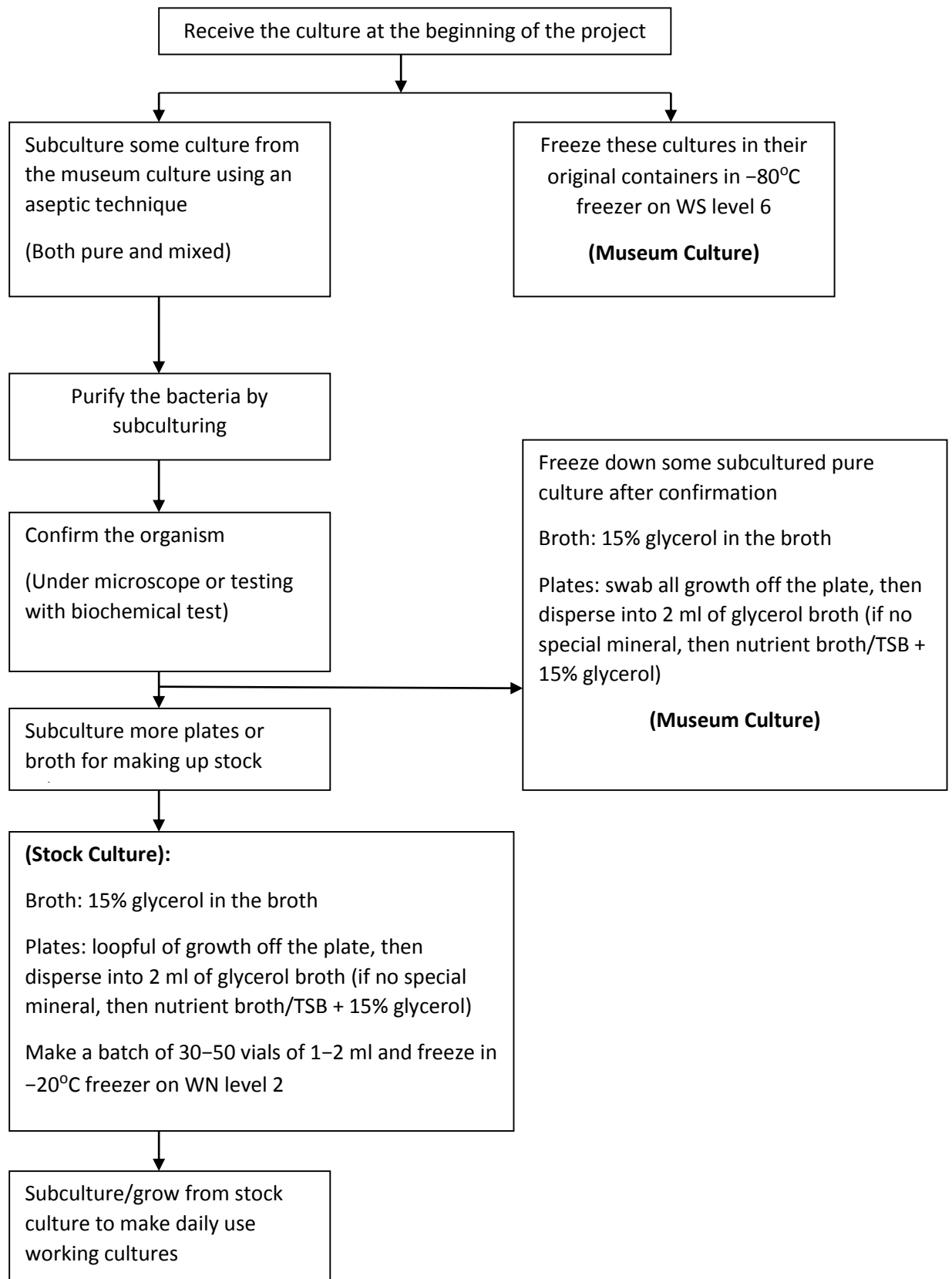
2. Definitions

Museum Culture: These cultures are the cultures received at the start of the project. They might be pure or mixed. They should be preserved immediately after receipt. They should be stored using conditions that aim for long term storage, such as -80°C freezer on level 6 of WS. A separate set of stock cultures should be purified from these cultures. (Freeze both the mixed culture and the pure culture, in case you purify the wrong bacteria. Keep the original culture untouched as much as possible. Make subcultures when you receive them. Freeze some of the subcultures as well because the amount received might be quite small.)

Stock Culture: These cultures should be purified from the 'museum culture' set at the beginning of the project. They should be pure and ready to use. They should be kept using conditions that aim for mid-long-term storage, i.e. freezing at -20°C on level 2 of WN. Sufficient amount of stock culture should be made up, such as 50 vials. The purity of the bacteria should be double checked before making up a big batch of subcultures or stock cultures. They should be stored in small aliquots or quantities as a large batch, e.g. 50 vials of 1 ml aliquots. Therefore, if any contamination occurs, the small aliquot of stock culture can be thrown out without interfering with the project.

Working Culture: These cultures should be consistent with the stock cultures. They should be subcultured from the stock cultures. They can be kept in broth or plates in the cold room or incubator just for daily use. They can be thrown away at any point if there are any concerns with them. Do not subculture too many times in sequence because genomic changes may occur within the bacteria. If you are concerned about this, just subculture from the stock culture again.

3. Procedure



Appendix 3 Minitab Output for Geo1 (Factorial Regression)

Factorial Fit: Growth Rate versus Temperature C, Solids%

* NOTE * Data in the worksheet do not appear to match the center point column.
 * NOTE * This design has some botched runs. It will be analyzed using a regression approach.

Estimated Effects and Coefficients for Growth Rate (coded units)

Term	Effect	Coef	SE Coef	T	P
Constant		0.6498	0.1339	4.85	0.005
Temperature C	0.4836	0.2418	0.1640	1.47	0.201
Solids%	-1.1700	-0.5850	0.1640	-3.57	0.016
Temperature C*Solids%	-0.1756	-0.0878	0.2009	-0.44	0.680

S = 0.401812 R-Sq = 75.10% R-Sq(adj) = 60.16%

Analysis of Variance for Growth Rate (coded units)

Source	DF	Seq SS	Adj SS	Adj MS	F	P
Main Effects	2	2.40411	2.40411	1.20205	7.45	0.032
2-Way Interactions	1	0.03084	0.03084	0.03084	0.19	0.680
Residual Error	5	0.80727	0.80727	0.16145		
Total	8	3.24221				

Estimated Coefficients for Growth Rate using data in uncoded units

Term	Coef
Constant	-0.04808
Temperature C	0.0549083
Solids%	-0.036500
Temperature C*Solids%	-0.00219500

* NOTE * Some factors have more than 2 levels, no alias table was printed.

Appendix 4 Minitab Output for Geo1 (Response Regression)

Response Surface Regression: Growth Rate versus Temperature C, Solids%

The analysis was done using coded units.

Estimated Regression Coefficients for Growth Rate

Term	Coef	SE Coef	T	P
Constant	1.03093	0.2877	3.584	0.037
Temperature C	0.24178	0.1576	1.534	0.222
Solids%	-0.58500	0.1576	-3.713	0.034
Temperature C*Temperature C	-0.37745	0.2729	-1.383	0.261
Solids%*Solids%	-0.19420	0.2729	-0.712	0.528
Temperature C*Solids%	-0.08780	0.1930	-0.455	0.680

S = 0.3860 R-Sq = 86.2% R-Sq(adj) = 63.2%

Analysis of Variance for Growth Rate

Source	DF	Seq SS	Adj SS	Adj MS	F	P
Regression	5	2.79530	2.79530	0.55906	3.75	0.153
Linear	2	2.40411	2.40411	1.20205	8.07	0.062
Square	2	0.36036	0.36036	0.18018	1.21	0.412
Interaction	1	0.03084	0.03084	0.03084	0.21	0.680
Residual Error	3	0.44690	0.44690	0.14897		
Total	8	3.24221				

Estimated Regression Coefficients for Growth Rate using data in uncoded units

Term	Coef
Constant	-11.4822
Temperature C	0.4324
Solids%	0.3034
Temperature C*Temperature C	-0.0038
Solids%*Solids%	-0.0121
Temperature C*Solids%	-0.0022

Appendix 5 Preheating Pipe Model for Geo1

```

library(deSolve)

# all volumes are in ml and all times are in seconds.

flowrate_min <- 1.5 #NB: ml/min

flowrate <- flowrate_min / 60

incoming_milk_conc <- 1e5 # NB: bacteria per ml
Vol_pipe <- pi*0.3^2 * 60 # NB: volume in ml

parameters <- c(t0      = 3800, # settling efolding time, sec
                tG      = 8800, # growth efolding time, sec
                k        = 1e8,  # carrying capacity of the FILM of the pipe
                inflow   = incoming_milk_conc * flowrate
                )

## first specify the _start_ state, remember that 'M' is the number of
## CFU in the free-flowing mil in the pipe.
state <- c(M = Vol_pipe * incoming_milk_conc , P = 0)

bact <- function(t, state, parameters) {
  with(as.list(c(state, parameters)), {

    settling <- M / t0
    slough <- P^2/(k*tG)
    growth <- P/tG

    outflow <- M/Vol_pipe * flowrate

    # rate of change
    dM = (
      +inflow
      -outflow
      -settling
      +slough
    )

    dP = (
      +settling
      -slough
      +growth
    )
  }
}

```

```
# return the rate of change
  list(c(dM, dP))
}) # end with(as.list ...)
}

times <- seq(0, 24*3600, by = 30*60)

out <- ode(y = state, times = times, func = bact, parms = parameters)
head(out)
```

Appendix 6 Optimization of the Preheating Pipe Model for Geo1

```

source("try.R")

a <- read.table("observations.txt",header=T)

## convert to seconds:
a$time <- a$time * 3600

parameters <- c(t0      = 1800, # settling efolding time, sec
                tG      = 7800, # growth efolding time, sec
                k        = 1e7,  # carrying capacity of the FILM of the pipe
                inflow   = incoming_milk_conc * flowrate
                )

# First, plot observational data.
plot ((log10(Vol_pipe) + c1)^time, data=a, type='b', col='red')
points((log10(Vol_pipe) + c2)^time, data=a, type='b', col='blue')

points(out[, 1], log10(out[, 2]), col='green')

mismatch1 <- log10(out[, 2]) - (a$c1 + log10(Vol_pipe))
mismatch2 <- log10(out[, 2]) - (a$c2 + log10(Vol_pipe))

badness <- sum(mismatch1[-1]^2) + sum(mismatch2[-1]^2)

bad <- function(parameters, giveall=FALSE) {

  out <- ode(y = state, times = a$time, func = bact, parms = parameters)
  if(giveall) {return(out)}
  mismatch1 <- log10(out[, 2]) - (a$c1 + log10(Vol_pipe))
  mismatch2 <- log10(out[, 2]) - (a$c2 + log10(Vol_pipe))

  badness <- sum(mismatch1[-1]^2) + sum(mismatch2[-1]^2)
  return(badness)
}

objective <- function(x, giveall=FALSE) {
  print(x)
  if(any(x<0)) {return(1e99)}
  params <- c(x, inflow=2500)
  bad(params, giveall=giveall)
}

startvalue <- c(t0=1800, tG=7800, k=4e7)

```

```
ans <- optim(par = startvalue, fn=objective)
```

Note: The observation.txt is the observed 24 hour tube-only run data;

Appendix 7 Hexagonal Reactor Model for Geo1

```

#This file does the coupon reactor growth as well.

library(deSolve)

# all volumes are in ml and all times
are in seconds.

source("usefulfuncs.R") # this defines f() which gives the growth rate in the
coupon as a function of Temp.
flowrate_min <- 1.5 #NB: ml/min
flowrate <- flowrate_min / 60
incoming_milk_conc <- 1e4 # NB: bacteria per ml

Vol_pipe <- pi*0.3^2 * 60 # NB: volume in ml

Vol_coupon <- 4 # NB: volume in (milliliters)

Area_coupon <- Vol_coupon / 0.5 # 0.5 = height of coupon.

Area_pipe <- 2*pi*0.3*60 # curved surface area in square centimeters

settling_velocity <- Vol_pipe / (Area_pipe*48526)

carrying_capacity_perunitarea <- 4e8/Area_pipe

parameters <- c(t0 = Vol_pipe/(Area_pipe*settling_velocity), #
settling_efolding_time, sec
tG = 6473, # growth_efolding_time, sec
k = carrying_capacity_perunitarea * Area_pipe, #
carrying_capacity_of_the_FILM_of_the_pipe
inflow = incoming_milk_conc * flowrate,
t0_coupon = Vol_coupon / (Area_coupon *settling_velocity),
k_coupon = carrying_capacity_perunitarea * Area_coupon
)

## first specify the _start_ state, remember that 'M' is the number of
## CFU in the free-flowing mil in the pipe.
state <- c(M = Vol_pipe * incoming_milk_conc , P = 0, N_coupon = Vol_coupon *
incoming_milk_conc, R_coupon=0)

bact <- function(t, state, parameters) {

```

```

with(as.list(c(state, parameters)), {

  settling <- M / t0
  slough <- P^2/(k*tG)
  growth <- P/tG

  outflow <- M/Vol_pipe * flowrate

  # rate of change
  dM <- (
    +inflow
    -outflow
    -settling
    +slough
  )

  dP <- (
    +settling
    -slough
    +growth
  )

  if(FALSE) {
    tG_coupon <- growthrate_T(sine_wave(t, Tmin=35, Tmax=55, period=20)) # period
    in *minutes*
  } else {
    tG_coupon <- growthrate_T(square_wave(t, Tmin=30, Tmax=55, t_low=35, t_high=15))
    # 't_low' is time at low temperature
  }

  out_conc <- M / Vol_pipe # concentration in outflow from pipe = inflow to
  coupon.

  inflow_coupon <- out_conc*flowrate
  outflow_coupon <- (N_coupon / Vol_coupon) * flowrate
  settling_coupon <- N_coupon / t0_coupon

  slough_coupon <- R_coupon^2/(k_coupon*tG_coupon)
  growth_coupon <- R_coupon/tG_coupon

  dN_coupon <- (
    +inflow_coupon
    -outflow_coupon
    -settling_coupon
    +slough_coupon
  )

```

```
dR_coupon <-      (  
  +settling_coupon  
  -slough_coupon  
  +growth_coupon  
  )  
  
                                # return the rate of change  
  list(c(dM, dP, dN_coupon, dR_coupon))  
}) # end with(as.list ...  
}  
  
times <- seq(0, 86400, by = 7200)  
  
out <- ode(y = state, times = times, func = bact, parms = parameters)  
head(out)
```

Appendix 8 Hexagonal Reactor Model Wave Function

```

jj <- read.table("data.txt", header=T)

growthrate_T <- approxfun(jj$temp, (1/jj$growth)*3600, yleft=1e-6, yright=1e-6)
# divide by 3600 to give growth rate per second, not hour.
rm(jj)

sine_wave <- function(time, Tmin, Tmax, period) {
  # time in seconds,
  # period in minutes,
  # Tmin and Tmax min
  # and max temperatures
  # respectively

  p <- period*60
  (Tmin+Tmax)/2 - (Tmax-Tmin)*0.5*cos(2*pi*time/p) # cosine because time=0
means minimum temperature.
}

square_wave_basic <- function(time, t_high, t_low) {
  time <- time %% (t_high + t_low)
  ifelse(time < t_high, 1, 0)
}

square_wave <- function(time, Tmin, Tmax, t_low, t_high) {
  # time in seconds, period in minutes, Tmin and Tmax min and max
  # temperatures respectively. t_high and t_low are TIMES at high temp
  # and low temp respectively.

  t_low <- t_low * 60
  t_high <- t_high * 60

  Tmin + (Tmax-Tmin)* square_wave_basic(time, t_high, t_low)
}

```

Appendix 9 Hexagonal Coupon Reactor Model Data.txt

temp growth

30 1e-6

35 1e-6

40 0.8465

50 1.4661

60 1.1997

70 1.052

80 1e-6